Molecular Analysis of *Mycobacterium tuberculosis* Infection of Human Macrophages: The Role of Protein Tyrosine Phosphatase A

by

Valérie Poirier

B.Sc., Bishop's University, 2008

A THESIS SUBMITTED IN PARTIAL FULFILLMENT OF

THE REQUIREMENTS FOR THE DEGREE OF

DOCTOR OF PHILOSOPHY

in

THE FACULTY OF GRADUATE AND POSTDOCTORAL STUDIES

(Experimental Medicine)

THE UNIVERSITY OF BRITISH COLUMBIA

(Vancouver)

February 2015

Abstract

To survive in the human host macrophage, *Mycobacterium tuberculosis*, the etiological agent of Tuberculosis, infects human macrophages and inhibits two key cellular events required for the elimination of invading organisms; phagosome acidification and fusion with lysosomes. This is partially dependent on Protein tyrosine phosphatase A (PtpA) secreted into the cytosol of the macrophage. PtpA first disrupts phagosome acidification by binding to subunit H of the proton pump, and second, inhibits phagosome-lysosome fusion by dephosphorylating and inactivating the membrane fusion regulator, hVPS33B. The ability of *M. tuberculosis* to actively interfere with host trafficking events allows this pathogen to replicate and persist inside the macrophage and prevent antigen presentation required to initiate an adaptive immune response.

In this work, we explored the global macrophage's response to infection emphasizing on PtpA's role in this process. We analyzed the macrophage global proteomic responses and focused on the activity of signalling pathways by determining the phosphorylation status of host proteins upon infection with *M. tuberculosis* strains.

We found that PtpA affects the macrophage's response by modulating various proteins involved in RNA metabolism, immunity and defence, and cellular respiration pathways. We further show that PtpA promotes *M. tuberculosis* survival by dephosphorylating the host kinase GSK3α on amino acid Y^{279} leading to inhibition of GSK3α and arrest of macrophage apoptosis. GSK3α has pro- and anti-apoptotic activities and dephosphorylation of Y^{279} inhibits its ability to initiate apoptosis. In this regard, activation of the host apoptosis executioner, caspase-3, is

blocked in *M. tuberculosis*-infected macrophages compared to cells infected with Δ*ptpA* mutant strain.

Taken together, these findings reveal one of the long-sought effectors behind the inhibition of apoptosis of the host by virulent *M. tuberculosis*. Moreover, we are the first to simultaneously determine proteome-wide protein expression levels of human macrophages infected with *M. tuberculosis* and outline molecular signatures of the global and PtpA-dependent proteomic patterns of macrophages during infection.

We have now established that PtpA significantly contributes to successful infection and survival of *M. tuberculosis* inside the macrophage. Understanding the mechanism of action of PtpA during *M. tuberculosis* infection may lead to the development of novel anti-mycobacterial drugs.

Preface

Parts of this thesis have been published in the peer-reviewed journals listed below:

1. **Poirier, V.**, and Av-Gay, Y. (2012). *Mycobacterium tuberculosis* modulators of macrophage cellular events. *Microbes Infect.* 14, 1211-1219

   In this work, I was responsible for writing a review article on the current knowledge of *Mycobacterium tuberculosis* effectors for which a cognate substrate, a cellular partner or a signalling pathway have been experimentally identified within the human host. Y. Av-Gay participated in writing and editing the manuscript. This work is located in Sections 1.2.1 and 1.2.2.

2. **Poirier, V.**, Bach, H., and Av-Gay, Y. (2014) *Mycobacterium tuberculosis* promotes anti apoptotic activity of the macrophage by PtpA-dependent dephosphorylation of host GSK3α. *J Biol Chem.* 289, 29376-29385

   In this study, I designed and performed all experiments except those of work related to Figure 11, which was performed by H. Bach. I wrote the manuscript. Y. Av-Gay contributed to the designing of the study and writing the manuscript. A version of this published work is located in Sections 3.1 and 4.1.

3. A version of Chapter 3 and 4 (Sections 3.2 and 4.2) will be submitted for publication in the near future. In these sections, I designed and performed all experiments. G. Av-Gay performed

all statistical analyses. I wrote the manuscript except for Section 2.14, which was written by G. Av-Gay. Y. Av-Gay participated in designing the study and writing the manuscript.

The work presented in this thesis was conducted in accordance with the University of British Columbia Research Policies and Procedures, the University Biosafety Committee, the Public Health Agency of Canada guidelines, and with approval from the University of British Columbia Office of Research Services. Biohazard Approval Certificate: B10-0112. Work performed with radioactive materials was approved by the University of British Columbia Advisory Committee on Radioisotopes and Radiation Hazards. Radioisotope License: MEDI-3375-18.

Table of Contents

List of Tables

List of Figures

List of Abbreviations

2D	Two-Dimensional
ABCB10	ATP-Binding Cassette Sub-Family B Member 1
ALPHAScreen	Amplified Luminescent Proximity Homogeneous Assay Screen
AraLAM	Arabinofuranosyl-Terminated LAM
ATP	Adenosine-5'-Triphosphate
γ^{32}P-ATP	[γ^{32}P]-Adenosine-5'-Triphosphate
ATP5I	ATP Synthase Subunit ε
BCG	Bacillus Calmette-Guérin
BCL-2	B-Cell Lymphomal Leukaemia-2
BIRC6	IAP Repeat-Containing Protein-6
Brg1	Brahma-Related Gene-1
Ca^{2+}	Calcium
CaM	Calmodulin
CaMKII	Ca^{2+}/CaM Kinase II
cDNA	Complementary DNA
CIITA	Class II, Major Histocompatibility Complex, Transactivator
CIRBP	Cold-Inducible RNA-Binding Protein
CO	Complement (Δ*ptpA*::*ptpA M. tuberculosis*)
CO_2	Carbon Dioxide
COX7B	Cytochrome c Oxidase Subunit 7B
CR3	Complement Receptor 3
CTSG	Cathepsin G

DNA	Deoxyribonucleic Acid
DOCK10	Dedicator of Cytokinesis Protein-10
DTT	Dithiothreitol
ECL	Enhanced Chemiluminescence
EDTA	Ethylenediaminetetraacetic Acid
EEA1	Early Endosome Antigen-1
FACS	Fluorescence-Activated Cell Sorting
FBS	Fetal Bovine Serum
FcγR	Fc Gamma Receptor
GAPDH	Glyceraldehyde 3-Phosphate Dehydrogenase
GEF	Guanine Nucleotide Exchange Factor
GSK3α	Glycogen Synthase Kinase-3 Alpha
GSK3β	Glycogen Synthase Kinase-3 Beta
GST	Glutathione S-Transferase
GTP	Guanosine-5'-Triphosphate
H2AFZ	Histone H2A
HAT	Histone Acetyl Transferase
HCl	Hydrogen Chloride
HDAC	Histone Deacetylase
HEPES	4-(2-Hydroxyethyl)-1-Piperazineethanesulfonic Acid
His	Histidine
HOPS	Homotypic Vacuole Fusion and Protein Sorting
HPLC	High-Performance Liquid Chromatography

HRP	Horseradish Peroxidase
hVPS	Human Vacuolar Protein Sorting
hVPS34	Human Vacuolar Protein Sorting Protein 34
hVPS33B	Human Vacuolar Protein Sorting Protein 33B
ICAM1	Intercellular Adhesion Molecule-1
IFNγ	Interferon-Gamma
IgG	Immunoglobulin G
IL1β	Interleukin-1β
IPTG	Isopropyl-β-D-Thio-Galactoside
iTRAQ	Isobaric Tags for Related and Absolute Quantitation
K_d	Dissociation Constant
kDa	KiloDalton
KO	Knockout (Δ*ptpA M. tuberculosis*)
LAM	Lipoarabinomannan
LAMP	Lysosomal Associated Membrane Protein
LB	Luria-Bertani
LC	Liquid Chromatography
LLO	Listeriolysin O
LpqH	19 kDa Lipoprotein
ManLAM	Mannosylated LAM
MAPK	Mitogen-Activated Protein Kinase
M. bovis	*Mycobacterium bovis*
M. bovis BCG	*Mycobacterium bovis* Bacillus Calmette-Guérin

MDR	Multidrug-Resistant
MEK1/2	Mitogen-Activated Protein Kinase Kinase-1/2
$MgCl_2$	Magnesium Chloride
MHC-I	Major Histocompatibility Complex Class I
MHC-II	Major Histocompatibility Complex Class II
MIF	Migration Inhibitory Factor
M. kansasii	*Mycobacterium kansasii*
MMTS	S-Methyl Methanethiosulfonate
$MnCl_2$	Manganese Chloride
MOI	Multiplicity of Infection
MOWSE	Molecular Weight Search
mRNA	Messenger RNA
MS/MS	Mass Spectrometry
M. smegmatis	*Mycobacterium smegmatis*
MTBC	*M. tuberculosis* Complex
M. tuberculosis	*Mycobacterium tuberculosis*
MW	Molecular Weight
NaCl	Sodium Chloride
Na_2HPO_4	Disodium Hydrogen Phosphate
Na_3VO_4	Sodium Orthovanadate
NI	Uninfected
Ni-NTA	Nickel-Nitriloacetic Acid
NSF	*N*-Ethylmaleimide-Sensitive Factor

OADC	Oleic Acid Dextrose Catalase Complex
PAMP	Pathogen-Associated Molecular Pattern
PBS	Phosphate Buffered Saline
PCD	Programmed Cell Death
PCR	Polymerase Chain Reaction
PH	Pleckstrin Homology
P_i	Inorganic Phosphate
pI	Isoelectric Point
PI	Phosphatidylinositol
PI3K	Phosphatidylinositide 3-Kinase
PI3P	Phosphatidylinositol 3-Phosphate
PiLAM	Phosphoinositol-Capped LAM
PlcA	Phospholipase A
PlcB	Phospholipase B
PMA	Phorbol-12-Myristate-13-Acetate
PMSF	Phenylmethanesulfonyl Fluoride
*p*NP	*p*-Nitrophenol
*p*NPP	*p*-Nitrophenyl Phosphate
PRPF31	U4/U6 Small Nuclear Ribonucleoprotein Prp31
PRR	Pattern Recognition Receptor
PtpA	Protein tyrosine phosphatase A
qPCR	Quantitative Polymerase Chain Reaction
R	Gnu

RCF	Relative Centrifugal Force
RILP	Rab-Interacting Lysosomal Protein
RNA	Ribonucleic Acid
RPMI	Roswell Park Memorial Institute
SapM	Secreted Acid Phosphatase of *M. tuberculosis*
SARS2	Seryl-tRNA Synthetase-2
SD	Standard Deviation
SDS	Sodium Dodecyl Sulphate
SDS-PAGE	Sodium Dodecyl Sulphate-Polyacrylamide Gel Electrophoresis
Ser	Serine
SNAP	Soluble NSF Attachment Protein
SNARE	Soluble N-Ethylmaleimide-Sensitive Factor Attachment Protein Receptor
SNRPD1	Small Nuclear Ribonucleoprotein Sm D1
SOD2	Superoxide Dismutase-2
TB	Tuberculosis
TCEP	Tris(2-Carboxyethyl)phosphine
TEAB	Tetraethylammonium Bromide
TGN	*Trans*-Golgi Network
Thr	Threonine
TLR2	Toll-Like Receptor 2
TNF-α	Tumor Necrosis Factor-Alpha
Tyr	Tyrosine
V-ATPase	Vacuolar H^+-ATPase

VPS	Vacuolar Protein Sorting
VPS11	Vacuolar Protein Sorting 11
VPS16	Vacuolar Protein Sorting 16
VPS18	Vacuolar Protein Sorting 18
VPS33B	Vacuolar Protein Sorting 33B
VPS34	Vacuolar Protein Sorting 34
VPS39	Vacuolar Protein Sorting 39
VPS41	Vacuolar Protein Sorting 41
WHO	World Health Organization
WT	Wild-Type (*M. tuberculosis*)
XDR	Extensively Drug-Resistant
Y	Tyrosine

Acknowledgements

The first person that I wish to thank is my supervisor Dr. Yossef Av-Gay. The work presented in this thesis would not be possible had it not been from his strong and constant support to persevere through the hard work of my graduate studies. Dr. Av-Gay accepted me into his laboratory in 2008 as a Master's student, and throughout the entirety of my graduate studies Dr. Av-Gay presented me with numerous opportunities to learn and experience the various aspects of professional scientific research. These opportunities allowed me to meet leaders within the scientific community and benefit from participating in several international conferences. Dr. Av-Gay has inspired me to become a better scientist, to continue my work in this field and has made me more sensitive to a disease that ravages developing countries. I offer Dr. Av-Gay my enduring gratitude for his welcoming heart, expertise and for broadening my vision of science. He is a selfless human being and displayed nothing but patience and mentorship during my graduate studies.

I thank my committee members, Dr. Zakaria Hmama and Dr. Steven Pelech, for their support. They have provided me with helpful comments and questions over the years that helped me to question myself and my work on a fundamental level that is critical to scientific research.

I also thank all the past and present members of the Av-Gay laboratory, with special thanks to Mary Ko for all of her technical assistance, and Melissa Richard-Greenblatt for her enduring friendship over the years and her ability to create a lively environment in the laboratory.

I would like to acknowledge financial support from Canadian Institute of Health Research (CIHR) and the University of British Columbia, and also, the British Columbia Center for Disease Control for providing us access to a BCL-3 laboratory.

Special thanks are owed to my loving family who helped me get through the emotional ups and downs of being so far away from home during my Ph.D studies.

Finally, I thank my husband Stefan Szary for supporting me morally and financially throughout my years of education. His support gave me the luxury of choosing my path. But most importantly, I deeply thank him for his unconditional care, love and advice that helped me become the woman I am today.

"The Great White Plague, tuberculosis, is never done with its insidious work; for numberless years it has been silently, continuously and unrelentingly pursuing its destructive course, never remitting its deadly work, always reaching out for new victims, and today it is the most universal scourge of the human race."

Otis, Edward O. *The Great White Plague: Tuberculosis*. New York: Thomas Y. Crowell & CO, 1909. Print, p. 2.

Chapter 1: Introduction

1.1 Tuberculosis

1.1.1 Epidemiology of Human Tuberculosis

Among all infectious diseases, Tuberculosis (TB) is second to HIV/AIDS as the greatest killer worldwide (WHO Report, 2014). An estimated one-third of the world's population carries latent TB, implying that people have been exposed to *M. tuberculosis*, but show no signs of illness and cannot yet transmit the disease. TB is mostly prevalent in developing countries where over 95% of TB-related deaths occur. In 2013, an estimated 9 million people fell ill with TB and 1.5 million people died of the disease (WHO Report, 2014). Although the number of people falling ill due to TB is declining annually, TB is still the leading killer of people living with HIV representing one quarter of all deaths (WHO Report, 2014).

By the beginning of the 20th century, before the discovery of antibiotics, TB was the principal cause of death of human beings and was crowned with the names; "Great Killer" and "Captain of all Deaths" (1). The work of Albert Calmette and Camille Guérin led, in 1921, to the introduction of the first TB vaccine, known as the BCG vaccine, which relies on the administration of live attenuated *M. bovis* bacilli, the causative agent of bovine TB. The use of the BCG vaccine then became the prevalent strategy to combat human TB in the world (1). Although the vaccine has proven effective against severe forms of childhood TB and miliary TB (an extrapulmonary form of TB characterized by wide dissemination) (2), its efficacy varies widely against pulmonary TB, the most prevalent form of the disease in adults (3).

The introduction of first-line anti-mycobacterial drugs (antibiotics such as streptomycin, and chemotherapy such as isoniazid, ethambutol and pyrazinamide) in the late 1940s revolutionized TB treatment, and caused astonishing decreases in mortality rates worldwide (4). However, resistance to these drugs was observed soon after their introduction (5) and by the end of the 1960s, the antibiotic rifampicin had to be added to the anti-mycobacterial drug cocktail. This combination of drugs appeared so promising that the "TB plague" was widely considered resolved (6). In 1969, the medic chief of the National Institute of Health declared that "it was time to close the books about infectious diseases" (4), which led to a decline in funding and interest in TB control programs (7). This false sense of security and ensuing lack of precautionary measures culminated in the reemergence of TB in the 1980s at the cost of many more millions of lives.

Besides the lack of rigor from health authorities, the reemergence of TB has been attributed to several factors such as; the HIV/AIDS pandemic, the aging of the world population, and the increase in world travel, including immigration, from countries of high TB prevalence to developed nations. Social inequalities that generate poverty, malnutrition and unsanitary living conditions are also major contributing factors (8). With the arrival of HIV, improperly administered two-drug therapies were not sufficient to fight TB. For the first time, the world was facing both mycobacterial resistance to antibiotics and a pathogen of unprecedented strength.

Multidrug-resistant TB (MDR-TB), primarily caused by the inappropriate use of antibiotics, is a strain of *M. tuberculosis* that does not respond to the two most effective first-line anti-TB drugs, isoniazid and rifampicin (WHO). MDR-TB is treatable and curable but requires

extensive chemotherapy with second-line drugs such as aminoglycosides, fluoroquinolones and thioamides. The emergence of MDR-TB is of great concern since second-line drugs are difficult to procure to developing countries, are more expensive, and more toxic than first-line drugs. Treatment can also take up to two years with severe adverse effects in patients (9). The MDR-TB strain is found in all countries surveyed (Figure 1).

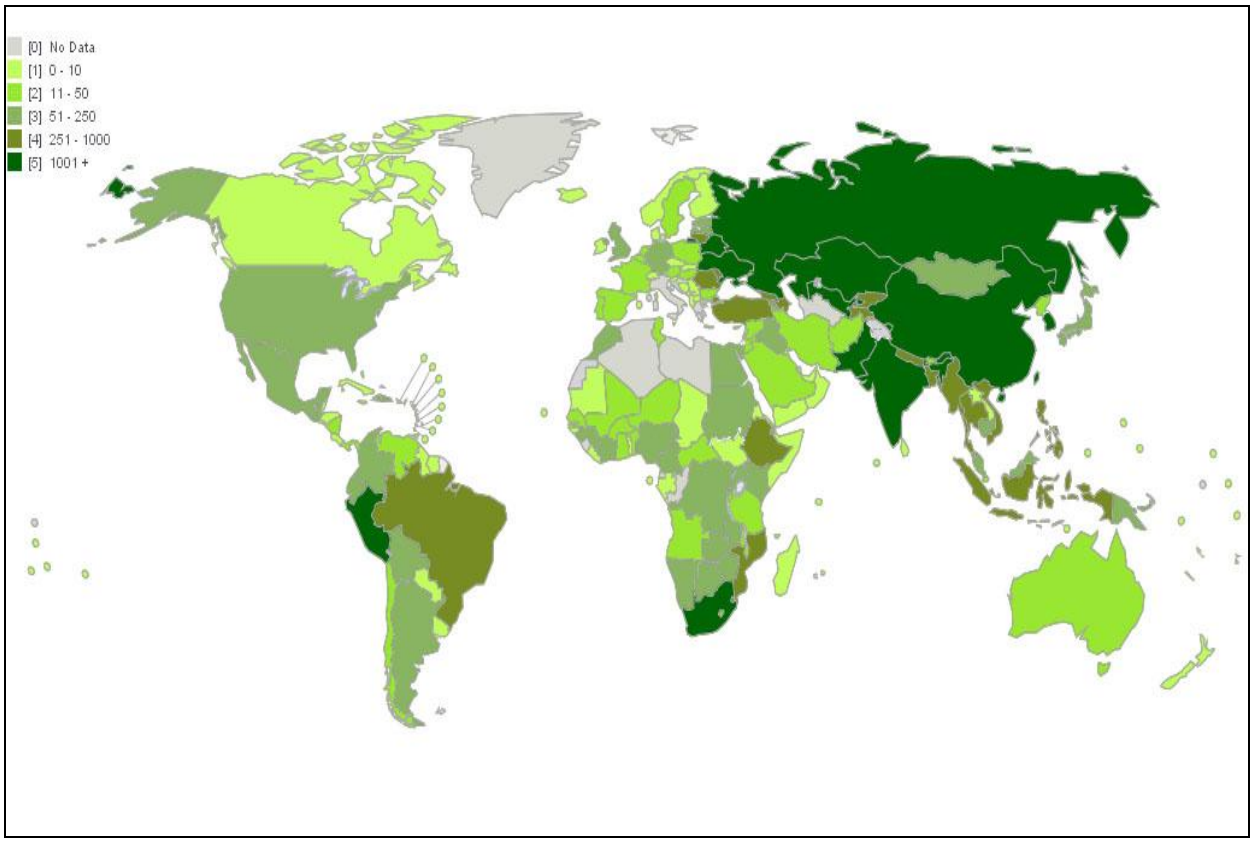

World Health Organization. Global Tuberculosis Control 2012. Reprinted with permission from World Health Organization.

Figure 1. Diagnosis and Notification of Multidrug-Resistant TB (2012)
Worldwide distribution of MDR-TB with the highest incidence rate in South Africa, the Russian Federation, India, and eastern European and central Asian countries with over 1001 cases identified (10).

Extensively drug-resistant TB (XDR-TB) is resistant to the two most powerful first-line anti-TB drugs (isoniazid and rifampicin), flouoroquinolones and at least one of the second-line anti-TB drugs (amikacin, kanamycin or capreomycin) (WHO). XDR-TB developed from MDR-TB as a result of the misuse or mismanagement of second-line drugs. Because of the resistance of XDR-TB to both first- and second-line anti-TB drugs, options for treatment are limited and the likelihood of success is much smaller than in patients with drug-susceptible TB or even with MDR-TB (WHO).

The combination of co-infection with HIV and the emergence of multidrug-resistant strains due to patient non-compliance pose a significant challenge to treating TB and increasing the survival rate. Despite intensive efforts to reduce the incidence of TB, no new anti-mycobacterial drugs had been deployed since the mid 1960s (11). However, in 2005, screening efforts led to the discovery of a novel molecule with anti-mycobacterial properties (12). This compound, now commercially known as bedaquiline, targets the *M. tuberculosis* proton pump Adenosine Triphosphate (ATP) Synthase and is reported to treat MDR-TB when administered in conjunction with second-line drugs (12). Due to the promising outcome of its use, bedaquiline was granted accelerated approval by the United States Food and Drug Administration in 2012 to treat MDR-TB (WHO). However, information regarding the safety of this new drug remains limited (WHO) and research focused on understanding the mechanism of action of *M. tuberculosis* should be a top priority in order to open new avenues for pharmaceutical interventions to treat TB.

1.1.2 Origin of Human Tuberculosis

In 1882, Dr. Robert Koch proved that the acid-fast bacillus *M. tuberculosis* causes TB (4). TB is caused by the highly virulent human pathogen *Mycobacterium tuberculosis* (*M. tuberculosis*). There is evidence of TB occurring in Ancient Egypt and the pre-Columbian societies of Central and South America as it has been identified in Egyptian and Peruvian mummies, a testament to the enduring threat it poses to every human society (13,14).

M. tuberculosis is a member of the *Mycobacterium tuberculosis* complex (MTBC). This complex includes the closely related species *M. bovis*, *M. microti*, *M. africanum* and *M. canettii* (15), which share 99.9% similarity at the nucleotide level in their genomes and identical 16S rRNA (16,17). Due to their extreme homogeneity, it is believed that the members of the MTBC are the clonal progeny of a single successful ancestor of the tubercle bacilli from East Africa approximately 3 million years ago (18). This indicates that our hominid ancestors may well have suffered from TB. It is surmised that clonal expansion took place only recently, following an evolutionary bottleneck that occurred 20,000 to 35,000 years ago, which gave rise to what we now know as the members of MTBC (17,19,20).

Despite their unusual high degree of conservation in housekeeping genes, and based on the assumption that they are all derived from a common ancestor, mycobacteria differ widely in phenotypic characteristics, including host preferences and pathogenicity (18). *M. tuberculosis*, *M. africanum* and *M. canettii* are exclusive human pathogens, whereas *M. microti* is a rodent pathogen, and *M.* bovis is a pathogen infecting a variety of hosts including cattle and man (19). These differences arise from genomic variations stemming from successive loss of DNA that

took place before the expansion of the *M. tuberculosis* clone (18,21), conferring the strains to a more or less pathogenic state and different host specificity (22). Furthermore, genomic studies show that *M. tuberculosis* is the direct descendant of tubercle bacilli that existed before clonal expansion (19) indicating that this common ancestor was already a human pathogen.

1.1.3 *Mycobacterium tuberculosis*

M. tuberculosis is a slow growing, aerobic facultative intracellular bacterium of the *Actinomycetales* order and *Corynebacterineae* suborder. It is an airborne pathogen that preferentially colonizes the respiratory system. In infected alveolar macrophages, *M. tuberculosis* normally goes into a dormant state as long as the immune system of the host predominates (23).

The genome of *M. tuberculosis* has a high G + C content of 65.6%, relative to *E. coli* (GC content ~ 50%), and contains approximately 4,000 genes. A genomic feature differentiating *M. tuberculosis* from other bacteria is its large amount of genes coding for fatty acid metabolic enzymes (about 250 genes in *M. tuberculosis* compared to 50 genes in *E. coli*, which has a similar genome size) (24). This unique characteristic of the tubercle bacillus confers it a complex cell envelope that is distinguished from the cell wall of Gram-positive and Gram-negative bacteria. Indeed, beyond the peptidoglycan, its envelope contains an additional layer exceptionally rich in unusual lipids, glycolipids and polysaccharides such as mycolic acids, mycocerosic acid, lipoarabinomannan, arabinogalactan and phenolthiocerol (Figure 2) (25,26). This thick lipid-rich coat contributes to host inflammatory reactions and forms a permeability barrier preventing entry of environmental solutes (27). This confers *M. tuberculosis* with high

intrinsic resistance to antibiotics and host antimicrobial mechanisms (28). Besides this highly hydrophobic cell wall, *M. tuberculosis* has gained resistance to antibiotics with mechanisms such as hydrolytic or drug-modifying enzymes and drug-efflux systems (25). Taken together, these unique features of *M. tuberculosis* contribute to "successful" infection and survival within the extremely hostile environment of the host macrophage.

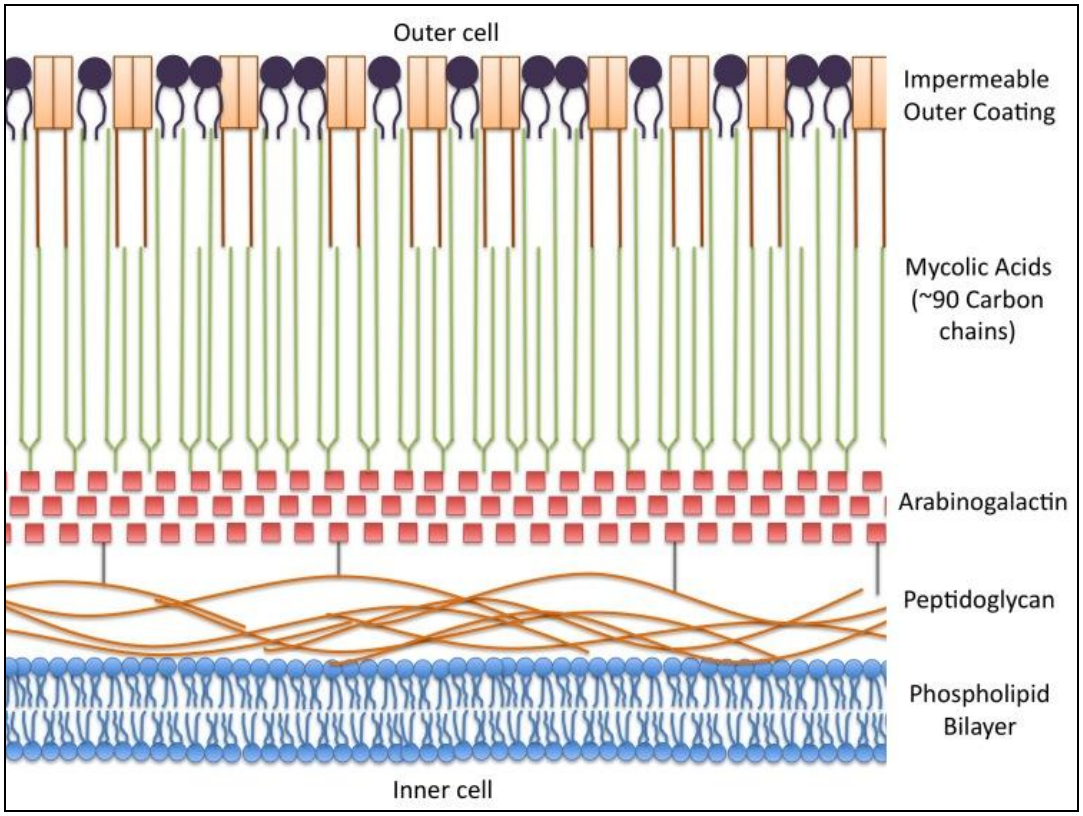

Smith. Yale J Biol Med. 2011. 84 (4): 361-369. Reprinted with permission from Elsevier.

Figure 2. Schematic Representation of the Mycobacterial Cell Wall
This illustration shows the cell wall of *M. tuberculosis* comprising of several layers of diverse cell wall lipid types ranging from simple fatty acids to complex long-chain lipids such as mycolic acids. The outer layers surround the traditional phospholipid bilayer of the cell.

1.2 Phagocytosis

1.2.1 Phagosome Formation and Maturation

M. tuberculosis infects the human lung and is internalized by circulating alveolar macrophages; the cells that provide the first line of defence against mycobacterial invasion (29). Macrophages, along with neutrophils and dentritic cells, are professional phagocytes. They phagocytose large particles, including microorganisms, destroy them and, if required, illicit an immune response by promoting antigen presentation that activates an adaptive immune response (30).

Phagocytosis occurs via the simultaneous recognition of pathogen-associated molecules by pattern recognition receptors or by opsonins; host factors, such as antibodies or complement proteins, that attach to the pathogen membrane allowing it to be recognized by phagocytic receptors (Figure 3) (30,31). The best characterized phagocytic receptors involved in the phagocytosis of *M. tuberculosis* are the Fc gamma receptor (FcγR), the mannose receptor and the complement receptor 3 (CR3).

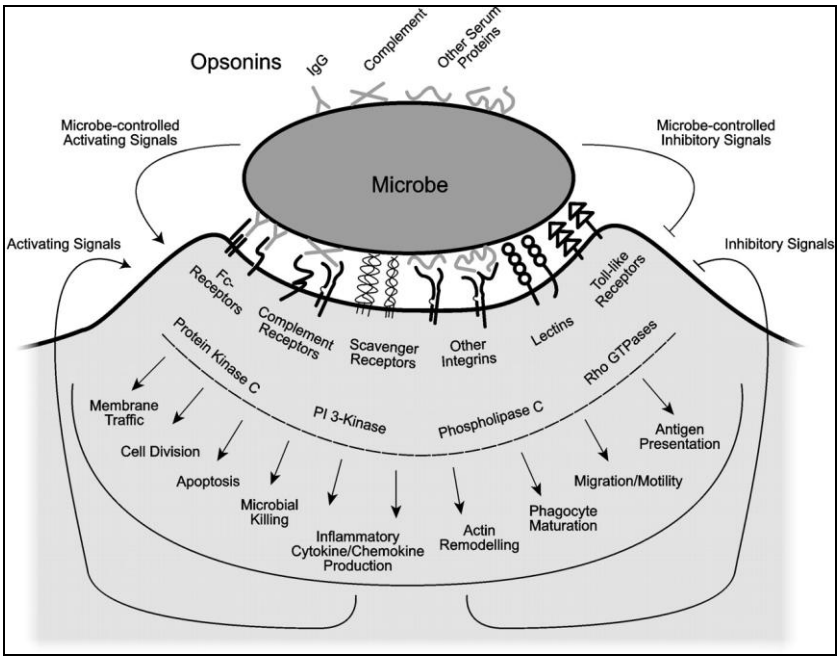

Underhill *et al*. Annu. Rev. Immunol. 2002. 20: 825-52. Reprinted with permission from Annual Reviews.

Figure 3. Receptor and Signalling Interactions During Phagocytosis of Microbes
Phagocytosis of the invader is initiated by the simultaneous binding of several pattern-associated molecules and opsonins to multiple host receptors. This binding causes a signalling cascade leading to phagocytosis and various other responses.

The FcγR binds to the Fc region of immunoglobulin G (32). It plays an important role in inducing phagocytosis and acting as a link between cellular and humoral branches of the immune system (33). The mannose receptor, expressed on the surface of tissue macrophages (34), mediates endocytosis and phagocytosis of microorganisms that express mannose-rich cell walls (35) such as *M. tuberculosis*. Lastly, the CR3 is a versatile receptor capable of recognizing diverse ligands (36). For instance, the CR3 binds to endogenous ligands such as extracellular matrix and coagulation proteins, and to glycoconjugates of pathogens such as *M. tuberculosis* lipopolysaccharides. Interactions with these ligands contribute to the host recognition of these

microorganisms and their clearance (37-39). These receptors work synergistically to augment their activity and trigger phagocytosis of the pathogen (40).

Upon phagocytosis, *M. tuberculosi*s is trapped within an organelle called a phagosome. Phagosomes are derived from the plasma membrane and must acquire microbicidal features, characteristic of innate immunity, to kill and digest the engulfed microbe (41). This process is known as phagosome maturation and includes fusion and fission events with compartments of the endocytic pathway, i.e. the route undertaken by vesicles derived from the plasma membrane to deliver their contents to lysosomes for degradation (30). As illustrated in Figure 4, phagosomes containing foreign particles, including invading microorganisms, interact with the endosomal pathway allowing for the exchange of endocytic solute materials and membrane components between the phagosomes and the endosomes. This results in the acidification of the phagosomes through the acquisition of vacuolar H^+-ATPase pumps (V-ATPase) and proteolytic enzymes (lysosomal hydrolases) (42). These fusion events modify the function of the phagosome to reflect the content of the lysosome (42). Moreover, they initiate the production of reactive oxygen intermediates and the processing of antigens for degradation of the organism (43).

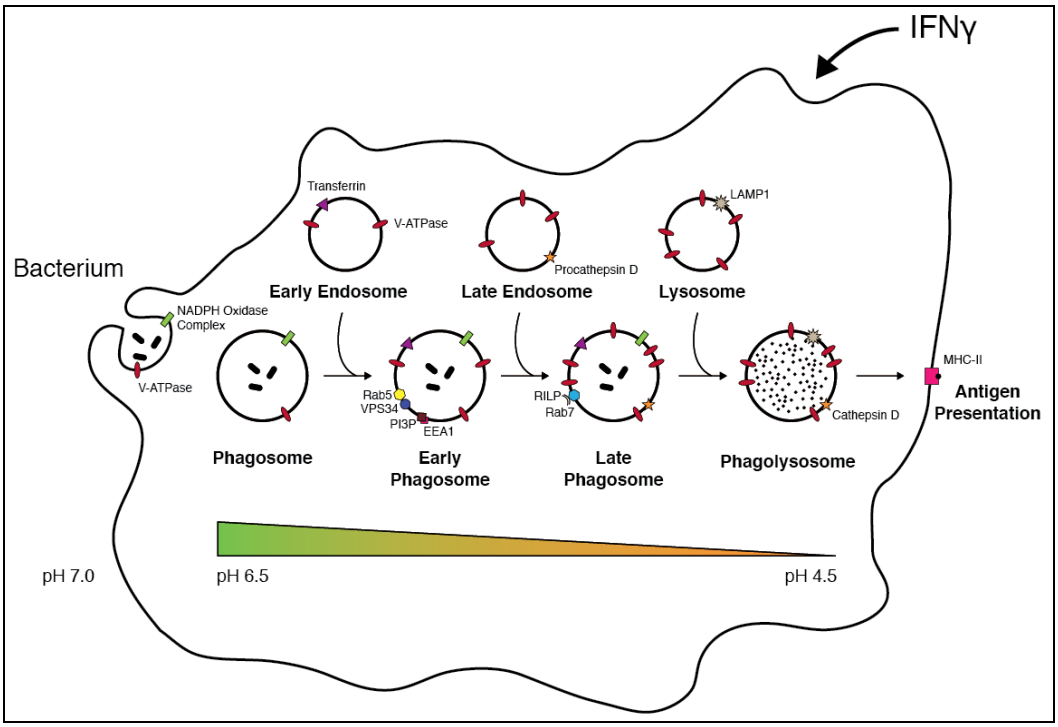

Poirier and Av-Gay. Microbes and Infection. 2012. 14 (13): 1211-1219. Reprinted with permission from Elsevier.

Figure 4. Stages of Phagosome Maturation Exemplified by *E. coli* Infection
Upon phagocytosis, the phagosome undergoes a series of fusion and fission events with vesicles of the endocytic pathway culminating in the formation of the phagolysosome. During this maturation, the phagosome acquires antimicrobial properties such as an acidic pH and a high concentration of hydrolytic enzymes. These events lead to the digestion of the invader and presentation of antigens on the surface of the phagocyte to initiate an adaptive immune response.

1.2.2 Inhibition of Phagosome Maturation by *M. tuberculosis*

Interference with host cellular pathways is a common trait of bacterial pathogenesis. For instance, once internalized, *Listeria monocytogenes* blocks the fusion of the phagosome with lysosomes and escapes the phagosome by secreting exotoxins LLO, PlcA and PlcB (44). *Salmonella enterica*, by contrast, activates acid tolerance genes allowing it to adapt to the low phagosomal pH (45). Lastly, *Legionella pneumophila* redirects phagosome maturation by altering maturation of the endocytic vesicle in which it resides. Rather than fusing with early

endosomes, late endosomes and lysosomes, phagosomes containing *L. pneumophila* fuse with membranes derived from the endoplasmic reticulum creating a niche suited for bacterial replication (46).

M. tuberculosis is also able to circumvent the macrophage killing machinery by inhibiting phagosome maturation and preventing the process of phagosome fusion with lysosomes (Figure 5). Armstrong and Hart (47) were the first to report on phagosome maturation arrest in macrophages infected with *M. tuberculosis*. They showed by electron microscopy that approximately 70% of phagosomes containing *M. tuberculosis* did not fuse with lysosomes (47). The blockage of phagosome maturation allows *M. tuberculosis* to avoid proteolytic degradation and antigen presentation required to initiate an adaptive immune response (47). Phagosomes containing *M. tuberculosis* are therefore characterized by the absence of several phagosomal markers: the V-ATPase pump (43), hydrolases such as cathepsin D (48,49), the small GTPase RAB7 (50,51) and lysosomal markers such as Lysosomal Associated Membrane Protein (LAMP) and Rab-Interacting Lysosomal Protein (RILP) needed for phagosome-lysosome fusion (52,53). The absence of phagosomal markers in *M. tuberculosis* infected macrophages indicates that active interference with macrophage trafficking events occurs within the majority of phagosomes containing *M. tuberculosis*.

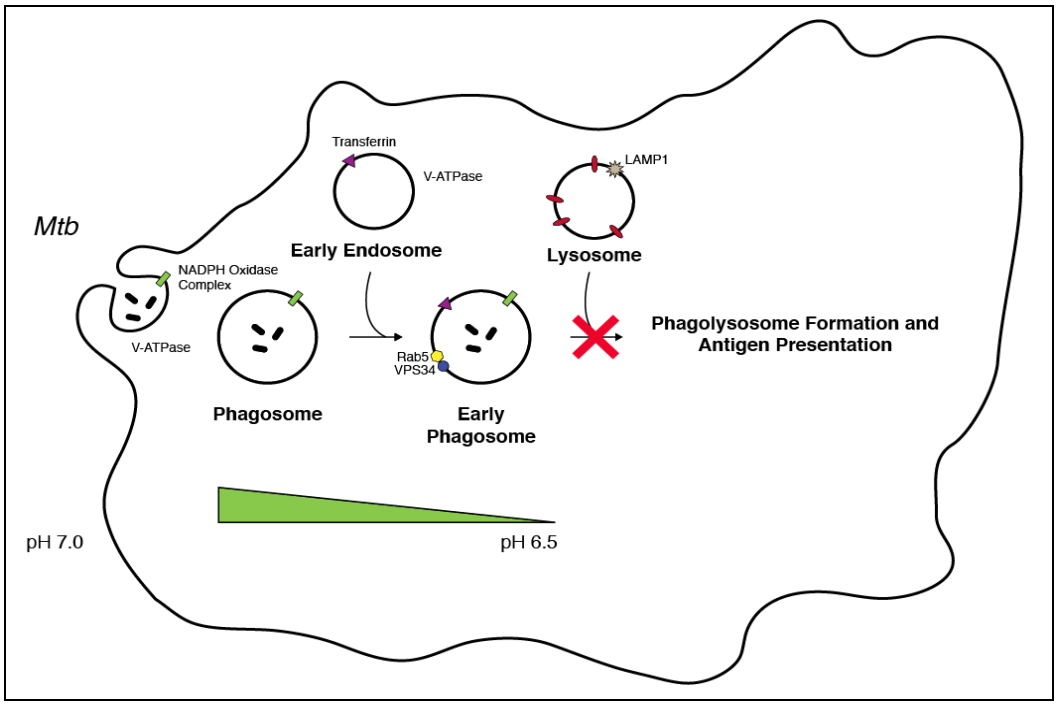

Poirier and Av-Gay. Microbes and Infection. 2012. 14 (13): 1211-1219. Reprinted with permission from Elsevier.

Figure 5. Blockage of Phagosome Maturation by *M. tuberculosis*
The fusion of the early endosome with the late endosome is inhibited by *M. tuberculosis*. The resulting phagosome lacks several markers required for phagolysosome formation, has a relatively neutral pH and contains few hydrolytic enzymes required for the pathogen degradation. *M. tuberculosis* remains intact in the phagosome.

1.2.2.1 Biological Effectors Mediating *M. tuberculosis* Survival in Macrophages

As a result of phagosome maturation arrest by *M. tuberculosis*, infected macrophages undergo impaired antigen processing and presentation (54), reduced responsiveness to interferon-gamma (IFNγ) (55), reduced production of cytokines, reactive oxygen and nitrogen intermediates (56), and suppression of host cell apoptosis (57). Attenuation of the host cells is attributed to an array of *M. tuberculosis* effectors composed of proteins, glycopeptides and lipids described below.

1.2.2.1.1 LAM

Lipoarabinomannan (LAM) is a major lipoglycan component of the *M. tuberculosis* cell wall (Figure 2) contributing to bacterial survival in the phagosomal milieu. LAM includes three types of lipoglycans classified according to the presence and structure of the capping motif: mannosylated LAM (ManLAM), phosphoinositol-capped LAM (PiLAM) and arabinofuranosyl-terminated LAM (AraLAM) (58). ManLAM is found in pathogenic mycobacterial species (e.g. *M. tuberculosis*, *M. leprae* and *M. bovis*) whereas PiLAM and AraLAM are mainly found on non-pathogenic mycobacterial species (59).

ManLAM is considered to be a key contributor to host-mycobacteria relationships by possessing immunomodulatory activities. Its main role is the inhibition of calcium (Ca^{2+}) concentration rise in macrophages upon infection, leading to interference with phagosome maturation (60). Ca^{2+} serves as an essential cell signalling molecule, especially for the phagosome maturation process (60). ManLAM specifically blocks the Ca^{2+} rise and interferes with a sorting pathway that delivers lysosomal hydrolases and V-ATPases from the *trans*-Golgi network (TGN) to the phagosome (61). ManLAM also inhibits the Ca^{2+}/calmodulin PI3K hVPS34 (human Vacuolar Protein Sorting protein 34) pathways and blocks the syntaxin 6-dependent delivery of cargo from the TGN to the early endosome (62).

Upon phagocytosis of a pathogen, intracellular Ca^{2+} concentration normally rises leading to the recruitment of the early endosomal marker, the small GTPase RAB5, to the phagosomal membrane. RAB5 facilitates fusion events between early and late organelles of the endocytic pathway (63). RAB5, along with calmodulin (CaM) and its effector Ca^{2+}/CaM kinase II

(CaMKII), recruit type III PI3K VPS34 to the phagosomal membrane (64). PI3K VPS34 is essential for the production of the lipid regulator phosphatidylinositol 3-phosphate (PI3P) on the phagosomal membrane (65). PI3P serves as a membrane tag that signals phagosomes to mature down the phagolysosome biogenesis pathway (62) and affects localization and function of proteins containing PI3P-binding domains (FYVE zinc finger, PH and PX). Proteins containing these domains are involved in membrane trafficking, endosomal protein sorting, multisubunit enzyme assembly at the membrane and fusion (66). One protein containing the FYVE domain is Early Endosome Antigen-1 (EEA1), which is a tethering molecule and a RAB5 effector essential for fusion of early and late endosomes (62). Its FYVE domain binds to PI3P causing membrane fusion by interacting with a family of proteins termed SNARE (Soluble N-ethylmaleimide-sensitive factor Attachment protein REceptor) composed of syntaxin 6, syntaxin 13 and additional elements such as the priming factor NSF and alpha-SNAP (67). SNARE proteins drive fusion of membranes (67) and interaction between PI3P and SNAREs cause early endosomes to fuse with late endosomes allowing for the delivery of the endosomal cargo between them (68).

Phagocytosis of *M. tuberculosis* results in a decrease in Ca^{2+} level in the macrophage by an unknown mechanism (60) and is linked to the mycobacterial inhibition of the Ca^{2+} effector protein CaMKII (69). This inhibition hinders the recruitment of PI3K VPS34 to the phagosomal membrane, the production of PI3P via the PI3K dependent pathway and the subsequent recruitment of EEA1, which drives fusion of early and late endosomes (Figure 6) (61,64). Although studies have shown that ManLAM is behind the blockage of intracellular Ca^{2+} rise leading to phagosome maturation arrest, it is still not known how ManLAM prevents intracellular Ca^{2+} levels from rising.

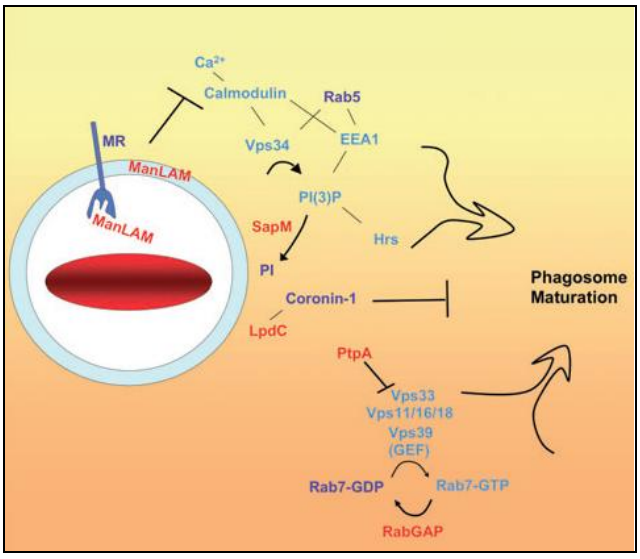

Philips. Cell Microbiol. 2008. 10 (12): 2408-15. Reprinted with permission from John Wiley and Sons.

Figure 6. Inhibition of Phagosome Maturation by *M. tuberculosis* Effectors
Mycobacterial effectors (depicted in red) impair different pathways by diminishing or inhibiting activity of host proteins (shown in blue) required for phagosome maturation. The cell wall glycolipid ManLAM and the PI3P phosphatase SapM interfere with the recruitment of EEA1 to and the production of the phagosomal membrane protein PI3P at the mycobacterial phagosome. The secretion of PtpA dephosphorylates VPS33B impairing membrane fusion between the phagosome and the lysosome.

1.2.2.1.2 SapM

Prior to the discovery of SapM in *M. tuberculosis*, acid phosphatases were thought to play a role in microbial pathogenicity (70,71). Saleh *et al.* (72) isolated a 28-kDa protein from *M. tuberculosis* culture filtrate and characterized it as acid phosphatase SapM, for secreted acid phosphatase of *M. tuberculosis*. SapM functions in an acidic-to-neutral pH range (70); the optimum pH for enzymatic hydrolysis of the artificial protein-tyrosine phosphatase substrate *p*NPP (*p*-nitrophenyl phosphate) was observed at pH 6.5-7.5 (72) by quantitation of released *p*NP (*p*-nitrophenol) (73) and P_i (74).

SapM was the first mycobacterial acid phosphatase to be identified and it appears to be the only one secreted by *M. tuberculosis*. Vergne and colleagues observed that SapM takes an active part in preventing *M. tuberculosis* phagosome maturation. They found that the exclusion of the membrane tag PI3P from phagosomes was only partly explained by the decrease in Ca^{2+} levels (75) and that SapM hydrolyzes the phagosomal membrane protein PI3P to PI (Figure 6) (75). They concluded that SapM dephosphorylation of PI3P prevents the recruitment of EEA1 to the phagosomal membrane and the fusion of phagosomes with late endosomes (75). Vergne *et al*. (75) also tested whether intracellular Ca^{2+} levels can restore PI3P levels on phagosomes containing live mycobacteria. They found that despite the Ca^{2+} rise, a transient spike in PI3P levels occurs in only 10% of all phagosomes observed. This indicated that reduced Ca^{2+} levels alone are not sufficient to explain the reduction of PI3P levels on mycobacterial phagosomes and reinforces the role of SapM in phagosome maturation arrest (75). To accomplish complete arrest, *M. tuberculosis* maintains a PI3P-free environment during its long-term stay in infected macrophages (60,75). Thus, in addition to ManLAM, a second mycobacterial macromolecule, SapM, is required for complete inhibition of PI3P accumulation at the phagosomal membrane, impeding EEA1 recruitment and fusion with late endosomes (75).

The role of SapM in infection remains a conundrum as it is found to be secreted into the lumen of the phagosome but the mechanism by which it gains access to the cytoplasmic face of the phagosome where it hydrolyzes PI3P is unknown (75). It is predicted that SapM contains an export signal allowing it to be exported to the cytosol. Nevertheless, SapM was experimentally proven to directly interfere with host cellular pathways by hydrolyzing host PI3P into PI, resulting in phagosome maturation arrest (75,76).

1.2.3 Inhibition of Antigen Processing and Presentation

As a result of phagosome maturation arrest, *M. tuberculosis* is able to alter antigen processing and presentation and evade the host adaptive immune response. Major histocompatibility complex class II (MHC-II) molecules loaded with bacterial antigenic peptides, the products of bacterial digestion in phagolysosomes, traffic to the cell surface and present specific *M. tuberculosis* antigens to helper T cells, which initiate an adaptive immune response. Once the antigens are presented to helper T cells, the proinflammatory cytokine IFNɣ is secreted to activate infected macrophages by inducing a microbicidal response through the generation of reactive oxygen and nitrogen species, and by further amplifying antigen processing and presentation (77). IFNɣ plays a crucial role in activating an immune response and controlling macrophage infection by increasing the expression of MHC-II molecules and accessory molecules required for antigen presentation (78). Interestingly, upon binding to Toll-like receptor 2 (TLR2) located on macrophages, *M. tuberculosis* triggers a potent proinflammatory immune response early during infection. In later stages of infection, the proinflammatory response results in inhibition of antigen processing and presentation. It has been shown that this inhibition of the proinflammatory response is required to combat the infection (79).

1.2.3.1 19 kDa Lipoprotein

The *M. tuberculosis* cell wall 19 kDa lipoprotein (LpqH) is identified as a pathogen-associated molecular pattern (PAMP) protein (79,80). The function of LpqH in *M. tuberculosis* grown *in vitro* and its biological activity are not yet identified, but it is proposed to have a role as an antigenic modulator of host immune processes (79). LpqH is shown to bind to the macrophage TLR2 and selectively inhibit IFNγ induction of the CIITA gene, the MHC-II gene

and accessory protein genes required for antigen presentation (81,82). CIITA, the MHC-II transactivator, regulates the expression of genes encoding MHC-II molecules and other genes involved in antigen processing and presentation by promoting the binding of transcription factors to the *MHC-II* promoter (82). Upon binding to TLR2, LpqH elicits a proinflammatory immune response in the host. This immune response helps combat infection by inducing expression of cytokines, bacterial killing and apoptosis (83). Interestingly, LpqH seems to have a pleiotropic effect on the immune system, i.e. its presence results in the activation of an immune response contributing to host defence, but also results in the inhibition of a subset of IFNγ responsive genes leading to persistence of the infection (84). However, over a prolonged period of time some of these proinflammatory innate immune responses are downregulated to limit damage to surrounding tissues (82).

The mechanism by which LpqH inhibits expression of MHC-II and antigen processing and presentation remains unclear. It is known, however, that the inhibition is dependent on TLR2 and Mitogen-Activated Protein Kinase (MAPK) signalling (p38 and/or ERK) (85), and that the expression of CIITA is suppressed (81,85). Chromatin remodeling has been suggested to be responsible for the inhibition of a subset of IFNγ-induced genes by *M. tuberculosis*, since CIITA expression is dependent on changes in chromatin structure (82,85).

Eukaryotic DNA transcription is controlled by chromatin structure wrapped around histones. Unstructured histone tails can be targeted for post-translational modifications (such as phosphorylation, methylation and acetylation) that modulate gene transcription. Histone acetylation is a transcription activator and it was observed that *MHC2TA*, the gene encoding

CIITA, is silenced by deacetylation of histone in response to LpqH (86). Pennini and colleagues (85) showed that *CIITA* promoter activity is inhibited by LpqH by a mechanism that involves inhibition of chromatin remodeling in a TLR2- and MAPK-dependent manner. They also showed that IFNγ-induced acetylation of histones H3 and H4 was inhibited by LpqH. This indicates that the inhibition of chromatin remodeling and histone acetylation at the *CIITA* promoter accounts for the inhibition of CIITA mRNA expression (85). Two models were developed by the same group in order to explain the inhibition of chromatin remodeling by LpqH. One model involves the reduced expression of histone acetyl transferase (HAT), known to catalyze acetylation of histones H3 and H4, and/or an increased expression of histone deacetylase (HDAC) that suppresses transcription through the deacetylation of histones. LpqH is proposed to inhibit the expression/activity of HAT required at the *CIITA* promoter or increase the expression/activity of HDAC that regulates the *CIITA* promoter (85). The second model involves inhibiting the recruitment of certain transcription factors (e.g. Brahma-related gene-1 - Brg1) or the activation of CIITA repressors (85). Regardless of the mechanism, LpqH inhibits CIITA expression via TLR2 and MAPK signalling resulting in deacetylation of histones, a loss of chromatin remodeling and a decrease in subsequent expression of MHC-II and accessory molecules (85). Additional studies are required to confirm the exact mechanism of inhibition.

1.3 PtpA

1.3.1 Overview

Upon macrophage infection, *M. tuberculosis* actively expresses a low molecular weight phosphatase, named Protein-tyrosine phosphatase A (PtpA), which was shown to play an essential role in *M. tuberculosis* pathogenicity (87). PtpA is secreted into the macrophage's

cytosol (87) where it interferes with and disrupts key components of the macrophage endocytic pathway. PtpA blocks phagosome acidification and maturation via interaction with V-ATPase subunit H and dephosphorylation of VPS33B, respectively (Figure 6) (76,88).

1.3.2 VPS33B and the HOPS Complex

Vacuolar Protein Sorting 33B (VPS33B), a substrate of PtpA within human macrophages, is a key cytoplasmic, peripheral membrane protein ubiquitously expressed in eukaryotic cells (76). VPS33B is recruited from the cytosol and, along with three other vacuolar sorting proteins (VPS11, VPS16 and VPS18), forms what is known as the Class C complex (89). The Class C complex binds two additional proteins (VPS39 and VPS41) forming the HOPS (HOmotypic fusion and vacuole Protein Sorting) complex, a large multimeric tethering factor essential for vesicle fusion (Figure 7) (90). The HOPS complex is localized to the phagosomal membrane where it is required for phagosomal trafficking to the lysosome (91). It is needed during the tethering and docking stages of vesicle fusion between phagosomes and lysosomes (92) where it plays a role in regulating the assembly of SNAREs, and cytosolic or membrane-bound proteins required in several membrane fusion steps in secretory and endocytic pathways (93-95), through interaction with endolysosomal Rab GTPases (96,97). Specifically, the HOPS complex associates with GTP-RAB7 through the interaction of VPS39 and VPS41 to promote tethering, SNARE-mediated membrane fusion of the phagolysosome and degradation of the pathogen (98). These interactions permit the exchange of cytosolic contents and subsequent degradation of the invader (99).

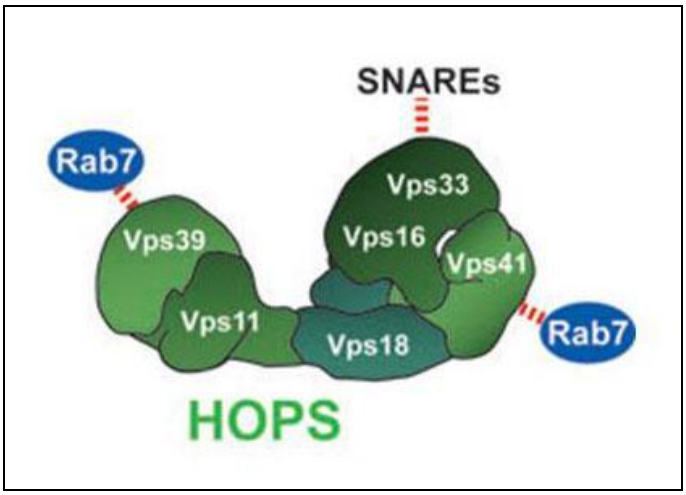

Solinger and Spang. FEBS J. 2013. 280 (12): 2743-57. Reprinted with permission from John Wiley and Sons.

Figure 7. Subunit Arrangement of the HOPS Complex
The organization of the HOPS complex according to Brocker *et al*. (100). The HOPS complex regulates membrane fusion events at lysosomes through interaction with RAB7 and SNAREs.

Recently, studies from our laboratory showed that *M. tuberculosis* PtpA interferes with the process of phagosome-lysosome fusion by dephosphorylating VPS33B (76). VPS33B dephosphorylation blocks the assembly of the HOPS complex and prevents its interaction with RAB7 and SNAREs. To support this finding, phagosomes harboring a *M. tuberculosis* mutant (where PtpA was deleted; Δ*ptpA*) were shown to undergo increased fusion with lysosomes and increased transfer of lysosomal contents when compared to phagosomes containing the parental strain, H37Rv *M. tuberculosis* (76). Therefore, dephosphorylation of VPS33B inhibits fusion between the phagosome and the lysosome allowing *M. tuberculosis* to survive and grow within the enclosed and protected environment of the phagosome (76).

1.3.3 Subunit H of the V-ATPase Pump

The V-ATPase pump is key to the cell's ability to combat infections. V-ATPase controls phagosome acidification by transporting protons across phagosomal membranes (101). During phagosome maturation, lysosomes extend along microtubules to fuse with and deliver the V-ATPase to the phagosome where the proton pump recruits the HOPS complex to allow for phagolysosome fusion (102). This fusion generally results in a reduction in phagosomal pH from 6.5 to approximately 4.5, and in the activation of hydrolytic enzymes required to eliminate pathogens (103).

Studies from our laboratory showed that *M. tuberculosis* PtpA binds to subunit H of the V-ATPase pump, which brings PtpA in close proximity to VPS33B (Figure 8) (88). PtpA then dephosphorylates VPS33B and prevents the formation of the HOPS complex required for proper phagolysosome fusion and pathogen elimination (88). Since PtpA is responsible for disrupting the interaction between V-ATPase and the HOPS complex, dephosphorylation of VPS33B by PtpA occurs as a consequence of PtpA binding to subunit H (88). Hence, the inhibition of the phagolysosome fusion and phagosome acidification is dependent on both PtpA phosphatase activity (dephosphorylation of VPS33B) and its ability to bind to subunit H of V-ATPase (88).

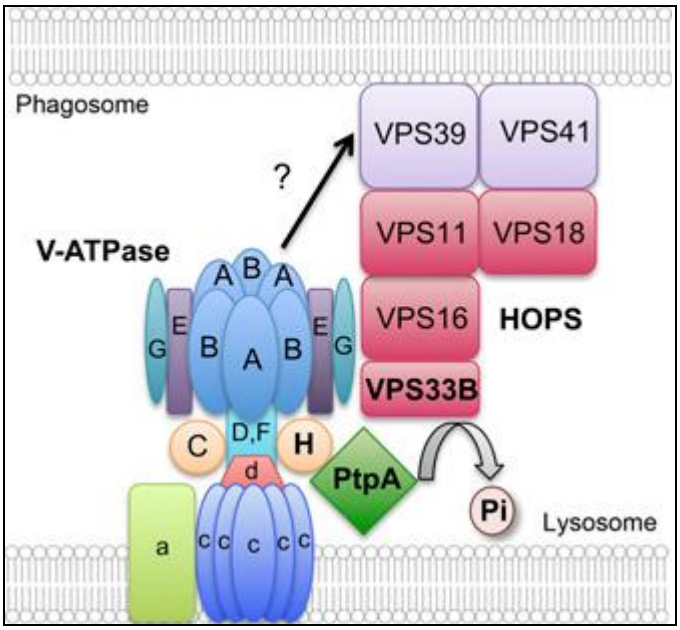

Wong *et al.* Trends in Microbiology. 2013. 21 (2): 100-109. Reprinted with permission from Elsevier.

Figure 8. Schematic Representation of V-ATPase Exclusion and Inhibition of Phagosome Acidification by PtpA
During phagosome maturation, the V-ATPase pump recruits the HOPS complex for fusion of the phagosome and lysosome membranes. PtpA, secreted into the cytosol, binds to subunit H of the V-ATPase pump and disrupts the interaction between the pump and the HOPS complex. The binding to subunit H brings PtpA in proximity to VPS33B and dephosphorylates it. This results in the shutting down of the membrane fusion machinery and a phagosome with a pH too high to activate hydrolytic enzymes for *M. tuberculosis* degradation.

1.4 Host Responses to *M. tuberculosis* Infection

1.4.1 Apoptosis Versus Necrosis

Macrophages infected with *M. tuberculosis* can undergo two types of cell death; programmed cell death (PCD) or necrosis. Apoptosis and autophagy are examples of PCD and are phenomena of widespread biological importance in which unwanted cells or damaged cellular contents are neatly removed without causing damage to tissues or initiating an inflammatory response (104,105). PCD is also an important innate defence mechanism against intracellular pathogens that prevents the spreading of infections (106,107). On the one hand,

apoptosis is regulated by a variety of cellular signalling pathways that culminate in the activation of a set of enzymes named caspases (108). Caspases are cysteine proteases that play key biological roles in the apoptotic, necrotic and inflammatory response pathways (109). Caspases are usually activated by the release of apoptotic mediators from the mitochondria or by ligation of a death receptor (108). Moreover, apoptosis is characterized by structural changes in the nucleus, such as nuclear condensation and fragmentation, chromosomal DNA cleavage, and packaging of deceased cells into apoptotic bodies whose specific morphological features are recognized by surrounding phagocytes (105,110). All of these morphological changes are achieved without the breakdown of the plasma membrane to avoid triggering an inflammatory response and damage to surrounding tissues (110). On the other hand, autophagy functions primarily as an intracellular recycling mechanism (111), which includes the sequestration of long-lived proteins and large cytoplasmic organelles into vesicular compartments followed by their delivery to lysosomes for degradation (112). The degraded metabolites are then reused by the cell for energy needs or macromolecule synthesis (111). Autophagy is triggered by various signals such as nutrient deprivation, damaged organelles, accumulated misfolded proteins, and oxidative stress (113). Autophagy can also provide cytoprotective functions to the host cell as it can be triggered by infection (113). The autophagic response then contributes to the elimination of invading pathogens (114). Several years ago, a link between autophagy activation and *M. tuberculosis* infection was revealed (115). The induction of autophagy led to a decrease in *M. tuberculosis* survival rates in infected macrophages, which indicated that the fusion of autophagosomes containing *M. tuberculosis* with lysosomes for degradation overcame the phagosome maturation block imposed by *M. tuberculosis* (115). Therefore, autophagy also acts as an important defence mechanism against pathogens (107).

Contrary to PCD, necrosis has traditionally been regarded as unorganized and disruptive cell death sharing more similarities with a train wreck than with surgical culling. Necrosis is the end result of a bioenergetic catastrophe initiated by toxic insults, ischemia or physical damage (110). Morphologically, necrosis is different from PCD and is characterized by rapid permeabilization of the membrane causing general swelling of the cell, vacuolation of the cytoplasm, loss of cell membrane integrity, and induction of inflammation due to the release of potentially toxic intracellular contents and proinflammatory molecules in the extracellular space from lysed cells (116). Unlike apoptosis and autophagy, necrosis provides detrimental effects to the surrounding cells and tissues (117).

The ability of *M. tuberculosis* to manipulate and control the mode of death of infected host cells plays an essential role in its survival and transmission. On the one hand, apoptosis of *M. tuberculosis*-infected macrophages is directly associated with mycobacterial killing (118) and with enhanced stimulation of T cell responses from antigen presentation (119). Necrosis, on the other hand, has also been observed in *M. tuberculosis* infection and serves to propagate infection. Indeed, necrosis is an essential part of the *M. tuberculosis* granuloma. The granuloma is a pathologic feature characteristic of TB and forms in later stages of infection when the immune system cannot eliminate foreign particles (77). It is characterized by the accumulation of immune cells such as infected alveolar macrophages surrounded by monocytes, lymphocytes, giant cells, neutrophils, and foamy macrophages (120,121). Lymphocytes localize to the periphery of the granuloma and associate with collagen fibers and other extracellular matrix components forming a capsule around the cells (120). At this stage, the infected human host does not show signs of disease or transmit the infection to others, and the granuloma remains an organized structure as

long as the immune system prevails over the pathogen (120). However, when the immune system fails to contain the infection (e.g. when the host becomes immunocompromised), *M. tuberculosis* reactivates and the granuloma is marked by a caseous necrotic center (121). This leads to the rupture of the granuloma into a mass of formless cell debris, releasing viable infectious bacilli into the airways and spreading of TB (121). Thus, necrosis of the granuloma represents an important mode of spreading and transmission to surrounding phagocytes for *M. tuberculosis* (122).

A fine balance exists between the two types of cell death during *M. tuberculosis* infection; one allows the host cell to have complete control of cell death leading to apoptosis and elimination of the pathogen, the other allows *M. tuberculosis* to manipulate host cell death signalling pathways leading to necrosis, transmission of the bacteria and subsequent progression of the disease (123).

1.4.2 Apoptosis During Infection with Virulent Versus Avirulent *Mycobacterium* Strains

Alveolar macrophages clear bacteria from the lungs and thus are well equipped to phagocytose and kill ingested bacteria. Several microbes have developed strategies to prevent infected macrophages from eliminating pathogens via the conventional phagolysosome route. *M. tuberculosis* is an example of a pathogen that possesses a fundamental virulence strategy to block phagosome maturation allowing it to survive and replicate inside the macrophage phagosome (29). In such instances, macrophages turn to an additional level of defence to kill the pathogen, and thus resort to apoptosis as a disposal route (124,125). Despite efforts deployed by the macrophage to eliminate the invader, some pathogens have found ways to also block

apoptosis and evade this second layer of host defence. One pathogen that has developed such an anti-apoptotic tactic is the human blood parasite *Leishmania donovani* (126).

M. tuberculosis has been shown to interfere with apoptosis in macrophages both *in vitro* and *in vivo*, and this appears to be directly related to its virulence capacity (29,125,127,128). Virulent strains of mycobacteria, such as *M. tuberculosis* H37Rv, *M. tuberculosis* Erdman and *M. bovis*, inhibit apoptosis as a virulence mechanism whereas avirulent or attenuated strains, such as *M. kansasii*, the vaccine strain *M. bovis* BCG, and the laboratory strain H37Ra, activate apoptosis (29,57,129). The ability of virulent mycobacteria to block apoptosis is of great importance for the pathogen as death of the host cell removes its supportive growth environment. Thus, mycobacterial virulence factors that modulate the apoptotic response of macrophages promote host cell survival and allow pathogen replication (29).

This model, stipulating that virulent mycobacteria inhibit apoptosis whereas attenuated or avirulent mycobacteria stimulate apoptosis, is controversial due to conflicting results obtained in several studies. Some studies have reported that the deletion of the virulent *M. tuberculosis* anti-apoptotic genes, *nuoG*, *secA2* and *ndk*, conferred a pro-apoptotic phenotype to the pathogen (130-132). Conversely, it has been reported that infection of macrophages with pathogenic *M. tuberculosis* in which the *nuoG* and *secA2* anti-apoptotic genes had been reintroduced, stimulated macrophage death by apoptosis to an extent greater than even avirulent strains (133-135). This discrepancy can be partly attributed to bacterial load, the type of host cells, periods of infection and the stimulatory milieu used in the different studies.

Moreover, recent work provides evidence that pathogenic *M. tuberculosis* does indeed have the ability to evade the host immune response by blocking apoptosis and favouring necrosis (Figure 9) (136-139). According to these studies, virulence is a determining factor in the balance between apoptotic versus necrotic cell death; virulent mycobacteria inhibit apoptosis of macrophages early in infection, but stimulate necrosis at later time points where the host cell lyses resulting in the spreading of the infection. Moreover, Butler and colleagues observed that different strains of pathogenic *M. tuberculosis* (GC1237 and H37Rv) induced equivalent levels of cell death, but caused apoptosis and necrosis in cells to a different degree, indicating that the balance between apoptotic and necrotic cell deaths could be strain-specific (140).

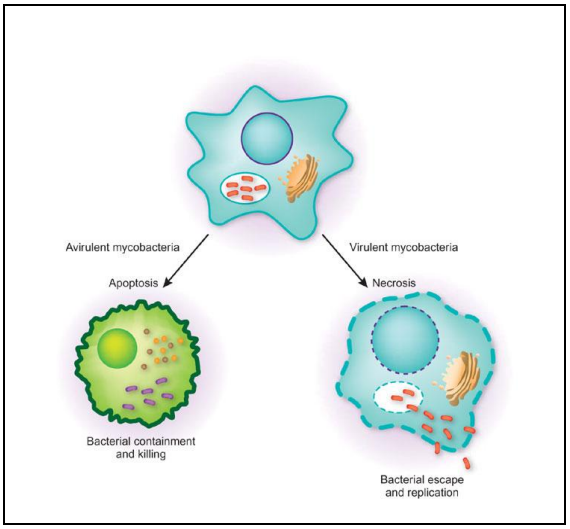

Porcelli and Jacobs. Nat Immunol. 2008. 9 (10): 1101-1102. Reprinted with permission from Nature Publishing Group.

Figure 9. Modes of Macrophage Cell Death Caused by Virulent and Avirulent Mycobacteria
Avirulent mycobacteria induce apoptosis of the host. The phagocyte sequesters the bacteria within apoptotic bodies that are taken up by surrounding macrophages. Apoptosis clears the microbial content of the phagocyte and prevents the release of toxic intracellular contents avoiding tissue inflammation. In contrast, virulent mycobacteria possess virulence factors that cause the host cell to undergo necrosis; a process that permeabilizes the phagocyte's membrane, allowing the bacteria to escape and spread to surrounding phagocytes.

A great degree of uncertainty remains in elucidating the relationship between virulence of mycobacteria and control of host cell death. It is clear, however, that macrophage cell death results from a complex meshing of pro- and anti-apoptotic stimuli partly shaped by the virulence of the invader. Other virulence-independent or anti-apoptotic mechanisms such as the binding of ManLAM and LpqH to TLR2 (141,142), the activities of NuoG (130), SecA2 (131) and Ndk (132), and the up-regulation of host anti-apoptotic proteins such as the BCL-2 family members (143), may also directly stimulate necrosis and determine the mode of death undertaken by the macrophage. Nonetheless, the detailed relationship between the control of cell death pathways and virulence of mycobacteria has yet to be characterized and it is necessary to understand how *M. tuberculosis* achieves intracellular growth while modulating host cell death to its advantage.

1.5 Techniques for Identifying Intracellular Substrates for *M. tuberculosis* Effectors During Infection

1.5.1 Phosphoproteome Analysis

Signal transduction mediated by protein kinase catalyzed phosphorylation is a key post-translational modification needed to analyze cellular phosphorylation events occurring in macrophages infected with different strains of *M. tuberculosis*. The experimental approach chosen to analyze signal transduction in this instance is a refined proteomics method, termed phosphoproteome analysis.

Phosphoproteome analysis is a large-scale Western assay that utilizes phosphosite-specific antibodies against a predefined set of key signalling proteins to identify modification events and quantify global protein kinase phosphotransferase activity in cells (144). One notable

advantage of phosphoproteome analysis is its high customizability with respect to phosphorylation events involved in specific cellular processes characterized for a particular species. The technique is usually protein phosphosite-specific and targets defined signalling proteins identified as taking active roles in major eukaryotic signalling networks (145). The assay can also be applied to protein kinases mediating cellular phosphorylation events of the cell population of interest under the desired treatment conditions. For this project, we monitored and compared the phosphorylation status of a predefined set of signalling protein kinases from cellular extracts of uninfected human macrophage-like cells and of macrophage-like cells infected with *M. tuberculosis* H37Rv and Δ*ptpA M. tuberculosis*. These modification events were verified using biochemical assays such as Western blotting.

1.5.2 iTRAQ

To understand the mechanism by which macrophages fight *M. tuberculosis* and to analyze the extent of proteomic reprogramming macrophages undergo during infection, a multiplexed peptide quantitation methodology, termed Isobaric Tags for Related and Absolute Quantitation (iTRAQ), was employed. iTRAQ is a quantitative mass spectrometry (MS)-based proteomics approach used to perform a global proteomic analysis of cellular proteins (146), in conjunction with tandem mass spectrometry (MS/MS), to identify the resultant peptides (147). iTRAQ precisely quantifies and identifies cellular proteins for quantitative protein analysis by placing isobaric mass labels on peptides in a peptide mixture (Figure 10) (147).

To better understand the evasive nature of *M. tuberculosis* and its molecular manifest on the macrophage response to infection, we conducted a global quantitative proteomic profiling of

infected macrophages. By examining four independent controlled infection experiments, we identified hundreds of proteins whose expression is modulated upon infection in all replicates. We showed that the macrophage response to *M. tuberculosis* infection mainly includes simultaneous and concerted up-regulation of proteins while the down-regulated response appears unorganized and random. The contribution of the *M. tuberculosis* secreted virulence factor PtpA was also assessed.

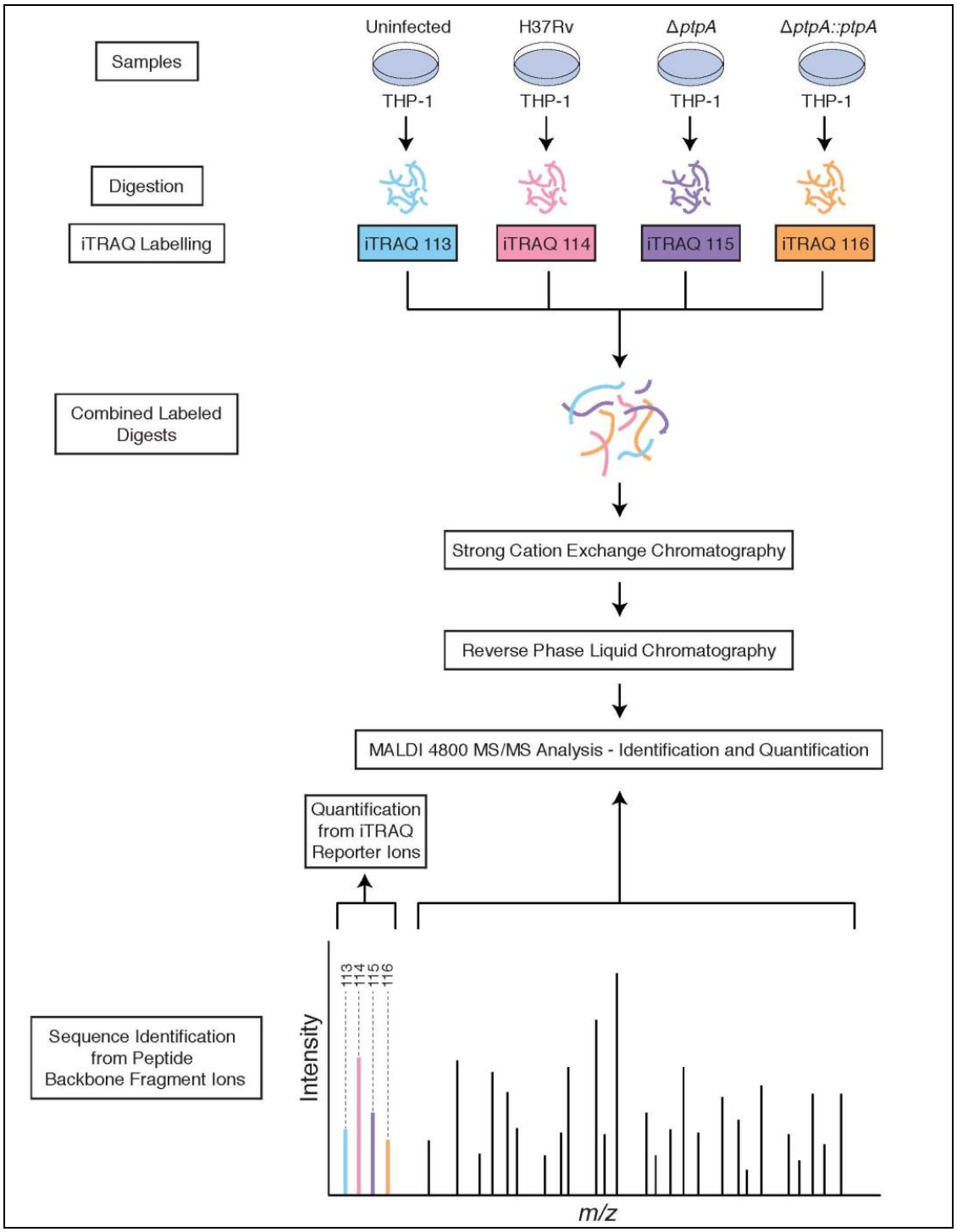

Figure 10. Sample Processing and Analysis Workflow for Global Proteome Profiling with Quantification Using Mass Tag Labeling of Peptides

Proteins derived from each sample were labeled with distinct iTRAQ labels (113-116). Identification and quantification took place in the MS/MS scan by comparing the peak intensities of the iTRAQ reporter ions. An iTRAQ 4-plex chemical labeling is presented in this figure, although an 8-plex was also used in the experiments. Author's own work.

1.6 Aims of the Study

Data assembled from studies of *M. tuberculosis* infection of human macrophages indicates that PtpA's role in infection extends beyond acting on its two known substrates; VPS33B and subunit H of the V-ATPase pump (76,88). In fact, recombinant PtpA was found to dephosphorylate multiple substrates in macrophage cell extracts (148). These findings suggested that *M. tuberculosis* PtpA actively affects multiple host macrophage signalling pathways.

We explored *M. tuberculosis*-host interactions using two approaches: a kinome analysis to identify host protein kinases modulated by PtpA and a proteomic assay to analyze global and PtpA-dependent proteomic changes during *M. tuberculosis* infection.

The first part of this thesis was assigned to the study of the kinome response of the human macrophage-like cell line, THP-1, upon *M. tuberculosis* and Δ*ptpA M. tuberculosis* infection. Performing a phosphoproteome analysis, the phosphorylation status of a set of predefined host protein kinases involved in key signalling pathways was identified. The modulation effect of PtpA on the host protein kinase, GSK3α, was assessed by performing various biochemical assays and the impact of this PtpA-dependent modulation on the host in *M. tuberculosis* infection was identified.

The second part focused on analyses of the global proteomic response of THP-1 cells to *M. tuberculosis* infection. Using the multiplex iTRAQ proteomic strategy, the proteome-wide protein relative expression levels of human macrophages infected with different strains of *M. tuberculosis* (H37Rv, Δ*ptpA* and Δ*ptpA*::*ptpA*) were simultaneously determined. We

assembled data from four independent iTRAQ experiments and identified proteins that were consistently modulated by *M. tuberculosis*. We validated these findings by biochemical assays. We also examined the specific contribution of PtpA to the infection process. These experiments provide insight into the global and PtpA-dependent effects of *M. tuberculosis* from a proteomic view of infected human macrophages.

Chapter 2: Methods and Materials

2.1 Reagents and Chemicals

2.1.1 Commercial Reagents

Endotoxin-free RPMI 1640 medium, phorbol-12-myristate-13-acetate (PMA), protease inhibitor mixture, phosphatase inhibitor cocktail, PMSF and glutathione-agarose beads were purchased from Sigma-Aldrich (St. Louis, MO). FBS and kanamycin were purchased from Gibco Laboratories (Burlington, ON), L-glutamine, penicillin and streptomycin from StemCell Technologies (Vancouver, BC), gentamicin from Invitrogen (Burlington, ON), and hygromycin from Roche Diagnostics (Laval, QC). Ni-NTA polyhistidine-tag purification resin was purchased from Qiagen (Mississauga, ON), ATP from PerkinElmer (Boston, MA), and LB broth from Thermo Fisher Scientific (Waltham, MA). OADC was purchased from Difco Laboratories (Detroit, MI) and 7H9 culture media from Becton, Dickinson and Company (Sparks, MD).

2.1.2 Antibodies

Affinity purified rabbit polyclonal anti-phosphoGSK3α (pY^{279}) antibody was purchased from Invitrogen, rabbit polyclonal anti-GSK3α from Abcam (Toronto, ON), rabbit polyclonal anti-caspase-3 IgG from Cell Signalling Technology (Danvers, MA), mouse monoclonal anti-ICAM1 from eBioscience (San Diego, CA), and rabbit polyclonal anti-CTSG and rabbit polyclonal anti-IL1β from Antibodies-online.com (Atlanta, GA). Secondary HRP-conjugated goat anti-rabbit antibody was purchased from Sigma-Aldrich, Alexa Fluor 680-conjugated goat anti-rabbit IgG from Invitrogen, and Alexa Fluor 780-conjugated goat anti-mouse from Mandel Scientific (Guelph, ON). The specificity of the commercial antibodies was tested with Western blot analysis and immunostaining control experiments.

2.2 Bacteria

2.2.1 Strain Maintenance

M. tuberculosis H37Rv and its derivative strains were grown in Middlebrook 7H9 broth supplemented with 10% (v/v) OADC and 0.05% (v/v) Tween 80 (Sigma-Aldrich) at 37 °C standing in the incubator. The PtpA-null mutant and the PtpA complemented strains were generated in our laboratory by allelic replacement and were isolated by a sequential two-step selection protocol as previously described (149).

2.2.2 Bacterial Preparation for Infection

Bacteria in mid-log phase were harvested by 5 min centrifugation at 2,602 relative centrifugal force (RCF) and were subsequently washed three times with 7H9 with 0.05% Tween 80. For infection of differentiated THP-1 macrophage-like cells, bacteria were opsonized with human serum for 30 min at 37 °C.

2.2.3 *In Vivo* Bacterial Uptake by Macrophage

To ascertain that infection with the different *M. tuberculosis* strains investigated resulted in comparable rates of infection of macrophages, THP-1 cells (1.0×10^6) were seeded on six-well plates and differentiated as explained in Section 2.3.1. Bacteria were washed three times with 7H9 broth with 0.05% Tween 80, labeled with 100 μg/ml Alexa Fluor 488 carboxylic acid SS (Invitrogen), and opsonized with 10% human serum. THP-1 cells were infected with the labeled bacteria at a multiplicity of infection (MOI) of 10:1 for 2 h at 37 °C in a humidified atmosphere of 5% CO_2. Noninternalized bacteria were washed away, and cells were incubated for another 2 h at 37 °C in a humidified atmosphere of 5% CO_2. THP-1 cells were then washed

with PBS, scraped off the plate, and fixed with 2.5% paraformaldehyde as described by Wong and colleagues (88). Uptake was measured with FACS in a FACSCalibur Flow Cytometer (BD Bioscience) and data was analyzed using the FlowJo 8.7 software. The mean fluorescence intensities (the geometric mean from the distribution in FACS histograms) of Alexa Fluor 488 (FL1) were used to calculate bacterial uptake. The mean fluorescence intensities of uptake of wild-type *M. tuberculosis* were used as a reference.

2.3 Cell Culture

2.3.1 Tissue Culture Maintenance and Differentiation

The human monocytic leukemia cell line THP-1 (TIB-202; American Type Culture Collection, Manassas, VA) was cultured in 125 cm^2 tissue culture flasks (Corning Inc., Corning, NY) in RMPI 1640 medium supplemented with 10% FBS, 1% L-glutamine, 1% penicillin and 1% streptomycin. Cells were seeded in 10 cm (diameter) tissue culture dishes at a density of 7.0 x 10^6 cells/dish and differentiated into a macrophage-like cell line with 20 ng/ml PMA in RPMI 1640 medium supplemented with 10% FBS and 1% L-glutamine (incomplete RPMI) at 37 °C in a humidified atmosphere of 5% CO_2 for 18 h.

2.3.2 Macrophage Infection

Bacterial cells were washed with Middlebrook 7H9 broth supplemented with 0.05% (v/v) Tween 80 (Sigma-Aldrich). Infection of THP-1 macrophage-like cells was performed using human serum-opsonized *M. tuberculosis* at a MOI of 10:1 in RPMI 1640 medium. After 3 h of incubation at 37 °C and 5% CO_2, cells were washed with RPMI 1640 medium to remove non-

internalized bacteria and re-incubated at 37 °C and 5% CO_2 in incomplete RPMI containing 100 μg/ml gentamicin for a predetermined number of hours.

2.3.3 Macrophage Cellular Extraction for Western Blot Analysis

At defined time points after infection, infected THP-1 macrophage-like cells were washed twice with cold PBS and cellular extracts were harvested in lysis buffer (20 mM Tris-HCl, 5 mM EDTA, 1% Triton X-100, 1 mM DTT, 1 mM PMSF, 1 mM phosphatase inhibitor cocktail (Sigma-Aldrich), pH 7.2) by drawing the solution in and out of a blunt syringe 15-20 times. The cellular extracts were centrifuged for 10 min at 20,199 RCF and passed through a 0.22 μm filter column (Millipore Corporation, Billerica, MA).

2.3.4 Macrophage Cellular Extraction for iTRAQ Analysis

Four hours post-infection, *M. tuberculosis*-, Δ*ptpA M. tuberculosis*- and Δ*ptpA*::*ptpA M. tuberculosis*-infected THP-1 cells were washed twice with RPMI 1640 medium and scraped in 3 ml of the medium. Cells were centrifuged for 10 min at 180 RCF, resuspended in 490 μl iTRAQ lysis buffer (25 mM ammonium bicarbonate, 5 mM sodium fluoride, 5 mM sodium orthovanadate, 10 mM sodium β-glycerophosphate pentahydrate, pH 7-7.5) and transferred to screw-cap tubes containing 0.5 g of 0.5 mm glass beads. Ten μl of 10% sodium dodecyl sulphate (SDS) were added to the tubes and cellular extracts were bead-beated (BioSpec Products Inc., Bartlesville, OK) for 2 min (30 sec on/30 sec off) at a speed of 5.0. The lysates were then centrifuged for 20 min at 20,199 RCF and the supernatants were passed through a 0.22 μm filter column.

2.4 DNA Manipulation

2.4.1 RNA Extraction and cDNA Synthesis

Total RNA was extracted from *M. tuberculosis*-infected THP-1-derived macrophages (7.0×10^6 cells) at defined time points using the RNAspin Mini Kit according to the manufacturer's instructions (GE Healthcare, Burnaby, BC). RNA was reversed transcribed to cDNA using the EasyScript cDNA Synthesis Kit following the manufacturer's protocol (ABM, Richmond, BC). For each cDNA synthesis, 1 µg of total RNA, measured by an Epoch Microplate Spectrophotometer (BioTek, Winooski, VT), and 0.5 µM oligo(dT) oligonucleotide primers were used.

2.4.2 DNA Cloning

The plasmid pANT7-GSK3α was purchased from DNASU Plasmid Repository (Tempe, AZ). Because this vector was not created for bacterial inducible expression, *GSK3α* was PCR-amplified from the plasmid DNA using the GSK3α F primer with a BamH1 site and GSK3α R primer with an EcoR1 site. The amplified gene was digested and inserted into the pGEX-6P-3 vector (GE Healthcare) to generate the pGEX-6P-3-GSK3α plasmid for GST-tagged GSK3α fusion protein expression.

The human GSK3α His-tagged fusion protein expression plasmid, pBO1-GSK3α, was purchased from GeneCopoeia Inc. (Rockville, MD). The gene encoding *RAB7* was PCR-amplified from cDNA from prepared THP-1 cells using the RAB7 F primer with a BamH1 site and RAB7 R primer with an XhoI site. The amplified gene was inserted into the pET22b vector

(Millipore Corporation) to generate the pET22b-RAB7 plasmid for His-tagged RAB7 fusion protein expression.

The *M. tuberculosis ptpA* gene was previously PCR-amplified from *M. tuberculosis* H37Rv genomic DNA using the PtpA F primer with an EcoR1 site and the PtpA R primer with an Xho1 site. The amplified gene was inserted into the pGEX-6P-3 vector to generate the pGEX-6P-3-PtpA plasmid for GST-tagged PtpA fusion protein expression.

All plasmid constructs were verified by sequencing at Eurofins MWG Operon (Ebersberg, Germany). The oligonucleotides used for DNA cloning in this study are described in Table 1.

Oligonucleotides	Sequence (5' → 3')*
GSK3α F	TATATAGGATCCATGAGCGGCGGCGGGCCTTCG
GSK3α R	TATATAGAATTCGGAGGAGTTAGTGAGGGTAGG
PtpA F	ATATATGAATTCCGTGTCTGATCCGCTG
PtpA R	ATATATCTCGAGTCAACTCGGTCCGTTC
RAB7 F	TATATAGGATCCATGACCTCTAGGAAGAAAGTG
RAB7 R	TATATACTCGAGTCAGCAACTGCAGCTTTC

*The recognition sequence for the restriction site is underlined.

Table 1. Oligonucleotides Used for DNA Cloning

2.4.3 Quantitative Polymerase Chain Reaction (qPCR)

Total RNA from lysates of *M. tuberculosis*-infected THP-1-derived macrophages was extracted at defined time points and reversed transcribed as previously described (Section 2.4.1). Primers specific for the mRNA of the genes of interest were designed using Primer-BLAST (National Center for Biotechnology Information, Bethesda, MD) (Table 2). Control PCR

amplifications for the expression of gene-specific mRNAs were performed on cDNA templates from uninfected PMA-differentiated THP-1 cells to confirm the specificity of the designed primers. Each qPCR reaction contained 2 X EvaGreen qPCR Mastermix (ABM), 15 ng cDNA and 1 μM of each primer, and was analyzed in quantification mode on a DNA Engine Opticon instrument (Bio-Rad Laboratories, Mississauga, ON). The following cycling conditions were used: 95 °C for 10 min, 40 cycles of 95 °C for 15 sec, 52 °C for 15 sec, and 60 °C for 30 sec with data collection during each cycle. Mock reactions (no reverse transcriptase) were also included with each experiment to confirm the absence of genomic DNA contamination. Ct values were converted to copy numbers using standard curves. Results were analyzed using GraphPad Prism 5.0 software. All values of gene-specific mRNA were internally normalized to cDNA expression levels of housekeeping gene *GAPDH*.

Oligonucleotides	Sequence (5' → 3')
Caspase-3 F	TGAGGCGGTTGTAGAAGAGTTT
Caspase-3 R	GCTCGCTAACTCCTCACGG
CTSG F	ATGACGAGGAAGCGATGGTG
CTSG R	TGGCAGGAAGTACTGGAGTAGA
GAPDH F	GAAGGTGAAGGTCGGAGTC
GAPDH R	GAGGGATCTCGCTCCTGGAAGA
GSK3α F	GCTCACCCCTGGACAAAGGTGTT
GSK3α R	CGCACAGGCCTCTAGTGGGGA
ICAM1 F	GACCATCTACAGCTTTCCGGC
ICAM1 R	CATTCAGCGTCACCTTGGCT
IL1β F	AGATGAAGTGCTCCTTCCAGG
IL1β R	CATGGCCACAACAACTGACG
MIF F	CCGGACAGGGTCTACATCAACT
MIF R	TGGGCGGGCCTAGAACA
SOD2 F	GTGGAGAACCCAAAGGGGAG
SOD2 R	GAAACCAAGCCAACCCCAAC

Table 2. Oligonucleotides Used for Quantitative PCR

2.5 Protein Expression and Purification

2.5.1 Expression of Recombinant Proteins in *E. coli*

To express and purify His-tagged recombinant protein, pBO1-GSK3α and pET22b-RAB7 plasmids were transformed into chemically competent BL21 *E. coli* cells. The transformed cells were used to grow starter cultures overnight at 37 °C, and were then inoculated into 2 L of LB media (Thermo Fisher Scientific) supplemented with 100 μg/ml ampicillin (Bio Basic Inc., Toronto, ON). The cultures were then grown to an OD_{600} of 0.6 at 37 °C, and expression was induced with 0.4 mM IPTG (Bio Basic Inc.) at room temperature overnight. The bacteria were harvested by centrifugation at 4,066 RCF, resuspended in lysis buffer (50 mM Na_2HPO_4, 290 mM NaCl, 10 mM imidazole, pH 8.0, and 1 mM PMSF) and lysed by sonication. The soluble fraction of the bacterial lysates was obtained by centrifugation at 20,199 RCF and His-tagged proteins were purified from the soluble fraction by affinity chromatography on Ni-NTA polyhistidine-tag purification resin.

GST-tagged PtpA and GSK3α were expressed in BL21 *E. coli* cells transformed with pGEX-6P-3-PtpA and pGEX-6P-3-GSK3α plasmids. A starter culture of the transformed BL21 was grown overnight at 37 °C and inoculated into 2 L of LB media with 100 μg/ml ampicillin. The culture was grown at 37 °C to an OD_{600} of 0.6 and expression was induced with 0.4 mM IPTG at room temperature overnight. The bacteria were harvested by centrifugation at 4,066 RCF, resuspended in lysis buffer (50 mM Na_2HPO_4, 290 mM NaCl, 10 mM imidazole, pH 8.0, and 1 mM PMSF) and lysed by sonication. The soluble fraction of the bacterial lysates was obtained by centrifugation at 20,199 RCF and GST-tagged proteins were purified from the soluble fraction by affinity chromatography on glutathione-agarose resin (Sigma-Alrich).

2.5.2 Expression of Recombinant Proteins in *M. smegmatis*

The competent cells *M. smegmatis* were used for transformation of the pALACE-PtpA plasmid. Transformed bacteria were used to grow starter cultures over two nights in 7H9 media containing 0.05% Tween 80, 50 μg/ml hygromycin and supplemented with 1% ADS (0.5% bovine serum albumin-fraction V, 0.2% dextrose, 0.85% saline) enrichment. The starter cultures were inoculated into 2 L of 7H9 media containing 0.05% Tween 80, 50 μg/ml hygromycin and supplemented with 1% ADS and grown at 37 °C to an OD_{600} of 1.0. Cells were harvested by centrifugation at 4,066 RCF for 30 min and resuspended in 7H9 media supplemented with 0.05% Tween 80, and 50 μg/ml hygromycin. Expression of the protein was induced with 0.2% acetamide at room temperature for 24 h. The bacteria were harvested by centrifugation at 4,066 RCF for 30 min, resuspended in lysis buffer (50 mM Na_2HPO_4, 290 mM NaCl, 10 mM imidazole, pH 8.0, and 1 mM PMSF) and lysed by sonication. The soluble fraction of the bacterial lysates was obtained by centrifugation at 20,199 RCF and His-tagged proteins were purified by affinity chromatography on Ni-NTA polyhistidine-tag purification resin.

2.6 Phosphoproteome Analysis by Kinetworks™ Phospho-Site Screen (KPSS) Assay

THP-1 cells were infected with wild-type *M. tuberculosis* H37Rv or the H37Rv strain in which the *ptpA* gene was deleted (Δ*ptpA M. tuberculosis*) as previously described (Section 2.3.2) and cellular extracts were harvested 18 h post-infection (Section 2.3.3). The macrophage lysates were prepared for phosphoproteome analysis (KPSS 1.3) according to the manufacturer's instructions (Kinexus Bioinformatics Corporation, Vancouver, BC). Data was analyzed according to statistical confidence provided by experience in analyzing over ten thousand

screens. According to Kinexus, the significance levels of change are over 25% variability in intensity.

2.7 *In Vitro* Phosphatase Activity Assay

To assess for phosphatase activity of PtpA *in vitro*, the artificial chromogenic substrate *p*NPP was used. The reaction contained 100 mM Tris-HCl pH 8.0, 5 μM $MgCl_2$, 2 μM $MnCl_2$, 1 μM DTT and 30 mM *p*NPP with 5 μM of purified recombinant PtpA. The reaction was incubated at 37 °C for 1 h. The absorbance (A_{450}) was measured after 1 h using a Bio-Rad Model 680 microplate reader.

2.8 *In Vivo* and *In Vitro* Western Blot Analysis

Western blot analyses of cell extracts from infected THP-1 cells harvested 18 and 48 h post-infection (Sections 2.3.2 and 2.3.3) were performed as follow: 50 μg of THP-1 cell extracts were resolved by SDS-PAGE and transferred onto a nitrocellulose membrane (Bio-Rad Laboratories). The blots were probed with affinity purified rabbit polyclonal anti-phosphoGSK3α (pY^{279}) IgG, anti-GSK3α or anti-caspase-3 antibody (final IgG dilution for all antibodies, 1:1,000) and incubated overnight at 4 °C. For detection of phosphorylated GSK3α (Y^{279}) and non-phosphorylated GSK3α, HRP-conjugated goat anti-rabbit (final IgG dilution, 1:3,500) antibody was used as the secondary detection reagent and the blot was developed by enhanced chemiluminescence (ECL) (Thermo Fisher Scientific). For detection of caspase-3, Alexa Fluor 680 goat anti-rabbit antibody was used as the secondary detection reagent (final IgG dilution, 1:10,000) and detection was done using an Odyssey Infrared CLx Imager (LI-COR Biosciences, Lincoln, NE).

For iTRAQ analyses, lysates of infected THP-1 cells were harvested 4 h post-infection (Sections 2.3.2 and 2.3.4). Briefly, 100 μg of cell extracts were resolved by SDS-PAGE and transferred onto a nitrocellulose membrane. The blots were probed with affinity purified mouse monoclonal anti-ICAM1 antibody (final IgG dilution, 1:250), affinity purified rabbit polyclonal anti-IL1β IgG (final IgG dilution, 1:1,000), or affinity purified rabbit polyclonal anti-CTSG antibody (final IgG dilution, 1:500) and incubated overnight at 4 °C. For detection of ICAM1, Alexa Fluor 780 goat anti-mouse antibody was used as the secondary detection reagent (final IgG dilution, 1:5,000). For IL1β and CTSG, Alexa Fluor 680 goat anti-rabbit antibody was used (final IgG dilution, 1:10,000). An Odyssey Infrared CLx Imager (LI-COR Biosciences) was employed for chemiluminescence detection. To ensure identical protein loading of the different samples, Ponçeau staining of the blots was performed.

In other experiments, 1 to 4 μM of recombinant GSK3α were incubated with 0.15 mM ATP for 1 h at 37 °C. Then, a fixed concentration of recombinant PtpA (0.04 μM) was added to different GSK3α concentrations and incubation was continued for 45 min at 37 °C. Samples were then resolved by SDS-PAGE and transferred onto a nitrocellulose membrane. The blot was probed with rabbit anti-phosphoGSK3α (pY^{279}) IgG and HRP-conjugated goat anti-rabbit antibody was used as the secondary detection reagent as described above. The blots were developed by ECL. Blots were stripped and reprobed with anti-GSK3α antibody to confirm that total GSK3α protein levels were identical in each reaction samples.

2.9 Determination of PtpA and GSK3α Dissociation Constant

The interaction between PtpA and GSK3α was measured using a Fusion-α-HT Multimode Microplate Reader (PerkinElmer) and the ALPHAScreen Histidine (Nickel Chelate) Detection Kit (PerkinElmer). Purified GST-tagged recombinant PtpA was biotinylated using the EZ-Link Biotinylation Kit (Thermo Scientific) and diluted in the assay buffer (25 mM HEPES, 100 mM NaCl, and 0.1% Tween 20, pH 7.4) in 384-well microplates (PerkinElmer). Purified His-tagged recombinant GSK3α was added to wells containing PtpA. Nickel chelating acceptor beads were further added to the proteins and the microplate was incubated for 30 min at room temperature. Streptavidin donor beads were then added to the reactions and incubation was continued for 1 h at room temperature. Kinetics of the reactions was monitored in the ALPHAScreen apparatus by luminescence signals generated from protein-protein interactions (counts per second (cps)). Dissociation constants were determined using GraphPad 5.0 software.

2.10 *In Vitro* Protein Kinase Assay

Three separate subsets of reactions containing 2, 3 and 4 μM recombinant GSK3α were autophosphorylated in a kinase buffer (50 mM Tris-HCl, 5 mM $MgCl_2$, 2 mM $MnCl_2$, 1 mM DTT, pH 7.5) containing 10 μCi γ^{32}P-ATP (PerkinElmer) for 30 min at 37 °C. After this incubation period, 0.04 μM of PtpA was added to the second subset of reactions and 0.04 μM of PtpA and 1.5 mM or 5 μM of the phosphatase inhibitors, sodium orthovanadate (Na_3VO_4) or BVT 948, to the third. The first subset of reactions served as controls. Incubation of all three subsets was continued for 15 min at 37 °C. At the end of the incubation period, reactions were stopped with the addition of SDS sample loading buffer and heated at 95 °C for 8 min. The samples were resolved by 12% SDS-PAGE. The gel was silver-stained, dried and exposed to a

screen overnight. The ^{32}P-radioactively labeled protein bands were detected by a PhosphorImager SI apparatus (GE Healthcare). Bands corresponding to phosphorylated GSK3α were cut, submerged in scintillation fluid (Beckman Coulter Inc.) and analyzed by scintillation counting using a Beckman Coulter LS 6500 (Beckman Coulter, Mississauga, ON).

2.11 Radiometric Protein Kinase Assay

The kinase assay was performed as previously described (Section 2.10) until the end of the second incubation period. Reactions were spotted onto phosphocellulose paper (GE Healthcare), dried and washed thoroughly with 1% phosphoric acid six times for 10 min. Radioactivity levels were measured by submerging the phosphocellulose papers in scintillation fluid and analyzed by scintillation counting.

2.12 Isobaric Tags for Related and Absolute Quantitation (iTRAQ) and LC-MS/MS Analyses

THP-1 cells were infected with *M. tuberculosis*, Δ*ptpA M. tuberculosis* and the complemented strain (Δ*ptpA*::*ptpA*), and cell extracts were prepared as described above (Sections 2.3.2 and 2.3.4, respectively). Protein concentrations in cell extracts were determined using a bicinchoninic acid assay (Sigma-Aldrich). Protein samples (200 μg from each test) were sent to the University of Victoria Genome British Columbia Proteomics Centre for iTRAQ analyses. In brief, 85 μg of each sample were precipitated overnight in acetone at 4 °C, then resolubilized in 0.5 M Tetraethylammonium Bromide (TEAB), 0.2% SDS. Proteins were then reduced with TCEP and alkylated with MMTS. Proteins were digested in solution with trypsin (Promega, Madison, WI) at 37 °C overnight and labeled with the appropriate iTRAQ label (113-119, 121),

an isobaric stable isotope tag, at room temperature for 1 h. iTRAQ labeled peptides were then combined and separated by strong cation exchange HPLC. HPLC fractions containing peptides were concentrated by speed-vac, then analyzed and quantified by LC-MS/MS. The length of the reverse gradient used was 2 h per HPLC fraction. Samples were analyzed by reversed phase nanoflow (300 nl/min) HPLC with nano-electrospray ionization using a LTQ-Orbitrap mass spectrometer (LTQ-Orbitrap Velos, Thermo Fisher Scientific) operated in positive ion mode.

2.13 Data Analysis and Interpretation

All data was analyzed using Proteome Discoverer 1.4 (Thermo Fisher Scientific) and the search engine MASCOT v2.4 (Matrix Science, Boston, MA). Raw data files were searched against the Uniprot-SwissProt database with allspecies filter and mammalian species only.

2.14 Statistical Analysis

Raw data files from each of the four experimental trials were collected and analyzed using R (gnu). All four trials included *M. tuberculosis*/uninfected ratios for detected proteins. Additionally, the first two trials included Δ*ptpA M. tuberculosis*/uninfected and Δ*ptpA*::*ptpA M. tuberculosis*/uninfected ratios. Approximately two thousand proteins were detected in each trial, of which only 845 were detected in all trials. All data was log-transformed and each trial was normalized individually. Trials were normalized before elimination of contaminants and missing data.

For detection of anomaly, protein ratios of uninfected and *M. tuberculosis*-infected macrophages were compared using two methods. The first involved isolating all proteins for

which the expression ratio in at least three of four assays was one standard deviation above/below the mean expression ratio. For normalized data, the mean for each assay is zero and the standard deviation is one. For instance, to isolate up-regulated proteins, all proteins with a normalized log-ratio above one in at least three of the four assays were kept. The second method involved taking the mean ratio for each protein over all four assays and isolating those proteins for which this mean was outside of the ±1 standard deviation interval about the mean.

A method was implemented for the initial two iTRAQ assays which included all three treatment conditions, i.e. infection with *M. tuberculosis*, Δ*ptpA M. tuberculosis,* and Δ*ptpA*::*ptpA M. tuberculosis*. This was inspired by the apparent co-linearity between each of these covariates. Proteins for which the infected/uninfected ratio was 1.8 standard deviations above the mean for all three possible infected/uninfected ratios were considered consistently up-regulated proteins for that sample, and therefore not PtpA-specific. The same was done to isolate proteins consistently down-regulated for each sample. These generally up- or down-regulated samples had proteins ranked based on their mahalanobis distances (150) from the mean of the given sample where the three variables used in calculation of the correlation matrix were the three infected treatment conditions. Furthermore, the remaining proteins were analyzed in accordance to their *M. tuberculosis*/Δ*ptpA M. tuberculosis* ratios, organized into up- and down-regulated lists based on the 1.8 standard deviation criterion, and ranked based on their distance from the mean.

Chapter 3: Results

3.1 *M. tuberculosis* Promotes Anti-Apoptotic Activity of the Macrophage by PtpA-Dependent Dephosphorylation of Host GSK3*α*

3.1.1 Introduction

M. tuberculosis pathogenicity partly relies on the inhibition of phagosome acidification and maturation (76,88). These processes are blocked, in part, by the low molecular weight protein-tyrosine phosphatase, PtpA, secreted by *M. tuberculosis* into the macrophage cytosol (76). We showed that PtpA dephosphorylates the macrophage protein-serine/threonine kinase GSK3α on the tyrosine residue 279. GSK3α is a multifunctional protein kinase that acts as a master regulator of numerous signalling pathways including the insulin response, glycogen regulation, cell survival and apoptosis (151,152). GSK3α's activity is positively regulated by the phosphorylation of the tyrosine residue located in the activation loop, Y^{279}, and this phosphorylation is essential for the full activity of the enzyme (153). Studies have shown that apoptotic stimuli increase GSK3α's activity by phosphorylation of Y^{279} (154), providing evidence for a role for tyrosine phosphorylation in apoptosis. Considering this, we demonstrated that dephosphorylation of GSK3α on amino acid Y^{279} leads to modulation of the enzyme's anti-apoptotic activity, promoting pathogen survival early during infection. This was exemplified by the inhibition of the proteolytic cleavage and activation of the apoptosis executioner, caspase-3, in *M. tuberculosis*-infected macrophages. These findings revealed that PtpA significantly contributes to inhibiting host cell apoptosis at early stages of infection.

3.1.2 PtpA Interferes with Multiple Host Macrophage Signalling Pathways

Protein phosphatases play key roles in signal transduction in a number of pathways (155). To decipher the multifaceted activity of PtpA on macrophage signalling pathways, we previously performed an *in vitro* dephosphorylation assay in which recombinant PtpA was incubated with macrophage cell extracts. As seen in Figure 11 and Table 3, this resulted in the dephosphorylation of multiple host proteins including human VPS33B (hVPS33B), a host substrate previously identified in our laboratory (76).

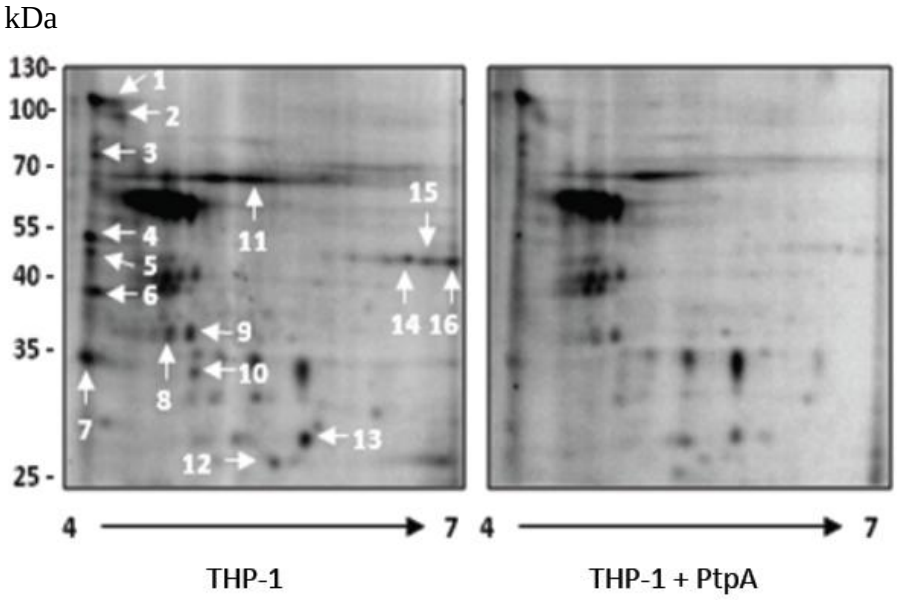

Figure 11. Phosphoproteomic Analysis of Host Macrophage Proteins Dephosphorylated by PtpA Revealed by 2D Gel Electrophoresis
A cellular extract of differentiated THP-1 cells was incubated with γ^{32}P-ATP in a kinase buffer for 30 min at 30 °C. Recombinant PtpA was added to one of the samples for 15 min and mixtures were electrophoresed onto 2D SDS-Polyacrylamide gels using isoelectric focusing in a 4-7 pH gradient for the first dimension and 10% SDS-PAGE for the second dimension. The radiolabeled spot profile was obtained by exposing overnight to a PhosphorImager screen. Sixteen spots demonstrating reduced phosphorylation upon addition of PtpA were identified by mass spectrometry (Table 3).

Spot No.	Protein identification*	MOWSE Score^	MW (pI)	Coverage (%)
1	Xin B (CAF25191)	$5.8e^{+16}$	122.1 (5.2)	15
	Phosphoinositide 3-Kinase Class-3 (NP002638)	$3.17e^{+15}$	101.5 (6.4)	12
2	Rabaptin (NP004694)	$3.25e^{+07}$	99.3 (4.9)	21
	Rabaptin-5 (AAC70781)	$3.25e^{+07}$	95.6 (4.9)	19
	Rabaptin-4 (3832516)	$1.63e^{+07}$	95.5 (4.9)	19
	VPS39 (AAH15817)	$1.61e^{+07}$	90.3 (6.6)	19
3	Exocyst Complex Component Sec6 (O60645)	$1.31e^{+02}$	86.8 (5.8)	12
	cGMP-Dependent Protein Kinase-1 (Q13976)	$1.21e^{+02}$	76.3 (5.7)	11
	Gamma Adducin (Q9UEY8)	$1.56e^{+02}$	79.1 (5.9)	7
4	Unknown (AAH04303)	$3.1e^{+103}$	52.5 (5.9)	64
	Hypothetical Protein	$8.36e^{+97}$	52.4 (5.5)	51
5	MHC Class I Antigen Cw*7 (P10321)	$5.31e^{+01}$	40.7 (5.6)	7
	MHC Class I Antigen Cw*1 (P30499)	$2.36e^{+01}$	40.9 (5.5)	6
6	Not Determined			
7	GTPase, IMAP Family Member-7 (Q8NHV1)	$1.06e^{+16}$	34.5 (6.1)	63
8	Annexin A13 (P27216)	$1.19e^{+31}$	35.5 (5.5)	60
9	N-Myc Interactor-STAT Interactor (Q13287)	$3.64e^{+43}$	35.1 (5.2)	57
	Cdc42 Effector Protein-4 (Q9H3Q1)	$3.7e^{+42}$	37.9 (5.1)	41
10	Not Determined			
11	Vacuolar Protein Sorting 33B (AAF91174)	$6.7e^{+52}$	70.6 (6.3)	64
12	Ras-Related Protein Rab-7L1 (O14966)	$2.15e^{+69}$	23.1 (6.7)	70
13	Ras-Related Protein Rab-28 (Rab-26) (P51157)	$6.5e^{+48}$	24.9 (5.7)	44
14	Syntaxin 18 (Q9P2W9)		38.7 (5.4)	21
	MHC Class I Antigen Cw*3 (70076)	$1.34e^{+04}$	40.7 (6.0)	15
15	Arfaptin-1 (P53367)	$1.86e^{+01}$	41.7 (6.2)	10
16	MHC Class I Antigen Cw*17 (Q95604)	$1.63e^{+01}$	41.2 (6.3)	19

* Accession numbers are shown in parenthesis, ^ Score based on peptide frequency.

Table 3. Identification of Proteins Dephosphorylated by the Addition of Recombinant PtpA to a Phosphorylated THP-1 Cellular Extract

A cellular extract of differentiated THP-1 cells was incubated with recombinant PtpA. The phosphorylation status of several THP-1 cell proteins was found to be modulated by PtpA. These proteins were identified by mass spectrometry. The numbers seen in Table 3 correspond to spots shown in Figure 11. MOWSE score or Molecule Weight Search allows calculation of the probability of matching N peaks by random chance and is based on the frequency of a peptide molecular weight being found in a protein of a given molecular weight range (156). Accession numbers are shown in parenthesis.

3.1.3 Kinetworks™ Analysis

To identify other macrophage signalling proteins that might be affected by *M. tuberculosis* PtpA, we conducted a specific large-scale proteomics analysis of signalling networks, termed Kinetworks™ analysis, which tracks the kinome and phosphoproteome (145). This multi-immunoblotting method uses an array of phospho-specific antibodies against defined

human signalling proteins and networks (145). To test PtpA's effect on signal transduction pathways, we monitored and compared the phosphorylation status of a predefined set of signalling proteins from uninfected macrophages, macrophages infected with *M. tuberculosis* and macrophages infected with Δ*ptpA M. tuberculosis*. We chose to investigate events occurring 18 h post-infection. Based on the selective phosphoproteome analysis, as seen in Figure 12, we observed that PtpA affects the phosphorylation pattern of a series of host signalling proteins.

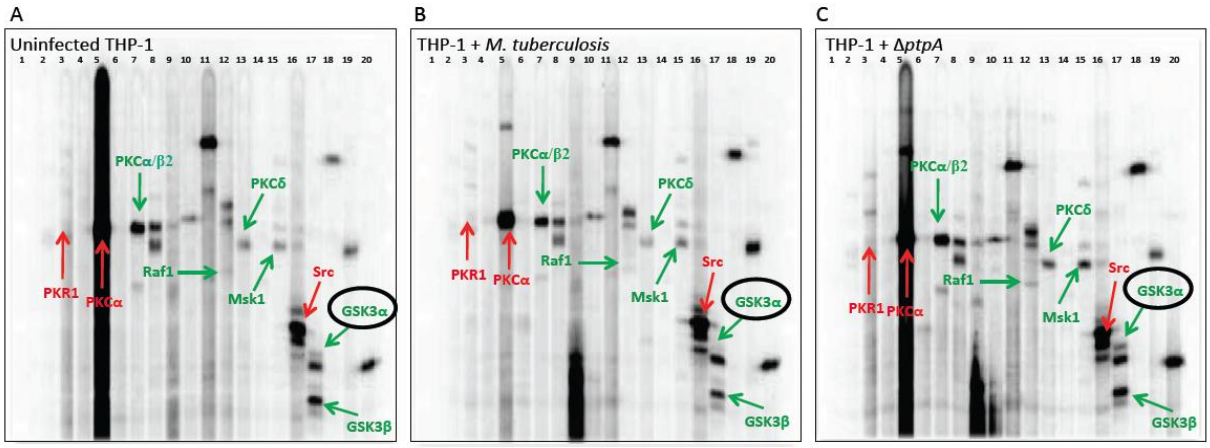

Figure 12. Global Phosphoproteome Analysis of THP-1 Cells Infected with *M. tuberculosis* and Δ*ptpA M. tuberculosis*

Simultaneous detection of selected host proteins and their activation status using a multiple immunoblotting technique. Accurate intensity values for each protein are the accumulated signal obtained over a given scan time for each blot. These are shown as numerical values in Table 4. The three gels represent (A) uninfected THP-1 cells, (B) THP-1 cells infected with *M. tuberculosis*, and (C) THP-1 cells infected with Δ*ptpA M. tuberculosis*. Each lane was probed with one or more antibodies. The highlighted proteins are host signalling proteins showing a phosphorylation change greater than 25% (red: upregulation, green: downregulation). Antibodies against the phosphorylated proteins were as follows: lane 1, molecular size standard; lane 2, NR1 (S^{896}); lane 3, PKR1 (T^{451}); lane 4, STAT5A (Y^{694}); lane 5, PKCα (S^{657}), Src (Y^{418}); lane 6, JNK (T^{183}+Y^{185}), RSK1/3 (T^{359}+S^{363}/T^{356}+S^{360}); lane 7, MEK3/6 (S^{189}/S^{207}), PKCα/β2 (T^{638}+T^{641}); lane 8, ERK1 (T^{202}+Y^{204}), ERK2 (T^{185}+Y^{187}), S6Kα p70 (T^{389}), S6Kα p85 (T^{389}); lane 9, PKCε (S^{729}), SMAD1/5/9 (S^{463}+S^{363}/S^{463}+S^{465}/S^{465}+S^{467}); lane 10, STAT3 (S^{727}); lane 11, JUN (S^{73}); lane 12, RAF1 (^{S259}), STAT1α (Y^{701}), STAT1β (Y^{701}); lane 13, PKBα (AKT1) (T^{308}), PKCδ (T^{507}); lane 14, PKBα (AKT1) (S^{473}); lane 15, GSK3α (S^{21}), GSK3β (S^{9}), MSK1 (S^{376}); lane 16, α-Adducin (S^{726}), γ-Adducin (S^{693}), CDK1/2 (Y^{15}), Src (Y^{529}); lane 17, GSK3α (Y^{279}), GSK3β (Y^{216}); lane 18, p38α MAPK (T^{180}+Y^{182}), RB (S^{780}); lane 19, NPM (S^{4}), MEK1/2 (S^{218}+S^{222}); and lane 20, CREB1 (S^{133}), RB (S^{807}+S^{811}).

As illustrated in Figure 12, cellular extracts of uninfected and *M. tuberculosis*-infected macrophages were subjected to simultaneous screens. Changes in phosphorylation were measured based on the intensity of 38 predefined phosphoproteins (Table 4) shown as bands in each gel. The phosphorylation levels of the three different treatments were compared in terms of the relative fold change in phosphorylation. The fold change was calculated by comparing the accumulated signal of proteins obtained over a given scan time (normalized counts per minute) from uninfected macrophages and macrophages treated with *M. tuberculosis*, to the accumulated signal of proteins from macrophages treated with Δ*ptpA M. tuberculosis* (control; accumulated signal set as 1) (Table 4). Due to the high sensitivity of the assay in determining the phosphorylation state of phosphoproteins, a change in phosphorylation greater than 25% between treated cells is considered significant according to the supplier of the screening kit (Kinexus Bioinformatics Corporation). Kinexus Bioinformatics Corporation has performed over ten thousand screens and thorough analysis of all data determined this value. A change in phosphorylation of less than this percentage may be due to experimental and/or biological variation.

Protein Full Name	Abbreviation	Epitopes	Control	Fold Change	
			Δ*ptpA* *M. tuberculosis*	Uninfected	*M. tuberculosis*
Adducin Alpha (ADD1)	α-Adducin	S^{726}	0		
Adducin Gamma (ADD3)	γ-Adducin	S^{693}	0		
B23 (Nucleophosmin, Numatrin, Nucleolar Protein NO38)	B23 [NPM]	S^{4}	0		
Cyclin-Dependent Protein Kinase-1/2	CDK1/2	Y^{15}	1	2.00	ND
cAMP Response Element Binding Protein-1	CREB1	S^{133}	1	0.70	0.84
Extracellular Regulated Protein Kinase-1 (p44 MAP Kinase)	ERK1	$T^{202} + Y^{204}$	0		
Extracellular Regulated Protein Kinase-2 (p42 MAP Kinase)	ERK2	$T^{185} + Y^{187}$	0		
Glycogen Synthase Kinase-3 Alpha	GSK3α	S^{21}	0		
Glycogen Synthase Kinase-3 Alpha	GSK3α	Y^{279}	1	0.65	0.33
Glycogen Synthase Kinase-3 Beta	GSK3β	S^{9}	0		
Glycogen Synthase Kinase-3 Beta	GSK3β	Y^{216}	1	0.93	0.61
Jun N-Terminus Protein Kinase (Stress-Activated Protein Kinase (SAPK))-1/2/3	JNK	$T^{183} + Y^{185}$	1	ND	1.15
Jun Proto-Oncogene-Encoded AP1 Transcription Factor S73	JUN	S^{73}	0		
MAPK/ERK Protein Kinase-1/2 (MKK1/2)	MEK1/2	$S^{217} + S^{221}$	0		
MAP Kinase Protein Kinase-3/6 (MKK3/6)	MEK3/6	S^{189}/S^{207}	0		
MAP Kinase Protein Kinase-6 (MKK6)	MEK6	S^{207}	0		
Mitogen- and Stress-Activated Protein Kinase-1	MSK1	S^{376}	1	0.57	0.67
N-Methyl-D-Aspartate (NMDA) Glutamate Receptor-1 Subunit Zeta	NR1	S^{896}	1	0.85	0.90
Mitogen-Activated Protein Kinase p38 Alpha	p38α MAPK	$T^{180} + Y^{182}$	0		
Protein Kinase B Alpha (Akt1)	PKBα [AKT1]	T^{308}	0		
Protein Kinase B Alpha (Akt1)	PKBα [AKT1]	S^{473}	0		
Protein Kinase C Alpha	PKCα	S^{657}	1	1.50	1.25
Protein Kinase C Alpha/Beta-2	PKCα/β2	T^{638}/T^{641}	1	0.94	0.62
Protein Kinase C Delta	PKCδ	T^{507}	1	0.81	0.51
Protein Kinase C Epsilon	PKCε	S^{729}	0		
Double-Stranded RNA-Dependent Protein Kinase	PKR1	T^{451}	1	1.31	1.54
Raf 1Proto-Oncogene-Encoded Protein Kinase	RAF1	S^{259}	1	0.88	0.47
Retinoblastoma-Associated Protein	RB	S^{780}	1	0.45	0.78
Retinoblastoma-Associated Protein	RB	$S^{807} + S^{811}$	0		
Ribosomal S6 Protein Kinase-1/3	RSK1/3	$T^{359} + S^{363}/ T^{356} + S^{360}$	0		
p85 Ribosomal Protein S6 Kinase-2	S6Kα p85	T^{412}	1	1.16	0.88
p70 Ribosomal Protein S6 Kinase Alpha	S6Kα p70	T^{389}	1	1.03	0.85
SMA- and Mothers Against Decapentaplegic Homologs-1/5/9	SMAD1/5/9	$S^{463} + S^{465}/S^{463} + S^{465}/S^{467}$	0		
Src Proto-Oncogene-Encoded Protein Kinase	Src	Y^{418}	0		
Src Proto-Oncogene-Encoded Protein Kinase	Src	Y^{529}	1	0.89	1.57
Signal Transducer and Activator of Transcription-1 Alpha	STAT1α	Y^{701}	1	0.56	0.86
Signal Transducer and Activator of Transcription-1 Beta	STAT1β	Y^{701}	1	1.04	0.90
Signal Transducer and Activator of Transcription-3	STAT3	S^{727}	1	0.79	0.86
Signal Transducer and Activator of Transcription-5	STAT5	Y^{694}	0		

ND, not determined.

Table 4. Phosphoproteome Analysis of Host Signalling Proteins Affected by PtpA

A total of 38 phospho-specific antibodies targeting key host signalling proteins were used. The trace quantity of each protein band was measured by the area under its intensity profile curve and corrected for the individual scan times (recorded time before saturation occurs). Values for the control samples were set to 1 or 0. A value of 0 indicates that no immunoreactive signal was detected for this protein. An immunoreactive signal was detected for only 17 proteins. Values for uninfected THP-1 cells and cells infected with *M. tuberculosis* show the fold change relative to their respective control samples (Δ*ptpA M. tuberculosis*).

Out of the 38 signalling proteins tested, an accumulated signal was detected for 17 macrophage phosphoproteins. Among these, several displayed significant changes in phosphorylation between macrophages infected with *M. tuberculosis* and the control Δ*ptpA* mutant. These include Protein Kinase C Alpha (PKCα; fold change of 1.25 compared to the control), Double-Stranded RNA-Dependent Protein Kinase (PKR1; 1.54), Protein Kinase C Alpha/Beta-2 (PKCα/β2; 0.62), Raf 1 Proto-Oncogene-Encoded Protein Kinase (RAF1; 0.47), Protein Kinase C Delta (PKCδ; 0.51), Mitogen- and Stress-Activated Protein Kinase-1 (MSK1; 0.67), Src Proto-Oncogene-Encoded Protein Kinase (Src; 1.57), Glycogen Synthase Kinase-3 Alpha (GSK3α; 0.33), and Glycogen Synthase Kinase-3 Beta (GSK3β; 0.61). From this list, Src kinase was the only protein previously shown to be associated with *M. tuberculosis* infection (157).

3.1.4 *M. tuberculosis* PtpA Dephosphorylates the Human Kinase GSK3α

Among all host signalling proteins whose phosphorylation status was affected by PtpA (Figure 12, Table 4), we identified human Glycogen Synthase Kinase-3 (GSK3) as another potential substrate for mycobacterial PtpA. We chose to investigate GSK3α for further analysis, because GSK3α Y^{279} showed a 67% decrease in phosphorylation in macrophages infected with *M. tuberculosis* compared to macrophages infected with the Δ*ptpA* mutant strain. GSK3α was identified as the protein with the greatest level of dephosphorylation by *M. tuberculosis*.

3.1.5 *GSK3α* Transcription Levels are not Decreased by PtpA

To rule out the possibility that the GSK3α dephosphorylation observed in the Kinetworks™ analysis (Figure 12, Table 4) was caused by reduced levels of expression due to

PtpA's effect on *GSK3α* transcription levels, we examined levels of *GSK3α* transcripts by qPCR. RNA from uninfected THP-1 cells and from THP-1 cells infected with *M. tuberculosis* and Δ*ptpA M. tuberculosis* was harvested 18 h post-infection corresponding to the time point at which lysates were harvested for the Kinetworks™ analysis. As seen in Figure 13, qPCR profiling revealed a general modest increase in *GSK3α* transcript levels in cells infected with both *M. tuberculosis* and the Δ*ptpA* mutant without significant difference between the two. The difference in *GSK3α* transcript levels between *M. tuberculosis*- and Δ*ptpA M. tuberculosis*-infected cells may be attributed to *GSK3α*'s response to its inhibition via PtpA's catalyzed dephosphorylation. Nonetheless, the difference is not significant and we concluded that PtpA does not affect *GSK3α* expression levels and that the dephosphorylation observed in the phosphoproteome analysis is due to a *bona fide* dephosphorylation of GSK3α by PtpA.

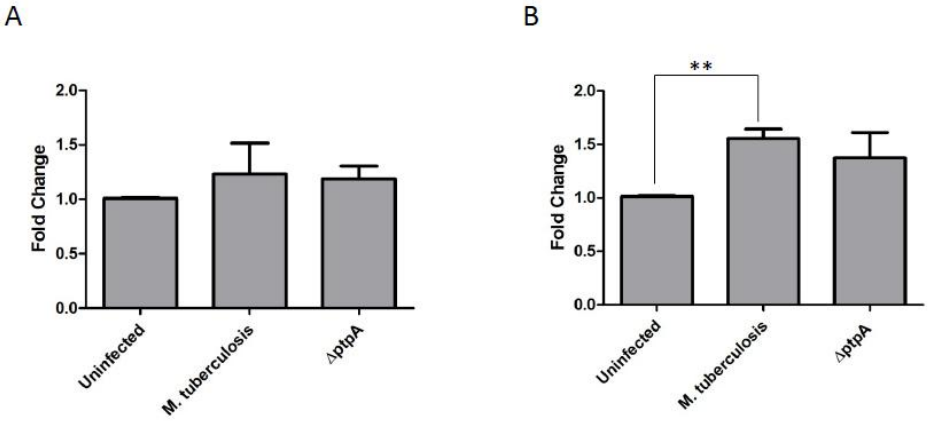

Figure 13. Transcriptional Levels of *GSK3α* Post-Infection
Quantitative PCR analysis comparing mRNA levels of *GSK3α* from different infection conditions. RNA from uninfected and treated THP-1 cells (treated with *M. tuberculosis* and Δ*ptpA M. tuberculosis*) was extracted (A) 4 h and (B) 18 h after infection and reversed transcribed. Data observed show the expression levels of *GSK3α*. Transcript abundance was determined relative to housekeeping gene *GAPDH*. Data shown are the means ± standard deviation of three independent experiments. The difference in *GSK3α* transcript levels between *M. tuberculosis*- and Δ*ptpA M. tuberculosis*-infected cells was not significant (*p*-value of 0.8868 for A and 0.5193 for B). **, $p < 0.001$. Significant differences were compared by Student's *t* test.

3.1.6 PtpA Dephosphorylates GSK3α Under *In Vivo* Growth Conditions

To further examine GSK3α dephosphorylation by PtpA, we conducted Western blot analyses in which we tested cell extracts from macrophages infected with *M. tuberculosis* and the Δ*ptpA* mutant (Figure 14). The phosphorylation level was monitored using the same anti-phosphoGSK3α (p^{Y279}) antibody used in the Kinetworks™ analysis (Figure 12). As seen in Figure 14, GSK3α phosphorylation levels were found to be higher in extracts obtained from macrophages infected with the Δ*ptpA* mutant compared to macrophages extracts obtained from infection by the parental *M. tuberculosis* strain, confirming our Kinetworks™ analysis screening. We used an anti-GSK3α antibody to confirm that total protein levels of GSK3α was not reduced in the lysates from macrophages infected with *M. tuberculosis* with functional PtpA.

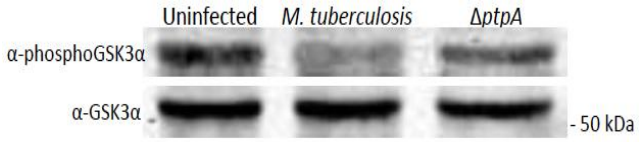

Figure 14. Western Blot Analyses of PtpA Dephosphorylation of GSK3α *In Vivo*
THP-1 cells were infected with *M. tuberculosis* or Δ*ptpA M. tuberculosis*. Cellular extracts were harvested 18 h post-infection and 50 μg were used for Western blotting in which the anti-phosphoGSK3α (p^{Y279}) antibody was utilized. The bottom panel represents the membrane probed with anti-GSK3α. The molecular mass of GSK3α is 50.981 kDa.

To determine whether GSK3α is a direct substrate of PtpA, we used two separate approaches: biochemical assays to monitor catalysis and a protein-protein interaction analysis to determine interaction between the two proteins. Western blot analysis of recombinant GSK3α to which PtpA was added was performed and we showed that Y^{279} is dephosphorylated by PtpA *in vitro* (Figure 15A). To confirm the dephosphorylating effect of PtpA on GSK3α, two Western blot analyses were performed in which the protein-tyrosine phosphatase inhibitors sodium

orthovanadate (Na_3VO_4) (Figure 15B) and BVT 948 (Figure 15C) were added to a GSK3α reaction containing PtpA. Although these are non-specific protein-tyrosine phosphatase inhibitors, their inhibitory effect on PtpA is noticeable bringing the GSK3α Y^{279} phosphorylation level closer to its basal level.

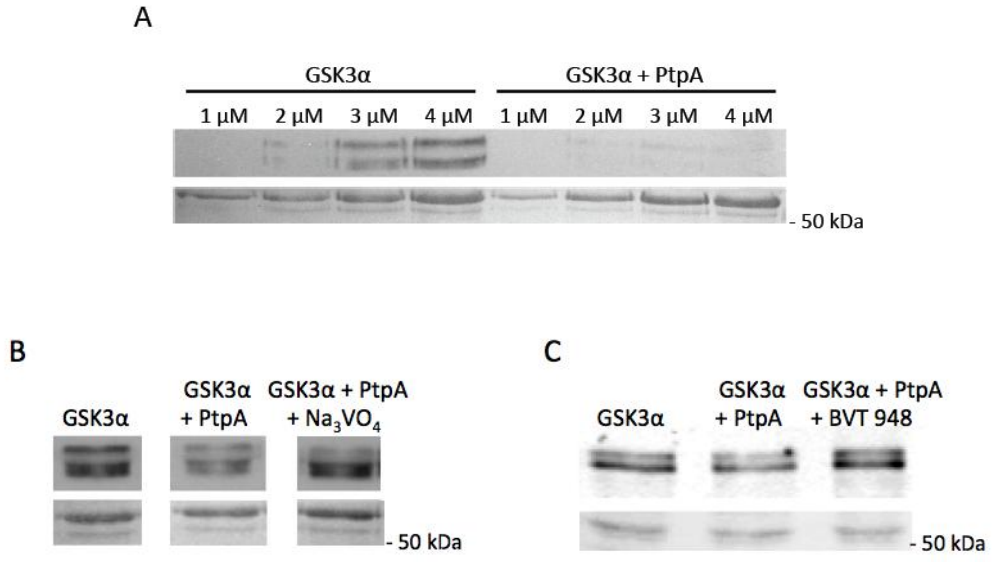

Figure 15. Western Blot Analyses of PtpA Dephosphorylation of GSK3α *In Vitro*
(A) Different concentrations of GSK3α (1, 2, 3 and 4 μM) with and without PtpA (0.04 μM) were incubated and developed by enhanced chemiluminescence. The anti-phosphoGSK3α (p^{Y279}) antibody was utilized. The bottom panel represents the Ponçeau stained membrane showing equal loading of samples. The molecular mass of GSK3α is 50.981 kDa. (B, C) A fixed concentration of GSK3α (3 μM) with and without PtpA (0.04 μM) to which the tyrosine phosphatase inhibitor Na_3VO_4 (1.5 mM) or BVT 948 (5 μM) was added was incubated and developed by enhanced chemiluminescence. The anti-phosphoGSK3α (p^{Y279}) antibody was utilized. The bottom panels represent the Ponçeau stained membranes showing equal loading of the recombinant GSK3α samples.

A more sensitive radioactive assay monitoring GSK3α kinase activity revealed that its autophosphorylation levels were significantly reduced in the presence of recombinant PtpA (Figure 16A). This phenomenon was improved upon addition of the protein-tyrosine phosphatase inhibitor Na_3VO_4 (Figure 16B) and completely reversed by the addition of BVT 948 (Figure

16C). The extent of γ^{32}P-ATP incorporation into GSK3α confirms that GSK3α is a self-phosphorylating autokinase dephosphorylated by PtpA.

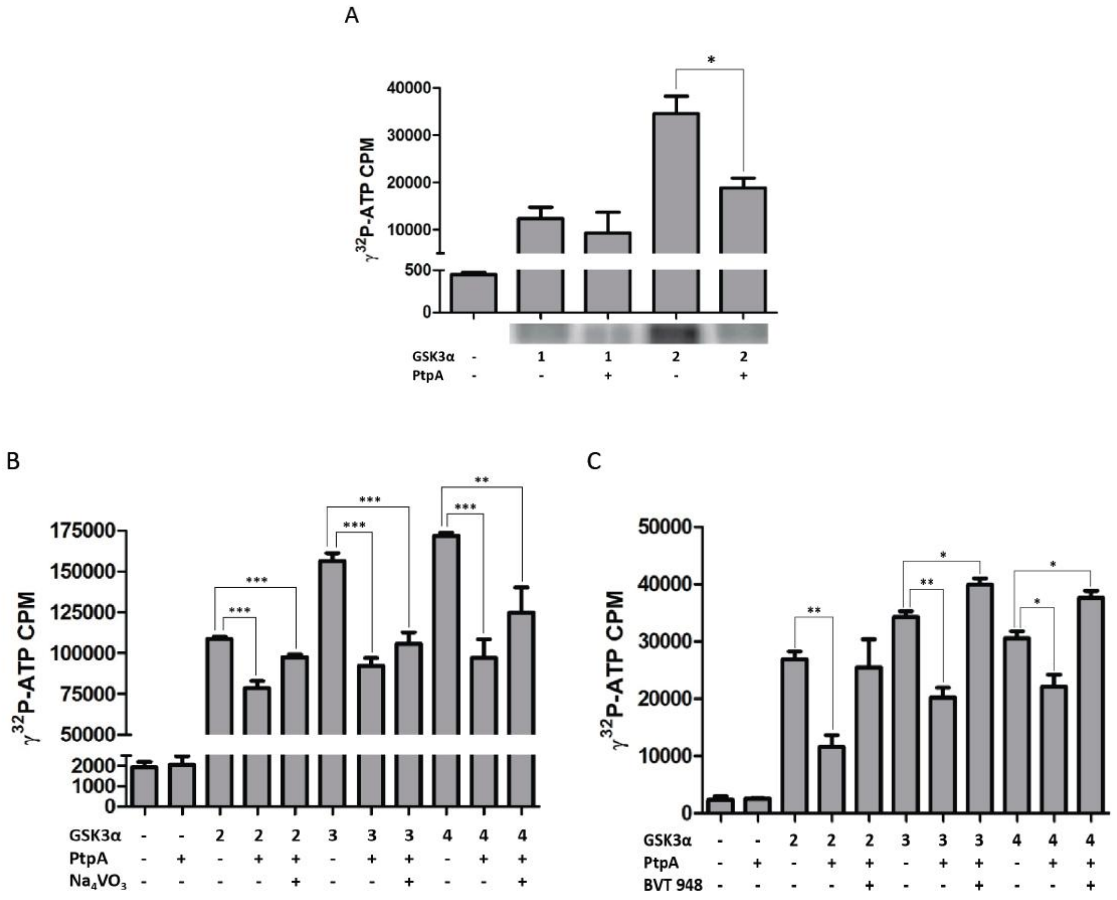

Figure 16. Kinase Assays of PtpA Dephosphorylation of GSK3α *In Vitro*
(A) Dephosphorylation of GSK3α by PtpA was tested in an *in vitro* kinase assay. GSK3α (1 and 2 μM) was autophosphorylated in a kinase buffer containing 10 μCi γ^{32}P-ATP with or without PtpA (0.04 μM) and was resolved onto a 12% SDS gel and exposed to a PhosphorImager screen for radiolabeled band localization. Bands corresponding to phosphorylated GSK3α were cut from the gel, and the radioactive incorporation was measured by a scintillation counter. This graph represents the radioactivity of the dried gel. Results are expressed as ± standard deviation of three independent experiments. The *p*-value of 2 μM GSK3α with PtpA is 0.0214. (B, C) The inhibiting effect of PtpA on GSK3α's activity was tested by radiometric analysis. GSK3α (2, 3 and 4 μM) was autophosphorylated in a reaction containing kinase buffer and 10 μCi γ^{32}P-ATP. PtpA (0.04 μM) and Na_3VO_4 (1.5 mM) or PtpA (0.04 μM) and BVT 948 (5 μM) were added to the sample mixtures and were spotted onto phosphocellulose paper. Radioactivity levels were measured by a scintillation apparatus. *, $p < 0.05$; **, $p < 0.001$; ***, $p < 0.0001$. Significant differences were compared by Student's *t* test.

To assess whether PtpA binds to GSK3α, ALPHAScreen (Amplified Luminescent Proximity Homogeneous Assay), which is used to monitor protein-protein interactions, was performed. Recombinant GSK3α was immobilized to beads by its His-tag while GST-PtpA was immobilized by biotinylation according to the manufacturer's protocol (PerkinElmer). The results show direct and dose-dependent interaction between PtpA and GSK3α (Figure 17). A hyperbolic curve fitting the 1:1 Langmuir binding model and a dissociation constant (K_d) of 4.0 $\times 10^{-9}$ M indicate a high level of affinity between the two proteins. PtpA binding to its known host substrate, hVPS33B, has a similar strength with an assessed K_d value of 2.1 x 10^{-9} M (76).

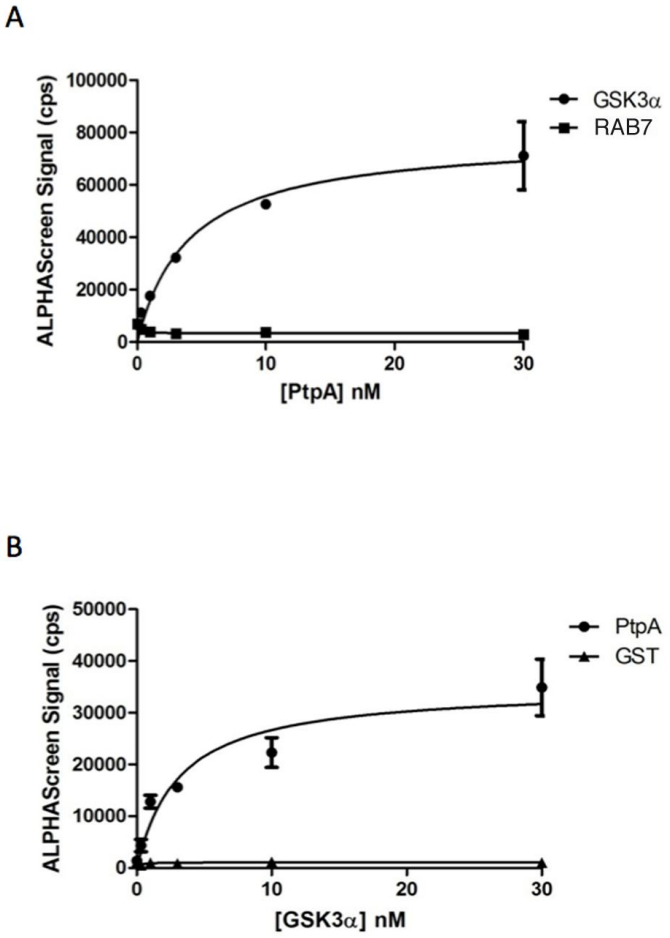

Figure 17. PtpA Interacts with GSK3α *In Vitro*
Protein-protein interaction between GSK3α and PtpA was determined using ALPHAScreen technology. (A) The K_d was calculated using biotinylated PtpA and increasing concentration of His-tagged GSK3α. His-tagged RAB7 protein served as the negative control. Curve fitting yielded a K_d of 4.0 x 10^{-9} M. (B) The reciprocal experiment with increasing concentration of PtpA yielded a K_d of 3.1 x 10^{-9} M. GST was used as negative control.

3.1.7 PtpA Interferes with Host Macrophages Apoptosis Early During Infection

GSK3α plays a key role in the control of cell fate in both pro- and anti-apoptotic manners (158,159). Previous studies have shown that phosphorylation of GSK3α Y^{279} is essential for the full activity of the enzyme (153) and that apoptotic stimuli increase its tyrosine phosphorylation activity (154). Although a low level of phosphorylation can be achieved by autophosphorylation, the protein kinases Mitogen-Activated Protein Kinase Kinase-1/2 (MEK1/2) are the most likely

protein kinases to phosphorylate GSK3α Y^{279} (Dr. Steven Pelech, personal communication). We observed that modulation of GSK3α's tyrosine phosphorylation activity correlates with an interference with apoptosis of the macrophage, the programmed self-destruction process considered to be a major defence mechanism against *M. tuberculosis*.

To investigate whether dephosphorylation of GSK3α Y^{279} by PtpA affected apoptosis, measurements of transcriptional and translational expression levels of the apoptotic executioner, caspase-3, were taken (160). Comparative qPCR levels of caspase-3 were performed on cellular extracts from either uninfected macrophages or infected with *M. tuberculosis*, the Δ*ptpA* mutant or with the complemented Δ*ptpA mutant* (Δ*ptpA*::*ptpA*) where the original *ptpA* gene was reintroduced via a replicative plasmid into the mutant strain. As seen in Figure 18, we observed a significant difference in the expression levels of caspase-3 between cells infected with *M. tuberculosis* and those infected with the Δ*ptpA* mutant. Eighteen hours post-infection, caspase-3 transcription levels were two-fold higher in the Δ*ptpA* mutant-infected macrophages compared to wild-type *M. tuberculosis*-infected macrophages (Figure 18A) indicating that suppression of caspase-3 expression by *M. tuberculosis* is PtpA-dependent early during infection. Caspase-3 expression levels were even lower in macrophages infected with *M. tuberculosis* than in uninfected macrophages. Interestingly, the inhibition of caspase-3 expression was overturned between 18 and 48 h post-infection where the caspase-3 transcript in *M. tuberculosis*-infected macrophages increased, surpassing its levels in the Δ*ptpA* mutant-infected macrophages (Figure 18B). This turn of events indicated that PtpA interference with the apoptotic pathway is transient and macrophages are capable of initiating apoptosis regardless of the presence of PtpA.

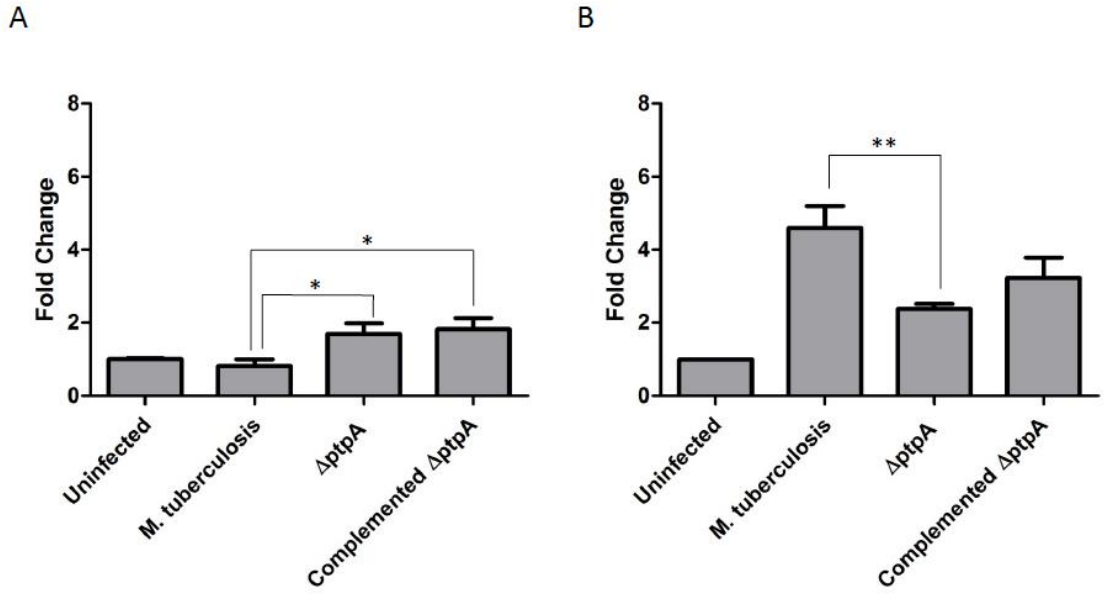

Figure 18. PtpA Reduces Trancriptional Levels of Caspase-3 Early in Infection
Quantitative PCR analysis comparing mRNA levels of caspase-3 from different infection conditions. RNA from uninfected and treated THP-1 cells (treated with *M. tuberculosis,* Δ*ptpA M. tuberculosis* and Δ*ptpA::ptpA M. tuberculosis*) was extracted (A) 18 h and (B) 48 h after infection and reversed transcribed. Data observed show the expression levels of caspase-3. Transcript abundance was determined relative to housekeeping gene *GAPDH*. Data shown are the means ± standard deviation of three independent experiments. The difference in transcript levels in cells infected with *M. tuberculosis* and Δ*ptpA M. tuberculosis* 18 and 48 h post-infection were significant (*p*-value of 0.0179 for A and 0.0097 for B). *, $p < 0.05$; **, $p < 0.001$. Significant differences were compared by Student's *t* test.

3.1.8 *M. tuberculosis* Blocks Proteolytic Cleavage of Inactive Caspase-3 into Active Caspase-3

To test whether PtpA's dephosphorylation of GSK3α resulted in modulation of caspase-3 activity, we monitored caspase-3 proteolytic degradation using the anti-caspase-3 antibody. As seen in Figure 19, *M. tuberculosis* infection inhibited the cleavage of inactive caspase-3 (31.6 kDa) into its active forms (17/19 kDa). Cellular extracts from uninfected cells and from cells infected with the Δ*ptpA* mutant showed both active and inactive caspase-3 whereas those from *M. tuberculosis*-infected macrophages showed only inactive caspase-3. Macrophages infected

with the Δ*ptpA*::*ptpA* strain showed similar activation of caspase-3 to macrophages infected with the Δ*ptpA* mutant strain, indicating that the observed effect of the complemented strain is not optimal and in agreement with other complementation phenotypes we have observed (76,161). Complementation of the Δ*ptpA* mutant strain was done using epichromosomal plasmid to reintroduce the *ptpA* gene to the genome. As observed in Figure 19, the Δ*ptpA*::*ptpA* strain does not exhibit a wild-type phenotype, but rather a Δ*ptpA* phenoptype. Since we know little about *ptpA* regulation of gene expression, it is possible that the plasmid did not get expressed from this plasmid. Moreover, the last step of specialized transduction, which was used to generate the original Δ*ptpA* mutant (76), requires alteration of the entire locus within *M. tuberculosis* genome which may have resulted in deletion of regulatory elements needed for full PtpA expression.

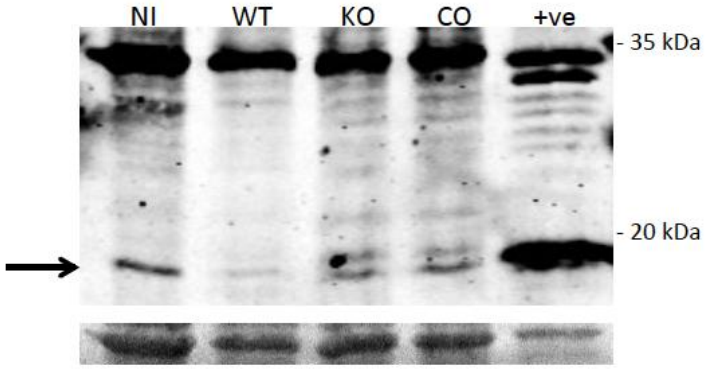

Figure 19. *M. tuberculosis* Blocks Activation of Caspase-3 *In Vivo*
THP-1 cells were uninfected (NI), infected with *M. tuberculosis* (WT), the Δ*ptpA* mutant (KO) or the complement Δ*ptpA* mutant (CO) and cellular extracts were harvested 48 h post-infection. A total of 50 μg of cellular extract were used for Western blotting in which the anti-caspase-3 antibody was utilized. The molecular mass of inactive caspase-3 is 31.608 kDa and 17/19 kDa for active caspase-3. The cellular extract of RAW 264.7 cells treated with 5 μM staurosporine for 5 h was used as the positive control (+ve). The bottom panel represents the Ponçeau stained membrane showing equal loading of samples.

3.2 Global Proteomic Analyses of Macrophage Response to *M. tuberculosis* Infection

3.2.1 Introduction

M. tuberculosis possesses multiple strategies to subvert recognition by the immune response. To better understand the evasive nature of the tubercle bacilli and its molecular manifest on the macrophage response to infection, we compared the proteome, i.e. the global protein expression profile, of macrophages infected with *M. tuberculosis* H37Rv to that of uninfected macrophages. In addition, due to its role in pathogenesis (76,88,148), we further extended our study to identifying the contribution of PtpA to the macrophage response by comparing the proteome of macrophages infected with the mutant Δ*ptpA M. tuberculosis* to that of macrophages infected with the parental *M. tuberculosis* strain.

In total, four independent proteomic experiments were performed and 9,784 host proteins were detected. Using a number of statistical methods (Section 2.14), we identified 27 proteins whose expression ratios lie outside of a 90% confidence interval about the mean. The majority of these proteins belong to functional classes as diverse as chromatin remodeling and transcription regulation, protein synthesis, immunity and defence, and cell signalling. We verified some of our findings by selecting five proteins whose expression showed significant modulation by infection for quantitative PCR for transcriptional analysis and Western blot for validation of protein expression. In addition, the contribution of the *M. tuberculosis* secreted virulence factor PtpA was assessed and showed a pronounced PtpA-dependent modulation of 11 proteins involved in RNA metabolism, immunity and defence, and cellular respiration.

3.2.2 Modulation of Host Protein Expression in Response to *M. tuberculosis*

Four independent sets of THP-1 cells infected with *M. tuberculosis* and the corresponding controls were analyzed by iTRAQ resulting in the detection of 42,007 peptides from cellular extracts of macrophages and in the identification of 9,784 proteins. After removing the repeats, 4,868 distinct proteins were identified. To determine the general effects of *M. tuberculosis* on host protein expression levels, assessment of expression ratios of identified proteins comparing uninfected to infected macrophages was performed using two-sided *t* tests for each sample‘s log-ratios. Using this approach we identified a total of 845 proteins in all four independent experiments.

Disparity in values obtained for the expression ratios was observed between experiments (Figure 20A); in three of the four infection experiments, infected versus uninfected log-ratios displayed a mean and a 95% confidence interval below zero. Log-ratios in the fourth experiment displayed a mean and 95% confidence interval above zero. Thus, we normalized the data so that each sample has a standard deviation of approximately one and a mean of zero (Figure 20B). In this manner, the relative modulation of protein expression could be measured in relation to all other proteins in the same experiment, across samples and between independent experiments.

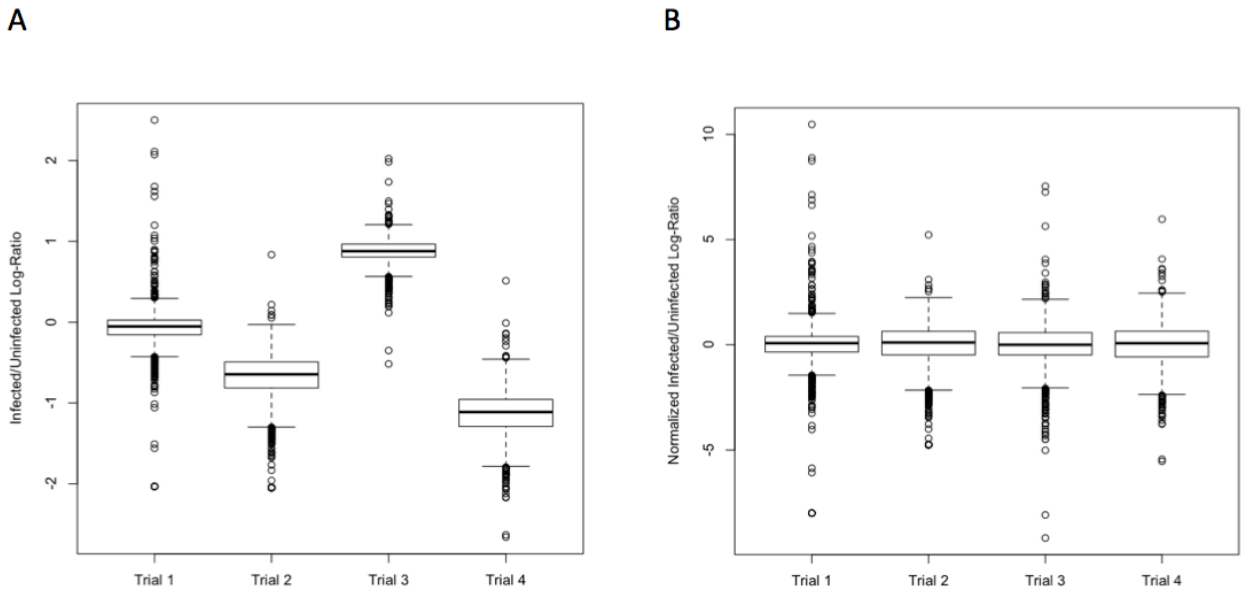

Figure 20. Boxplots of Host Proteins Obtained from Infected Versus Uninfected Macrophages

Log-ratios measured 4 h post-infection. (A) Log-ratios for four trials of experiments where ratios are between *M. tuberculosis*-infected and uninfected macrophages. (B) Normalized log-ratios for four trials of experiments where ratios are between *M. tuberculosis*-infected and uninfected macrophages. Each sample is normalized to have a mean and a standard deviation of approximately zero and one, respectively.

To study the effect of *M. tuberculosis* on the macrophage proteome, three different strains were used for the infection experiments; the wild-type H37Rv strain (WT), the gene knockout strain Δ*ptpA M. tuberculosis* (KO), and the corresponding complemented strain (CO). We identified proteins that are either consistently up- or down-regulated for each of the strains and determined their expression levels by means of the ratio between infected over uninfected macrophages. The ratios were plotted against one another for each individual sample. We observed that up-regulated proteins (Figures 21A and 21C) show a strong linear relationship between each ratio indicating that upon independent *M. tuberculosis* infection, similar proteins become up-regulated at similar rates. Alternatively, there appears to be a lack of linearity of the macrophage response in terms of down-regulated protein levels (Figures 21B and 21D).

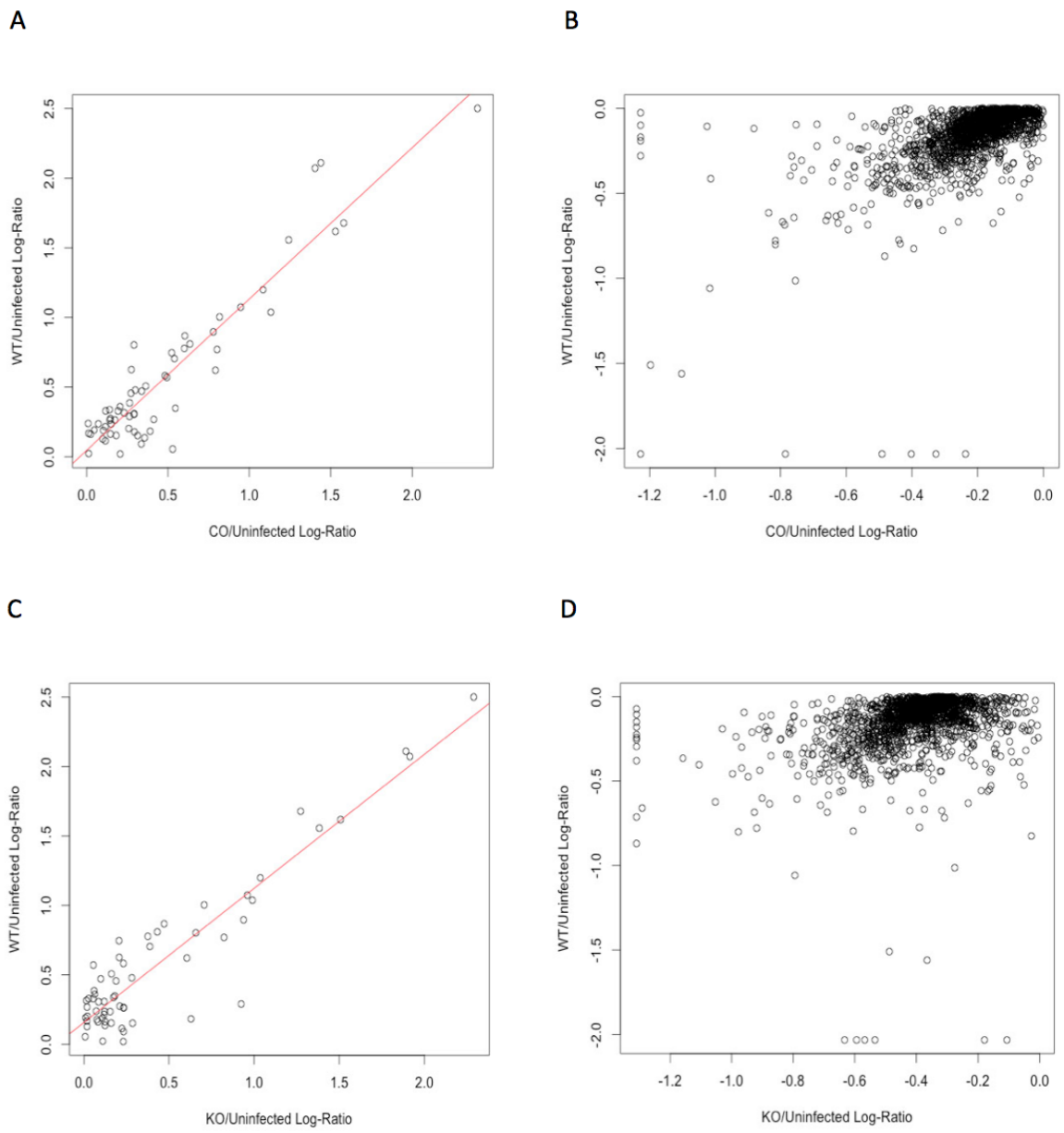

Figure 21. *M. tuberculosis*-Modulation of Host Protein Expression
Proteins for which the infected to uninfected expression ratios are above and below the mean 4 h post-infection. (A) The *M. tuberculosis*/Δ*ptpA*::*ptpA M. tuberculosis* log-ratio is plotted and shows a strong linear relationship between these expression ratios for up-regulated proteins. (B) The *M. tuberculosis*/Δ*ptpA*::*ptpA M. tuberculosis* log-ratio is plotted and shows little to no linear relationship between these expression ratios for down-regulated proteins. (C) The *M. tuberculosis*/Δ*ptpA M. tuberculosis* log-ratio is plotted and shows a strong linear relationship between these expression ratios for up-regulated proteins. (D) The *M. tuberculosis*/Δ*ptpA M. tuberculosis* log-ratio is plotted and shows little to no linear relationship between these expression ratios for down-regulated proteins. Proteins for which one of these ratios was not present in the sample were not included.

3.2.3 Identification of Macrophage Proteins Modulated by *M. tuberculosis* Infection

To identify host proteins modulated by *M. tuberculosis* infection, we plotted the average infected over uninfected expression level ratios of the 845 distinct proteins. We then determined the statistically relevant proteins by selecting those whose average expression level ratios fell outside of ±1 standard deviation from the global mean for at least three of the four experiments (Table 5). We further shortlisted proteins by taking the mean ratio for each protein over all four trials and excluded those whose ratios were within 1.8 standard deviations of the mean (Table 5). Using these two methods, we identified 27 unique biomarker proteins to be modulated in *M. tuberculosis* infection (Figure 22, Table 5).

Up-Regulated Proteins						Down-Regulated Proteins					
Proteins	**Num. of Peptides**	**Avg. Normalized Inf./Uninf. Ratio**	***p*-value**	**SD**	**Involved in Infection (Ref.)**	**Proteins**	**Num. of Peptides**	**Avg. Normalized Inf./Uninf. Ratio**	***p*-value**	**SD**	**Involved in Infection (Ref.)**
GPNMB	2	1.26	0.1836	1.4664	(162)	DOCK10	2	-1.77	0.1307	1.7113	
SNRPD1	2	2.05	0.0299	1.0531		**CTSG**	6	-1.91	0.3969	3.8686	(164)
HMGN2	3	1.16	0.2011	1.4271	(163)	ADRBK1	5	-1.33	0.0535	0.8619	(165)
ICAM1	6	2.16	0.1018	1.8507	(166,167)	RANBP2	8	-1.40	0.0519	0.8951	(168)
H2AFZ	4	1.56	0.0355	0.8525		ITPR1	4	-1.10	0.2812	1.6859	(170)
ATP5D	2	1.12	0.0091	0.3700	(169)	CEP170	3	-1.53	0.0367	0.8469	
RPL23A	4	1.52	0.0019	0.2920		ARHGEF2	5	-1.19	0.0903	0.9619	(171)
HIST1H4	8	1.54	0.0809	1.1920	(85)	NCAPG	2	-1.06	0.1538	1.1115	
FAU	1	1.33	0.0059	0.3786		**BIRC6**	2	-2.28	0.0804	1.7579	(179)
IL25	2	0.53	0.4318	1.1594	(172-174)	WDR3	2	-1.31	0.2572	1.8737	
DPY30	2	0.88	0.0967	0.7349		MIF	3	-1.97	0.0804	2.5254	(180)
GRPEL1	2	1.17	0.0166	0.4796							
FIS1	1	1.18	0.0444	0.7091	(175)						
CHTOP	2	1.39	0.0649	0.9750							
IL1β	4	2.24	0.2461	3.1216	(176,177)						
SOD2	7	1.92	0.0776	1.4506	(176,178)						

Table 5. *M. tuberculosis*-Infected Macrophage Proteins Modulated One Standard Deviation Above or Below the Mean
This list was obtained by eliminating all proteins for which less than three sample ratios were within one standard deviation of the mean. Proteins in bold are proteins for which the average standardized *M. tuberculosis*/uninfected ratio (over all samples) was above or below 1.8 standard deviations of the mean. For each protein, two-tailed *p*-values were calculated using a *t* test over the four trials. *p*-value < 0.05 indicates significance at the 95% level. *p*-value < 0.1 indicates significance at the 90% level.

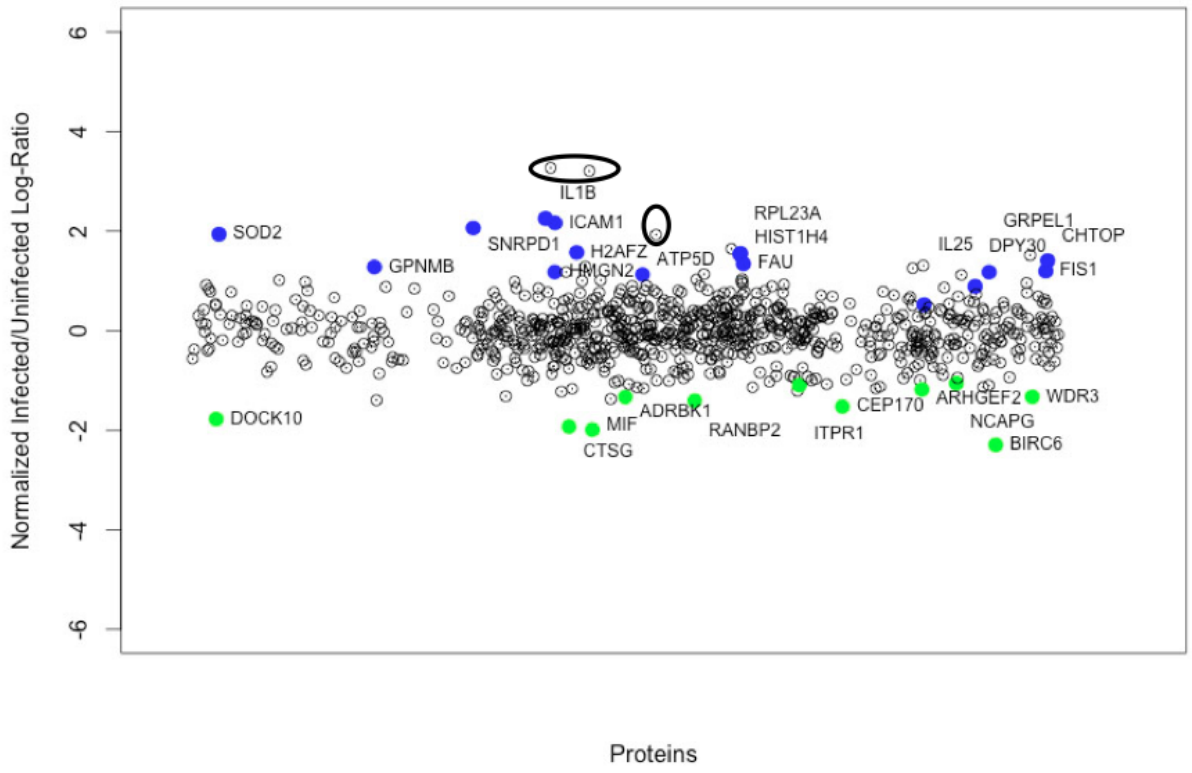

Figure 22. Global Expression Level Scatterplot of Normalized Infected Versus Uninfected Log-Ratios
Includes 845 proteins detected in all four trials of the experiments where highlighted proteins are those with mean expression ratios above or below a one standard deviation confidence interval about the mean. Blue dots correspond to up-regulated proteins, and green dots correspond to down-regulated, as per Table 5. The extreme values marked by a circle were determined to be contaminants (P35527, P04264, P13645).

Sixteen of the identified proteins were previously reported to be involved in the macrophage response to microbial infections. Up-regulated proteins include the innate immune proteins Superoxide Dismutase-2 (SOD2) (176,178), Intercellular Adhesion Molecule-1 (ICAM1) (166,167), and Interleukin-1β (IL1β) (176,177). Among known down-regulated proteins, we recognized Cathepsin G (CTSG) (164), Migration Inhibitory Factor (MIF) (180), and IAP Repeat-Containing Protein-6 (BIRC6) (179).

Eleven proteins were never previously shown to be associated with or affected by infection. These include the up-regulated RNA metabolism protein Small Nuclear Ribonucleoprotein Sm D1 (SNRPD1) and the chromatin remodeling and transcription protein Histone H2A (H2AFZ), and the down-regulated signalling protein Dedicator of Cytokinesis Protein-10 (DOCK10).

3.2.4 Validation of Proteomics Expression Levels

To experimentally validate our findings, we selected five representative proteins, previously reported to be modulated in microbial infections, from those listed in Table 5 and compared our iTRAQ findings to those obtained from either Western blot analysis (for protein levels) or quantitative PCR (qPCR for transcription levels).

Western analysis was conducted for ICAM1, IL1β and CTSG. Based on the iTRAQ results (Table 5), protein levels of ICAM1 and IL1β were expected to be up-regulated in infected cells and those of CTSG, to be down-regulated. As anticipated, levels of ICAM1 and IL1β in *M. tuberculosis*-infected cells were up-regulated (Figure 23A-B) correlating with and confirming the modulations observed in our proteomic analyses. However, as seen in Figure 23C, in contrast to our iTRAQ findings, CTSG levels remained unchanged when comparing infected to uninfected macrophages.

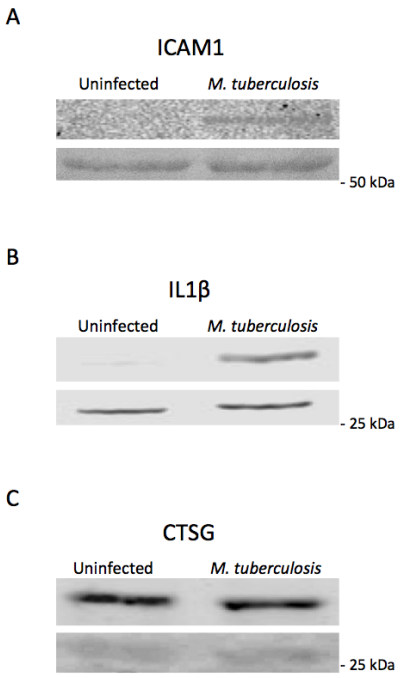

Figure 23. Western Blot Analyses of *M. tuberculosis*-Dependent Host Protein Expression Levels
THP-1 cells were infected with *M. tuberculosis* and cellular extracts were harvested 4 h post-infection. A total of 100 µg of cellular extract were employed for Western blotting in which (A) anti-ICAM1, (B) anti-IL1β, and (C) anti-CTSG antibodies were utilized. The molecular mass of ICAM1 is 57.825 kDa, of IL1β is 30.748 kDa, and of CTSG is 28.837 kDa. The bottom panels represent the Ponçeau stained membrane showing equal loading of samples.

The mRNA levels of *ICAM1*, *IL1β, SOD2*, *CTSG*, and *MIF* were quantified by qPCR. The average mRNA fold change was assessed 2, 4 and 18 h post-infection and was compared to the relative change in protein levels observed in the corresponding iTRAQ experiments. As seen in Figure 24, qPCR analysis revealed up-regulation in mRNA levels of *ICAM1*, *IL1β* and *SOD2* in cells infected with *M. tuberculosis* 4 h post-infection (Figure 24A-C). The increase in mRNA abundance correlates with our proteomic data (Table 5). Transcription levels of *CTSG* and *MIF* in infected cells were unchanged contradicting the proteomic results that detected down-regulation 4 h post-infection (Figure 24D-E, Table 5). Levels of *CTSG* mRNA remained

unchanged in infected macrophages and increased 18 h post-infection (Figure 24D) while mRNA levels of *MIF* showed no significant change in any of the time points monitored (Figure 24E).

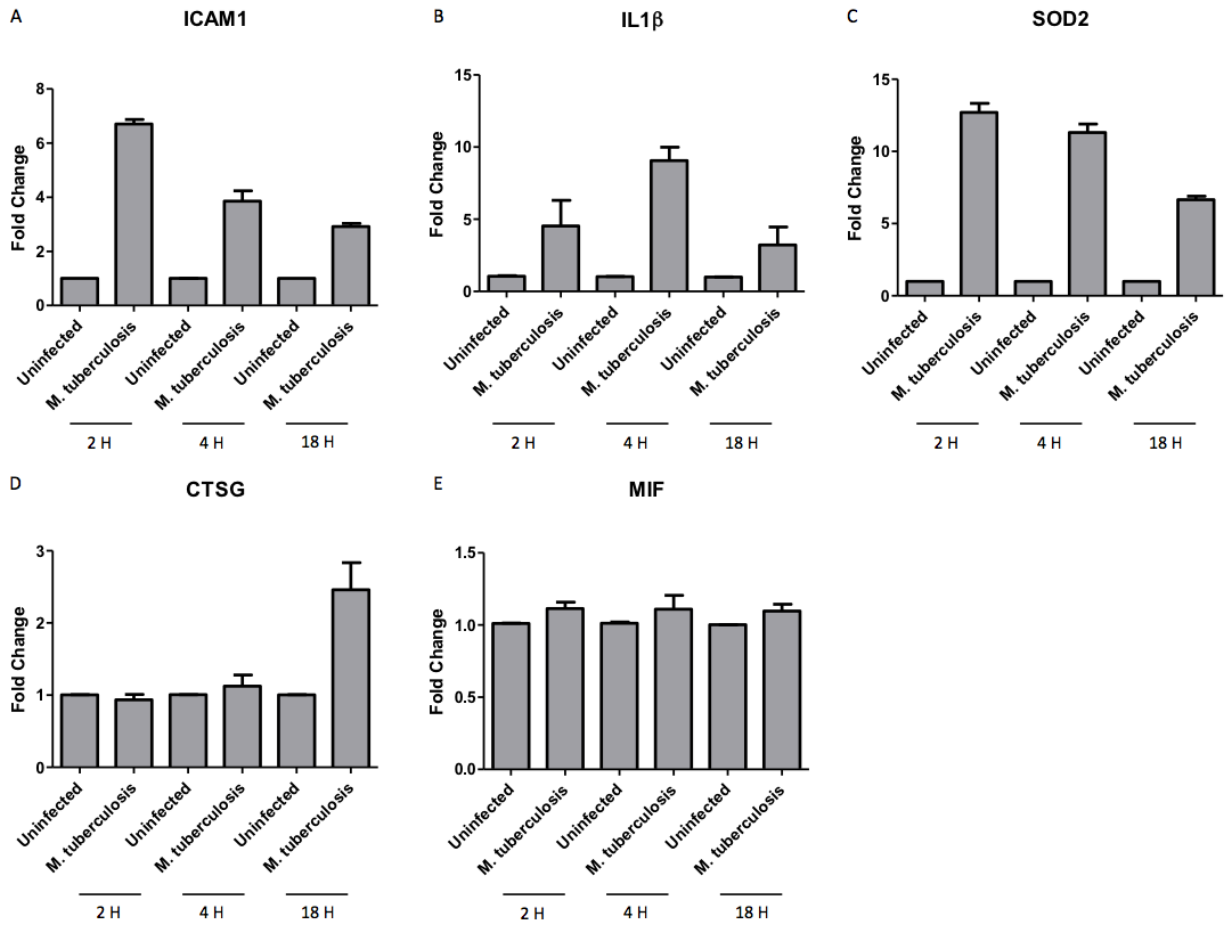

Figure 24. Transcriptional Levels of Five *M. tuberculosis*-Modulated Proteins
Quantitative PCR analysis comparing mRNA levels of (A) *ICAM1*, (B) *IL1β*, (C) *SOD2*, (D) *CTSG* and (E) *MIF* from uninfected and infected cells. RNA from uninfected and *M. tuberculosis*-infected THP-1 cells was extracted 2, 4 and 18 h after infection and reversed transcribed. Data observed show the expression levels of all genes. Transcript abundance was determined relative to the housekeeping gene *GAPDH*. Data shown are the means ± standard deviation of three independent experiments.

3.2.5 PtpA Effect on Macrophage Protein Expression Levels

To assess the contribution of PtpA to the macrophage's response to infection, we compared the macrophage proteome in response to infection with WT or Δ*ptpA* KO strains 4 h post-infection and normalized the data as described above to give each sample a mean of zero and a standard deviation of approximately one (Figure 25A-B).

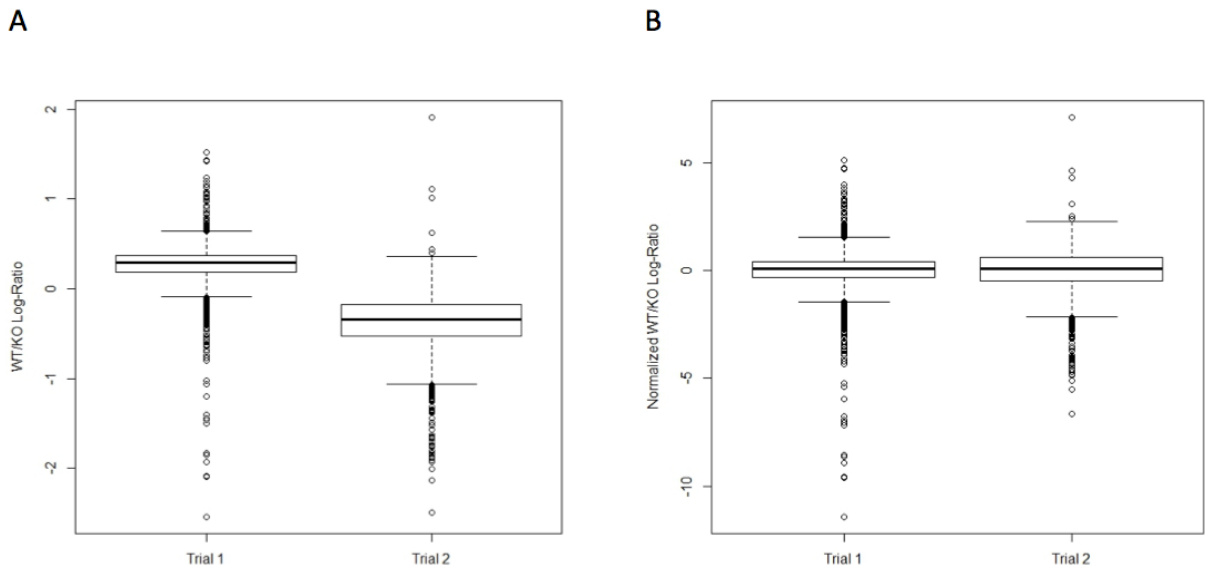

Figure 25. Boxplots of Host Proteins Obtained from Infected Versus Uninfected Macrophages
Log-ratios measured 4 h post-infection. (A) Log-ratios for two trials of experiments where ratios are between *M. tuberculosis*- and Δ*ptpA M. tuberculosis*-infected macrophages. (B) Normalized log-ratios for two trials of experiments where ratios are between *M. tuberculosis*- and Δ*ptpA M. tuberculosis*-infected macrophages. Each sample is normalized to have a mean and a standard deviation of approximately zero and one respectively.

In total, we identified 1,281 proteins with 11 macrophage proteins whose expression ratios fell outside of a ±1.8 standard deviation interval for macrophages infected with the KO strain (Figure 26, Table 6). Among these PtpA-dependent proteins, three have previously been reported to be involved in the infection process; the up-regulated stress response protein Cold-

Inducible RNA-Binding Protein (CIRBP) (181), and the down-regulated cell death regulator Glycogen Synthase Kinase-3 Alpha (GSK3α) (182), and transporter ATP-Binding Cassette Sub-Family B Member 1 (ABCB10) (183). GSK3α is the only PtpA-dependent protein that has been identified before to be involved in mycobacterial infections (148,184-186). Among the eight other proteins, the most modulated ones include the down-regulated RNA metabolism protein splicing factor U4/U6 Small Nuclear Ribonucleoprotein Prp31 (PRPF31), and protein synthesis protein tRNA synthetase Seryl-tRNA Synthetase-2 (SARS2).

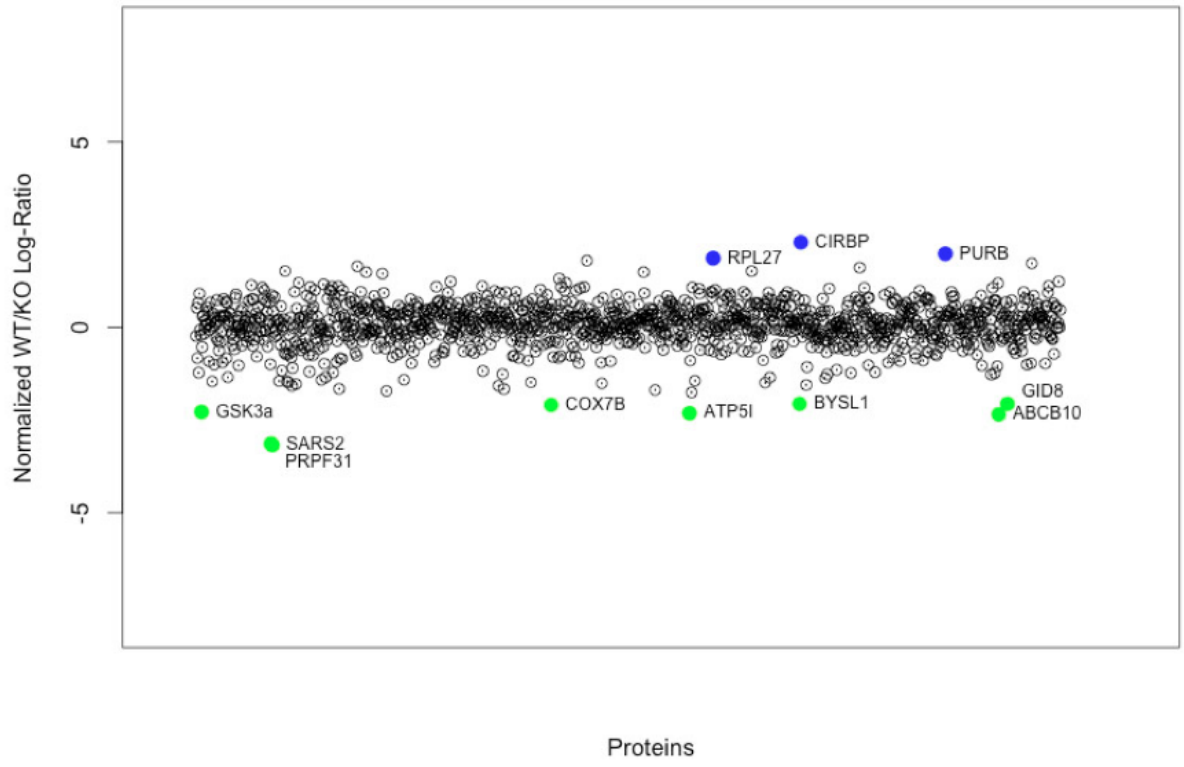

Figure 26. Global Expression Level Scatterplot of Normalized *M. tuberculosis* Versus Δ*ptpA M. tuberculosis* Log-Ratios
Includes 1,281 proteins detected in two trials of the experiments. Highlighted proteins are those with mean *M. tuberculosis*/Δ*ptpA M. tuberculosis* ratios above or below a 1.8 standard deviation confidence interval about the mean. Blue dots correspond to up-regulated proteins, and green dots correspond to down-regulated proteins, as per Table 6.

Up-Regulated Proteins						Down-Regulated Proteins					
Proteins	**Num. of Peptides**	**Avg. Normalized WT/KO Ratio**	***p*-value**	**SD**	**Involved in Infection (Ref.)**	**Proteins**	**Num. of Peptides**	**Avg. Normalized WT/KO Ratio**	***p*-value**	**SD**	**Involved in Infection (Ref.)**
RPL27	2	1.86	0.2470	1.0763		GSK3α	1	-2.28	0.5163	3.4015	(148,182,184-186)
CIRBP	2	2.29	0.2589	1.3966	(181)	PRPF31	2	-3.14	0.5464	5.1394	
PURB	1	1.98	0.3189	1.5345		SARS2	3	-3.18	0.5523	5.3055	
						COX7B	1	-2.10	0.6820	5.4357	
						ATP5I	2	-2.32	0.4905	3.1823	
						BYSL1	2	-2.07	0.1992	0.9451	
						ABCB10	2	-2.35	0.4462	2.8042	(183)
						GID8	3	-2.07	0.5259	3.1700	

Table 6. Δ*ptpA M. tuberculosis*-Infected Macrophage Proteins Modulated 1.8 Standard Deviations Above or Below the Mean
The list was obtained using two methods: (i) eliminating all proteins for which the *M. tuberculosis*/Δ*ptpA M. tuberculosis* sample ratios were within 1.8 standard deviations of the mean for both samples, and (ii) eliminating all proteins for which the mean *M. tuberculosis*/Δ*ptpA M. tuberculosis* ratio was within the ±1.8 standard deviation interval about the mean. For each protein, two-tailed *p*-values were calculated using a *t* test over the two trials. *p*-value < 0.05 indicates significance at the 95% level. *p*-value < 0.1 indicates significance at the 90% level.

Chapter 4: Discussion

4.1 *M. tuberculosis* PtpA Inhibits Host Apoptosis Early During Infection

M. tuberculosis pathogenicity relies upon its ability to sense changes in the environment and respond to host defence assaults. One of the ways to do so is by actively interfering with macrophage physiological pathways (187). One specific strategy utilizes the secreted phosphatase, PtpA, to block both phagosome maturation and acidification (76,88); two key processes required for digestion of invading microorganisms and initiation of an adaptive immune response (47).

Earlier studies from our laboratory showed that several regulatory phosphoproteins in diverse signalling pathways in macrophages changed significantly in their phosphorylation status upon mycobacterial infection (186). Following the rationale that some of these changes are dependent on *M. tuberculosis*' PtpA, we comparatively monitored PtpA's contribution to the phosphorylation status of key human signal transduction proteins during *M. tuberculosis* infection. We have now shown that PtpA modulates global phosphorylation patterns of macrophage proteins and that these modulations can impact the fate of the host cell.

The original phosphoproteome analysis that we performed compared the effect of infecting macrophages with live or dead *Mycobacterium bovis* BCG on phosphoprotein levels (186). Notably, Glycogen Synthase Kinase-3 Beta (GSK3β) was amongst the most phosphorylated proteins upon *M. bovis* BCG infection (186). Interestingly, the phosphorylation pattern of the *M. bovis* BCG and the *M. tuberculosis* phosphoproteome analyses (Figure 12, Table 4) showed some contradicting results exemplified by GSK3α and GSK3β. In the *M. bovis*

BCG phosphoproteome analysis, GSK3α and GSK3β were hyperphosphorylated on $Y^{279/216}$ in cells infected with live *M. bovis* BCG with a fold change of 1.29 and 1.57, respectively, compared to the uninfected control cells (186). In the *M. tuberculosis* phosphoproteome analysis, GSK3α and GSK3β showed reduced phosphorylation in infected cells compared to uninfected cells and had a fold change of 0.51 and 0.66, respectively (Table 4). This discrepancy can be attributed to the genotypic differences of the two strains as *M. bovis* BCG is an avirulent vaccine strain (188). It is also well documented that macrophages respond differently to *M. bovis* BCG than they do to *M. tuberculosis* (189). PtpA is expressed in *M. bovis* BCG (87), but its function is still under investigation. Potential reduction or absence of secreted PtpA in this vaccine strain could explain the hyperphosphorylation occurring in macrophages harbouring this non-virulent strain.

It is worth noting that in comparison to uninfected cells, the relative fold change of the GSK3 isoforms in macrophages infected with Δ*ptpA M. tuberculosis* resembled that of the isoforms in macrophages infected with live *M. bovis* BCG. In fact, an increase in phosphorylation for GSK3α (fold change of 1.54) and for GSK3β (1.07) is observed in macrophages infected with Δ*ptpA M. tuberculosis* when compared to the phosphorylation status of these isoforms in uninfected macrophages (Table 4). This data is similar to the results obtained from our previous phosphoproteome analysis when comparing the phosphorylation status of the isoforms in *M. bovis* BCG-infected cells versus uninfected cells (186). Moreover, PKCα/β2, PKCδ, and RAF1 also had a similar relative fold change in Δ*ptpA M. tuberculosis*- and *M. bovis* BCG-infected macrophages when compared to uninfected macrophages (Table 4)

(186). It appears that the attenuation caused by the Δ*ptpA* mutation (76) makes the mutant strain behave more like the avirulent *M. bovis* BCG strain.

The observed dephosphorylation of GSK3α and GSK3β provided the first evidence that PtpA may be involved in apoptosis; an effective defence strategy employed by the immune system to limit the growth of intracellular pathogens. More than two decades ago, apoptosis was first recognized to be manipulated by intracellular pathogens to their own advantage (190,191). Apoptosis, as a host defence mechanism, plays such a crucial role in the destruction of microorganisms. Throughout evolution, pathogens have acquired apoptosis-modulating genes (29). GSK3α and GSK3β play an essential role in the regulation of the apoptotic pathway. Studies have shown that phosphorylation of GSK3 $Y^{279/216}$ is critical for the full activation of these kinases (153) and the induction of apoptosis (154,192,193). We have shown that infection of macrophages with an attenuated mycobacterial strain increases phosphorylation of GSK3 $Y^{279/216}$ (186), indicating that macrophages are primed for apoptosis. On the one hand, results from both phosphoproteome analyses indicate that the apoptotic pathway is turned on in macrophages infected with the attenuated strains, i.e. in *M. bovis* BCG and Δ*ptpA* *M. tuberculosis*, via phosphorylation of GSK3α and GSK3β $Y^{279/216}$. On the other hand, we have demonstrated that the virulent strain *M. tuberculosis* H37Rv inactivates GSK3α and GSK3β by dephosphorylation of $Y^{279/216}$, which promotes survival of the host cell (Table 4).

Several *in vitro* studies revealed that the rate of apoptosis is increased in macrophages infected with mycobacteria (194,195). However, virulent strains of mycobacteria were shown to minimize apoptosis of macrophages in comparison to avirulent or attenuated strains (29,57),

reinforcing the idea that *M. tuberculosis* has developed strategies to block apoptosis to promote its survival within the host cell. The ability of *M. tuberculosis* to block apoptosis is of great importance for the pathogen as death of the host cell restricts its supportive growth environment (29). In agreement with this, we demonstrated that GSK3α dephosphorylation of Y^{279} could be interpreted as an anti-apoptotic feature of this pathogen.

To confirm the role of PtpA in inhibiting macrophage apoptosis, we measured transcriptional levels of caspase-3, a protease that plays a critical role in the execution-phase of apoptosis of the host, and showed that mRNA levels of caspase-3 were significantly reduced in *M. tuberculosis*-infected cells (Figure 18). This indicates that *M. tuberculosis* blocks early expression of caspase-3 to prevent apoptosis. Moreover, we showed that a significant difference in caspase-3 transcript levels existed between cells infected with *M. tuberculosis* and those infected with Δ*ptpA M. tuberculosis* (Figure 18A) confirming that inhibition of caspase-3 gene expression is, in part, dependent on PtpA. The increased caspase-3 gene expression in the Δ*ptpA* mutant may be a result of the mutant's attenuated phenotype.

Dephosphorylation of host GSK3α by PtpA leads to prevention of host cell apoptosis during early stages of infection. In fact, PtpA's anti-apoptotic role lessens at later stages of infection (Figure 18B), but does not necessarily signify resumption of host macrophages apoptosis. Indeed, we found that proteolytic cleavage of caspase-3 in *M. tuberculosis*-infected macrophages is blocked 48 h post-infection despite PtpA's non-engagement. On the one hand, as shown in Figure 19, inactive caspase-3 is expressed in all four treatments, but is only cleaved to active caspase-3 in two treatments: in uninfected cells and in cells infected with Δ*ptpA*

M. tuberculosis. On the other hand, macrophages infected with *M. tuberculosis* and the complemented mutant strain show no cleavage and limited cleavage of caspase-3, respectively.

The inhibition of apoptosis by virulent strains of mycobacteria is a long-established paradigm. Virulent *M. tuberculosis* secretes bacterial proteins that inhibit apoptosis of the macrophage to promote immortality of the host cell (29). The identification of these proteins is essential to understand the pathogenesis of TB and to understand how these effectors manipulate the host defence mechanism. To date, only a few *M. tuberculosis* virulence factors have been reported to inhibit apoptosis. We present evidence that the inhibition of apoptosis of the host macrophage early in infection is directly attributed to *M. tuberculosis* secreted protein PtpA, which inhibits the cleaving of inactive pro-caspase-3 into active caspase-3. Other yet to be identified *M. tuberculosis* proteins may also be involved in this process. This provides novel insight into *M. tuberculosis*' pathogenicity within macrophages and better mechanistic understanding of how it is able to circumvent the macrophage's killing machinery.

In addition to its role in apoptosis and phagosome maturation, we have shown that PtpA is a versatile virulence factor that influences several signalling pathways to facilitate and maximize replication and intracellular survival. As illustrated in Figure 12 and Table 4, PtpA modulates the phosphorylation status of several signalling proteins such as RAF1, PKCδ, GSK3β, PKCα/β2, MSK1, PKCα, PKR1, and Src (148). Moreover, *in vitro* phosphorylation analysis of macrophage proteins by recombinant PtpA resulted in the identification of multiple host signalling substrates including hVPS33B, a cognate PtpA substrate we had identified before

(Figure 11, Table 3) (76,148). Future experiments will reveal the multifaceted characteristics of PtpA mechanisms enabling *M. tuberculosis*' invasion and survival inside the macrophage.

4.2 *M. tuberculosis* Causes Concerted Up-Regulation and Random Down-Regulation of Host Macrophage Proteins

In recent years, several large-scale expression studies investigating global transcriptional responses of macrophages exposed to *M. tuberculosis* have been performed (157,176,196-208). The emergence of these studies has undeniably contributed to a better understanding of the extent of transcriptomic reprogramming of the macrophage during mycobacterial infection. However, a broader systems-biology approach would provide a better understanding of TB specific host-pathogen interactions and insights into the macrophage biology. Furthermore, understanding the mechanisms by which *M. tuberculosis* manipulates the host response could provide fertile grounds for novel interventions by means of chemotherapy or vaccine development, especially with the targeting of the most consistent protein changes in infected macrophages. Proteomics provides us with a higher level of understanding of biological functions than transcriptomic analysis as it takes into account protein levels, post-translational modifications and stability, as well as protein subcellular localization.

In this study, we provided insight into the macrophage's global response to *M. tuberculosis* infection using a quantitative proteomic approach, and show how the specific virulence factor, PtpA, affects the macrophage proteome. Our first finding indicated that the macrophage acts mainly by modulating protein expression of a variety of specific "responder proteins" that are activated by all strains examined in the study in a concerted up-regulated

manner. Contrary to this, down-regulation of protein levels seems to be random and varies from strain to strain and between experiments. Retrospectively, it seems more logical from an energetic point of view to induce a well defined set of proteins required to cope with infection rather than shutting down specific set of housekeeping or resting state homeostasis proteins which will in turn affect the macrophage's general ability to sustain infection.

To the best of our knowledge this is the first study to simultaneously determine proteome-wide protein relative expression levels of human macrophage-like cells infected with *M. tuberculosis*, and outline molecular signatures of the global and PtpA-dependent proteomic pattern of macrophages during *M. tuberculosis* infection.

4.2.1 Host Proteins Targeted by *M. tuberculosis*

Using the iTRAQ methodology, we identified 845 distinct host proteins whose expression level was modified by *M. tuberculosis* infection. Among these, 27 were statistically validated and were shown to form the "responder" family of proteins. The immune response proteins (ICAM1, IL25, IL1β, SOD2) were found to be up-regulated. We also found proteins involved in chromatin remodeling and transcription regulation (HMGN2, H2AFZ, HIST1H4, DPY30, CHTOP) to be up-regulated as well as proteins involved in protein synthesis (RPL23A, FAU). This pattern indicates that upon infection, the host turns on the transcriptional and translational machineries to synthesize proteins to fight the pathogen. This is supported by the lack of down-regulation of proteins involved in transcription and translation as the majority of down-regulated proteins belong to the cell signalling (DOCK10, ADRBK1, ITPR1, ARHGEF2) and, surprisingly, immunity and defence (CTSG, MIF, BIRC6) functional classes. The

unexpected down-regulation of proteins involved in specific immunity may be a direct outcome of virulence factors secreted by *M. tuberculosis* that target these host proteins.

Of the 27 modulated proteins, we analyzed proteins with the highest variation index. These include BIRC6 (relative fold change of -2.28 (179)) which has previously been associated with bacterial or viral infections and SNRPD1 (2.05) and DOCK10 (-1.77), which had not been previously linked to infection (Table 5).

The pronounced down-regulation of the apoptosis inhibitor BIRC6 (relative fold change of -2.28) (209) may demonstrate the extent of stress the macrophage is exposed to during infection. Indeed, one of *M. tuberculosis*' fundamental virulence strategies is to block phagosome maturation (29). Thus, the macrophage cannot eliminate the pathogen by the conventional phagosome-lysosome fusion route and an additional level of defence is applied; that is, the macrophage turns to apoptosis as a disposal route (124,125). As such, the down-regulation of the apoptosis inhibitor BIRC6 may represent a host-mediated event reflecting the macrophage's attempt at eliminating *M. tuberculosis*.

The SNRPD1 protein is a component of the spliceosome; a complex molecular machine involved in the splicing of all cellular pre-mRNAs (210). Previous studies have shown that high concentrations of SNRPD1 result in the production of regulatory T cells (Tregs) (211), which actively suppress the immune system by inhibiting or down-regulating the induction, proliferation, differentiation and effector functions of immune cells such as T cells, B cells, and dentritic cells (212,213). The immunosuppressive activity of Tregs is suggested to be down-

regulated during immune responses to infectious microorganisms to facilitate their elimination. However, some pathogens, such as *M. tuberculosis* (214), manipulate Tregs to suppress the host immune response and prevent systemic inflammatory immune responses (215). A *M. tuberculosis*-induced SNRPD1 up-regulation (relative fold change of 2.05) could represent another tactic employed by the pathogen to reduce the host inflammatory response that contributes to its survival.

The guanine nucleotide exchange factor DOCK10 (relative fold change of -1.77) is also down-regulated. DOCK10 is an activator of Rho GTPases and thus promotes diverse functions dependent on Rho-family proteins (216). Studies have shown that interleukin-4 (IL4) induces expression of DOCK10 in B cells (217). Down-regulation of DOCK10 may be a result of the pathogen targeting DOCK10 as IL4 expression was shown to be induced during *M. tuberculosis* infection (218). A consequence of a reduced DOCK10 expression could be impaired signalling in B cells and therefore, impaired proliferation and differentiation of B cells, and production of immunoglobulin. Although humoral response to TB is not well understood and established as a protective response, down-regulation of DOCK10 could reduce levels of *M. tuberculosis*-specific antibodies circulating in the blood and impair the ability of the adaptive immunity to respond to infection.

To validate the iTRAQ data, we investigated the correlation between the transcriptional and translational levels of five proteins whose modulation has previously been reported in mycobacterial infections. We selected SOD2 (relative fold change of 1.92) (176,178), ICAM1

(2.16) (167), IL1β (2.24) (176,177), CTSG (-1.91) (164), and MIF (-1.97) (180) for further analysis (Table 5).

The proteomic data of the five modulated proteins was confirmed at the transcriptional level by performing gene expression profiling using qPCR. We also verified the protein expression levels of ICAM1, IL1β and CTSG by Western blotting. As observed in the iTRAQ data (Table 5), mRNA levels of *ICAM1*, *IL1β* and *SOD2* were up-regulated 4 h post-infection (Figure 24A-C). Their up-regulated expression observed between uninfected and *M. tuberculosis*-infected cells is persuasive.

ICAM1 exhibited a four-fold increase 4 h after infection (Figure 24A). ICAM1 is a glycoprotein expressed at the surface of immune cells. It plays a role in the migration of macrophages to the site of infection and in the presentation of antigens to T cells (167). Its expression has been reported to be significantly enhanced on macrophages harbouring *M. tuberculosis* (219). Western blot analysis of ICAM1 showed upregulated expression levels in *M. tuberculosis*-infected cells (Figure 23A), which is consistent with our iTRAQ results (Table 5) and reports in the literature.

The cytokine IL1β displayed a 10-fold increase in mRNA levels between uninfected and infected cells 4 h post-infection (Figure 24B). IL1β is produced by activated macrophages and acts as an important mediator of the inflammatory response through its involvement in several cellular activities such as T cell proliferation, B cell maturation and proliferation, cell differentiation, and apoptosis (177). IL1β was previously observed in the supernatants of

macrophages stimulated with *M. tuberculosis*. It is believed to have effector function in the cellular response to *M. tuberculosis* infection and play a role in the resistance of macrophages (220). Western blot analysis of IL1β showed a pronounced increase in expression levels in *M. tuberculosis*-infected macrophages (Figure 23B). Protein and mRNA expression levels of IL1β were up-regulated across both analytical platforms validating the iTRAQ results (Table 5) and reinforcing the affirmation that IL1β is an important player in the fight against *M. tuberculosis*.

The mRNA levels of the antioxidant *SOD2* increased 12-fold 4 h post-infection (Figure 24C). This up-regulation is justified by the sudden oxidative bursts generated by the macrophage upon phagocytosis of *M. tuberculosis*. Expression of SOD2 must be increased to defend the host from its own toxic assaults from superoxide anions ($O_2^{\bullet-}$) and reactive oxygen species (ROS) (221-223). In such instances, SOD2 scavenges $O_2^{\bullet-}$ offering the host cytotoxic protection. Up-regulation of SOD2 expression is, therefore, a crucial defence mechanism employed by the macrophage, but also a tool used by *M. tuberculosis* to protect itself from $O_2^{\bullet-}$ killing since the protection of the host from $O_2^{\bullet-}$ and ROS converts the macrophage into a sanctuary for *M. tuberculosis* to grow.

A lack of association exists between gene and protein expression levels of CTSG and MIF. As seen in Figure 24D-E, mRNA levels of *CTSG* and *MIF* from *M. tuberculosis*-infected cells show minimal up-regulation for most time points observed. This up-regulation does not correlate with their respective down-regulated protein levels identified by iTRAQ 4 h post-infection (Table 5) and results cannot be directly compared. Moreover, results from Western blot

analysis show no change in protein expression levels of CTSG, which seemingly contradict the iTRAQ data (Figure 23C). Transcription levels of *CTSG*, which encodes a serine protease that possesses antibacterial activities in the killing and digestion of engulfed pathogens, were shown to be down-regulated in macrophages upon *M. tuberculosis* infection (164), which is in agreement with our iTRAQ results. However, our Western blot and qPCR data does not compare with our iTRAQ results or the literature as expression levels of *CTSG* are unchanged (Figure 23C) or slightly above basal levels (Figure 24D). Moreover, a 2.5-fold increase in mRNA expression levels is even observed in infected cells 18 h post-infection (Figure 24D). These findings may indicate that *M. tuberculosis* is only marginally capable of inhibiting *CTSG* expression to basal levels early during infection.

Lastly, MIF is a proinflammatory cytokine involved in the innate immune response to pathogens. It has been shown to be secreted by and up-regulated in macrophages upon exposure to *M. tuberculosis* (224). MIF-deficient macrophages have revealed impaired mycobacterial killing (180). Our qPCR data did not correlate with the proteomic results as a slight up-regulation is noticed in infected cells at all time points observed (Figure 24E).

The interpretation of transcriptomic data can be variable due to the high frequency of false positives (225). An additional feature is that the level of transcription of a gene may not reflect its level of expression. Indeed, mRNA transcripts may not always be translated into proteins, may be degraded (226) or, through alternative splicing, may give rise to several different proteins (227). It is also possible that, in the case of CTSG, the protease is more stable within the macrophage by means of possessing a lower degradation rate or higher half-life during

infection. By contrast, *MIF* mRNA may be regulated post-translationally by events such as protein-targeted degradation. Post-translational modifications are strategies commonly employed by pathogens to modulate key host signalling pathways to their advantage. This would play a pivotal role in the pathogenesis of the infection due to MIF's important functions in immunity and explain why down-regulated protein levels were observed in the iTRAQ analyses, but not in the qPCR assay.

4.2.2 Host Proteins Targeted by *M. tuberculosis* PtpA

The proteomic response of macrophages infected with the PtpA mutant strain resembled that of macrophages infected with the parental or complement strains (Figure 21A-B). As observed in Figure 21C, a strong linear relationship exists between each of the ratios indicating that upon *M. tuberculosis* and Δ*ptpA M. tuberculosis* infection similar proteins become up-regulated at comparable rates. However, little concordance is observed in the rates of protein down-regulation, and, as for the other *M. tuberculosis* strains, infection with the PtpA mutant caused proteins to be down-regulated at seemingly random rates (Figure 21D). By examining two independent controlled infections, we were able to identify modulation of expression of 11 PtpA-dependent host proteins with statistical confidence (Table 6). Surprisingly, the majority of the PtpA-dependent proteins were down-regulated and included members of the immunity and defence (GSK3α, ABCB10) and cellular respiration (COX7B, ATP5I) functional classes. Protein synthesis and respiration require production of ATP by the host. The down-regulation of proteins involved in the electron transport chain leading to a reduction in ATP synthesis seems counterintuitive as reducing ATP production could be detrimental to the host and the pathogen. However, targeting the energy generator of the host may be a strategy employed by

M. tuberculosis to weaken the host. Indeed, reducing the production of ATP to levels that would affect protein synthesis of the host and impair its ability to counterattack while still serving as a niche for the pathogen may represent a tactic. Thus, we propose another role for PtpA, which is to facilitate interference with the energy generator of the host, and thereby secure the infiltration and survival of *M. tuberculosis*.

Among the PtpA-dependent proteins with the greatest modulation, we identified CIRBP (relative fold change of 2.29) (181), GSK3α (-2.28) (148,182), and ABCB10 (-2.35) (183), which have previously been shown to be involved in the infection process, and PRPF31 (-3.14), and SARS2 (-3.18) (Table 6), which have not yet been reported to be associated with infection.

CIRBP is a nuclear protein that responds to stresses such as mild hypothermia (228), exposure to UV irradiation (229), and hypoxia (230) by up-regulation. Recently, CIRBP was described as a new proinflammatory mediator of shock as it is up-regulated in macrophages during septic shock, induces inflammatory responses by stimulating the release of TNF-α, and causes tissue injury (181). The significant up-regulation (relative fold change of 2.29) observed in our iTRAQ results may reflect the stress level the macrophage endures and the corresponding measures it takes to eliminate the pathogen.

GSK3α is a protein-serine/threonine kinase that acts as a regulatory switch for numerous signalling pathways including cell survival and apoptosis (151). In a recent study, we showed that PtpA directly dephosphorylates human GSK3α promoting *M. tuberculosis* survival by blocking apoptosis of the host early in infection (148). This finding was exemplified by the

impaired activation of the apoptosis executioner, caspase-3, in *M. tuberculosis*-infected macrophages compared to Δ*ptpA* mutant-infected cells.

We showed in our previous study that mRNA levels of *GSK3α* are not affected by PtpA (148). Here we show that GSK3α protein levels are down-regulated by PtpA (relative fold change of -2.28). As observed for CTSG and MIF, GSK3α stability may contribute to the discrepancy between mRNA and protein levels. Regardless, we now show that PtpA contributes to both the protein levels and the phosphorylation status of GSK3α, which may reflect a common feedback mechanism.

The transmembrane protein ABCB10 is located in the inner mitochondrial membrane and is involved in intracellular trafficking and compartmentalization of peptides (183,216). Previous work done with the *Saccharomyces cerevisiae* ABCB10 homolog identified the protein as a mitochondrial peptide transporter (214). Degradation products of mitochondrial inner membrane proteins are exported via this transporter, released from the mitochondria (210,211), and presented on the cell surface by major histocompatibility class I (MHC-I) molecules (215). PtpA-dependent down-regulation of ABCB10 (relative fold change of -2.35) supports a putative physiological role in antigen processing (183).

PRPF31 is a protein involved in the formation of the spliceosome and in the splicing of pre-mRNAs (231). Studies have shown that depletion of PRPF31 inhibits spliceosome formation and pre-mRNA splicing (231). Modulation of PRPF31 has never been identified the context of bacterial infection. However, infected macrophages must synthesize large amounts of proteins

for self-defence. Therefore, the proper functioning of PRPF31 for RNA processing is deemed crucial for normal macrophage functions. Our iTRAQ analysis indicated a significant down-regulation of PRPF31 (relative fold change of -3.14). We therefore hypothesize that the high demand for spliced mRNA for protein synthesis in infected macrophages becomes a target for *M. tuberculosis*. The down-regulation of PRPF31 caused by PtpA could signify that splicing of pre-mRNAs is severely compromised and the host defence tactics, markedly weakened.

The aminoacyl-tRNA synthetase SARS2 is a component of the mitochondrial translational apparatus (232). This enzyme catalyzes the ligation of the serine amino acid to mitochondrial tRNA acceptors. Previous studies have shown that mutation in SARS2 greatly impacts acylation of tRNAs and the absence of acylated $tRNA^{Ser}$ leads to the degradation of nonacylated transcripts (233). The pronounced PtpA-dependent down-regulation of SARS2 (relative fold change of -3.18) observed in our iTRAQ analysis may result in decreased serine aminoacylation of mRNA transcripts and adversely affect mitochondrial translation systems. As such, an impaired mitochondrial protein synthesis apparatus would eventually lead to a defective energy supply provided by the mitochondria and impaired antigen processing. To support this claim, we have identified the expression levels of two mitochondrial proteins, COX7B and ATP5I, involved in the generation of ATP, to be significantly down-regulated in *M. tuberculosis*-infected macrophages (relative fold change of -2.10 and -2.32 respectively, Table 6). Moreover, the mitochondrial ABCB10 transporter potentially involved in antigen processing was also downregulated by PtpA (-2.35, Table 6). Thus, we suggest that to promote its survival, *M. tuberculosis* releases PtpA, which targets the mitochondrial translational machinery of the host and impairs its energy generator and weakens its self-defence strategies.

Previous studies from our lab analyzed the macrophage's phosphoproteome response to mycobacterial infection. We investigated the phosphorylation status of key host macrophage kinases during infection with live or heat killed *M. bovis* BCG (186) or *M. tuberculosis* or Δ*ptpA M. tuberculosis* (Figure 12) (148). Overall, we noted changes in host signalling pathways caused by mycobacterial infection including apoptosis (up-regulation of c-JUN, SAPK and GSK3β), cytoskeletal arrangement (up-regulation of α-Adducin), Ca^{2+} signalling (up-regulation of NR1) and macrophage activation (down-regulation of PKCε) (186). We also showed that *M. tuberculosis* PtpA dephosphorylates an abundance of macrophage proteins (Figures 11 and 12, Tables 3 and 4) (76,148). These events may contribute to downstream effects resulting in the observed protein expression changes we describe in this report. Future experiments will reveal the macrophage's multiphasic response that enables the symbiotic nature of *M. tuberculosis* infection.

M. tuberculosis is a host-adapted human pathogen and a deeper biological understanding of the host-pathogen interactome is necessary to get a general idea of what artillery is deployed by the host against *M. tuberculosis*, and to draw a more detailed picture of how *M. tuberculosis* manipulates the host response to its advantage. Despite overlooking many notable proteins in the process due to the high-throughput nature of our screening, we expand existing knowledge of the global response of macrophages to *M. tuberculosis* infection and show the PtpA-specific effect of *M. tuberculosis* on the organization of the macrophage proteome. We also present novel host targets never observed in *M. tuberculosis* infection or any other pathogenic infections. These findings provide novel insight into the global proteomic organization (pathways turned on or off) of the macrophage when challenged by *M. tuberculosis* and into the macrophage protein content.

They also help in the understanding of the complex and unique interplay between *M. tuberculosis* and the host macrophage, and of the manipulative nature of *M. tuberculosis* to circumvent the macrophage's killing machinery.

4.3 Future Directions

The *M. tuberculosis* virulence factor PtpA is known for its inhibitory action on phagosome maturation. Its export into the host cytoplasm indicates that secretion of PtpA is essential to the sabotage of the antimicrobial and defence mechanisms of the macrophage, allowing *M. tuberculosis* to establish growth within the human macrophage. In this thesis, we presented a new role for PtpA as an anti-apoptotic effector and described PtpA's influence on the host macrophage proteomic response upon infection. In particular, we demonstrated that PtpA can disrupt multiple host pathways, such as the cellular respiration pathway, to promote *M. tuberculosis*' intracellular survival. Based on our work thus far, the interference of PtpA with numerous signalling pathways can translate into several research directions.

The PtpA-dependent inhibition of caspase-3 proteolytic cleavage partially explains the mechanism behind the inhibition of apoptosis during macrophage infection with *M. tuberculosis*. As of now, we can only speculate that inhibition of caspase-3 cleavage and activation is due to GSK3α dephosphorylation by PtpA. Future work involving PtpA will aim at determining the exact signal transduction pathway engaged following dephosphorylation of GSK3α by PtpA and leading to the inhibition of caspase-3 activation. The pathway affected by PtpA will be established to confirm that inhibition of caspase-3 cleavage and activation in *M. tuberculosis* infection is truly caused by dephosphorylation of GSK3α Y^{279}. To achieve this, several

experiments can be performed such as an immunoprecipitation of GSK3α substrates by GSK3α. Using antibodies against GSK3α, cellular extracts of uninfected, *M. tuberculosis*- and Δ*ptpA M. tuberculosis*-infected cells will be immunoprecipitated, resolved on SDS-PAGE and proteins interacting with GSK3α will be identified by mass spectrometry. In the case that no stable complexes of GSK3α and interacting proteins form, a 2D SDS-PAGE assay will be carried out. In this instance, recombinant GSK3α will or will not be incubated with cellular extracts of uninfected and infected cells. Lysates will be incubated with anti-GSK3α antibodies. The immunocomplexes will be purified, resolved by 2D SDS-PAGE and phosphorylated proteins will be identified by mass spectrometry. Moreover, an antibody microarray using cellular extracts of uninfected, *M. tuberculosis*- and Δ*ptpA M. tuberculosis*-infected cells and anti-GSK3α can be performed to yield insights into the differential binding of macrophage proteins to GSK3α and examine how these interactions are affected by PtpA. Lastly, the use of a specific and potent GSK3α inhibitor is another way to determine if GSK3α's inhibition results in reduced caspase-3 cleavage and activation. The chemical compound lithium chloride, which selectively inhibits GSK3α, will be used.

In this work, we also showed that, in *M. tuberculosis* infection, PtpA dephosphorylates GSK3β (Figure 12, Table 4). GSK3α and GSK3β are two isoforms encoded by distinct genes. They share 98% homology in their kinase domain and perform similar functions in several settings (234). Despite their resemblance, GSK3α and GSK3β interact with proteins of their own and depending on the cell type, distinct functions of the isoforms have been demonstrated in cell survival (235-237). It would be interesting to examine whether dephosphorylation of GSK3β by PtpA also leads to inhibition of caspase-3 activation and if so, to what extent. One way to

determine the outcome of GSK3β dephosphorylation will be by obtaining macrophages from GSK3α knockout mice, infect them with *M. tuberculosis* and the Δ*ptpA* mutant (as described in Section 2.3.2), harvest the lysates (Section 2.3.3), and perform a Western blot analysis using anti-caspase-3 (Section 2.8). Knowing whether the inhibition occurs via GSK3α, GSK3β or both would allow us to look at the effects of this dephosphorylation on GSK3α- and GSK3β-specific pathways and understand the complex connections among all of the molecules involved in these pathways, as well as to understand how these work in *M. tuberculosis* infection.

Finally, we demonstrated both the global and PtpA-specific effect of *M. tuberculosis* on the macrophage proteomic response. On the one hand, we found that *M. tuberculosis* causes a general up-regulation of housekeeping proteins, such as those involved in transcriptional and translational regulation, as well as proteins involved in immunity and defence. On the other hand, we discovered that PtpA forces a down-regulation of proteins involved in cellular respiration, and, surprisingly, in immunity and defence. Based on these results, the number of new research avenues that can be pursued is vast.

One appealing area of research would be to investigate the global phosphoproteomic response of the host macrophage upon *M. tuberculosis* infection. A quantitative proteomic analysis approach, such as iTRAQ, would determine the phosphorylation status of thousands of proteins upon *M. tuberculosis* infection. Hypothetical knot research of modulated kinases would indicate downstream host signalling cascades affected by PtpA and the precise protein composition change of human macrophages infected with *M. tuberculosis*. Knowledge of the pathways affected would provide new information for comparative studies concerning

pathological states. Revealing downstream host signalling cascades affected by *M. tuberculosis* and, more specifically by PtpA, could have a major impact on drug discovery and development to prevent and better manage this notorious disease.

References

1. Ducati, R. G., Ruffino-Netto, A., Basso, L. A., and Santos, D. S. (2006) The resumption of consumption - A review on tuberculosis. *Mem Inst Oswaldo Cruz.* **101**, 697-714

2. Ten Dam, H. G., and Pio, A. (1982) Pathogenesis of tuberculosis and effectiveness of BCG vaccination. *Tubercle* **63**, 225-233

3. Fine, P. E., and Rodrigues, L. C. (1990) Modern vaccines. Mycobacterial diseases. *Lancet* **335**, 1016-1020

4. Bloom, B. R., and Murray, C. J. (1992) Tuberculosis: commentary on a reemergent killer. *Science* **257**, 1055-1064

5. Crofton, J., and Mitchison, D. (1948) Streptomycin resistance in pulmonary tuberculosis. *Br. Med. J.* **2**, 1009-1015

6. Ruffino-Netto, A. (2002) Tuberculosis: the negleted calamity. *Rev Soc Bras Med Trop.* **35**, 51-58

7. Johnson, R., Streicher, E. M., Louw, G. E., Warren, R. M., van Helden, P. D., and Victor, T. C. (2006) Drug resistance in *Mycobacterium tuberculosis*. *Curr Issues Mol Biol.* **8**, 97-111

8. Fätkenheuer, G., Taelman, H., Lepage, P., Schwenk, A., and Wenzel, R. (1999) The return of tuberculosis. *Diagn Microbiol Infect Dis.* **34**, 139-146

9. Espinal, M. A., Laszlo, A., Simonsen, L., Boulahbal, F., Kim, S. J., Reniero, A., Hoffner, S., Rieder, H. L., Binkin, N., Dye, C., Williams, R., and Raviglione, M. C. (2001) Global trends in resistance to antituberculosis drugs. *The New England Journal of Medicine* **344**, 1294-1303

10. WHO. (2012) Drug-resistance TB. in *WHO Report 2012: Global Tuberculosis Control 2012*. pp 41-51

11. Petrini, B., and Hoffner, S. (1999) Drug-resistant and multidrug-resistant tubercle bacilli. *Int J Antimicrob Agents* **13**, 93-97

12. Andries, K., Verhasselt, P., Guillemont, J., Göhlmann, H. W., Neefs, J. M., Winkler, H., Van Gestel, J., Timmerman, P., Zhu, M., Lee, E., Williams, P., de Chaffoy, D., Huitric, E., Hoffner, S., Cambau, E., Truffot-Pernot, C., Lounis, N., and Jarlier, V. (2005) A diarylquinoline drug active on the ATP synthase of *Mycobacterium tuberculosis*. *Science* **307**, 223-227

13. Nerlich, A. G., Haas, C. J., Zink, A., Szeimies, U., and Hagedorn, H. G. (1997) Molecular evidence for tuberculosis in an ancient egyptian mummy. *Lancet* **350**, 1404

14. Salo, W. L., Aufderheide, A. C., Buikstra, J., and Holcomb, T. A. (1994) Identification of *Mycobacterium tuberculosis* DNA in a pre-columbian peruvian mummy. *Proc Natl Acad Sci U S A.* **91**, 2091-2094

15. Baess, I. (1979) Deoxyribonucleic acid relatedness among species of slowly-growing mycobacteria. *Acta Pathol Microbiol Scand B* **87**, 221-226

16. Böddinghaus, B., Rogall, T., Flohr, T., Blöcker, H., and Böttger, E. C. (1990) Detection and identification of mycobacteria by amplification of rRNA. *J Clin Microbiol.* **28**, 1751-1759

17. Sreevatsan, S., Pan, X., Stockbauer, K. E., Connell, N. D., Kreiswirth, B. N., Whittam, T. S., and Musser, J. M. (1997) Restricted structural gene polymorphism in the *Mycobacterium tuberculosis* complex indicates evolutionarily recent global dissemination. *Proc Natl Acad Sci* **94**, 9869-9874

18. Gutierrez, M. C., Brisse, S., Brosch, R., Fabre, M., Omaïs, B., Marmiesse, M., Supply, P., and Vincent, V. (2005) Ancient origin and gene mosaicism of the progenitor of *Mycobacterium tuberculosis*. *PLoS Pathog* **1**, 55-61

19. Brosch, R., Gordon, S. V., Marmiesse, M., Brodin, P., Buchrieser, C., Eiglmeier, K., Garnier, T., Gutierrez, C., Hewinson, G., Kremer, K., Parsons, L. M., Pym, A. S., Samper, S., van Soolingen, D., and Cole, S. T. (2002) A new evolutionary scenario for the *Mycobacterium tuberculosis* complex. *Proc Natl Acad Sci* **99**, 3684-3689

20. Kapur, V., Whittam, T. S., and Musser, J. M. (1994) Is *Mycobacterium tuberculosis* 15,000 years old? *J Infect Dis.* **170**, 1348-1349

21. Reid, S. D., Hoe, N. P., Smoot, L. M., and Musser, J. M. (2001) Group A streptococcus: Allelic variation, population genetics, and host-pathogen interactions. *J Clin Invest.* **107**, 393-399

22. Garnier, T., Eiglmeier, K., Camus, J. C., Medina, N., Mansoor, H., Pryor, M., Duthoy, S., Grondin, S., Lacroix, C., Monsempe, C., Simon, S., Harris, B., Atkin, R., Doggett, J., Mayes, R., Keating, L., Wheeler, P. R., Parkhill, J., Barrell, B. G., Cole, S. T., Gordon, S. V., and Hewinson, R. G. (2003) The complete genome sequence of *Mycobacterium bovis*. *Proc Natl Acad Sci U S A.* **100**, 7877-7882

23. Mack, U., Migliori, G. B., Sester, M., Rieder, H. L., Ehlers, S., Goletti, D., Bossink, A., Magdorf, K., Hölscher, C., Kampmann, B., Arend, S. M., Detjen, A., Bothamley, G., Zellweger, J. P., Milburn, H., Diel, R., Ravn, P., Cobelens, F., Cardona, P. J., Kan, B., Solovic, I., Duarte, R., Cirillo, D. M., and Lange, C. (2009) LTBI: latent tuberculosis infection or lasting immune responses to *M. tuberculosis*? . *Eur Respir J.* **33**, 956-973

24. Neyrolles, O., and Guilhot, C. (2011) Recent advances in deciphering the contribution of *Mycobacterium tuberculosis* lipids to pathogenesis. *Tuberculosis (Edinb)* **91**, 187-195

25. Brennan, P. J., and Draper, P. (1994) *Tuberculosis: pathogenesis, protection, and control* ASM Press, Washington DC.

26. Kolattukudy, P. E., Fernandes, N. D., Azad, A. K., Fitzmaurice, A. M., and Sirakova, T. D. (1997) Biochemistry and molecular genetics of cell-wall lipid biosynthesis in mycobacteria. *Mol. Microbiol.* **24**, 263-270

27. Jarlier, V., and Nikaido, H. (1994) Mycobacterial cell wall: structure and role in natural resistance to antibiotics. *FEMS Microbiol. Lett.* **123**, 11-18

28. Jarlier, V., and Nikaido, H. (1990) Permeability barrier to hydrophilic solutes in *Mycobacterium chelonei J Bacteriol* **172**, 1418-1423

29. Keane, J., Remold, H. G., and Kornfeld, H. (2000) Virulent *Mycobacterium tuberculosis* strains evade apoptosis of infected alveolar macrophages. *J. Immunol.* **164**, 2016-2020

30. Flannagan, R. S., Cosio, G., and Grinstein, S. (2009) Antimicrobial mechanisms of phagocytes and bacterial evasion strategies. *Nature Reviews Microbiol.* **7**, 355-366

31. Underhill, D. M., and Ozinsky, A. (2002) Phagocytosis of microbes: complexity in action. *Annu Rev Immunol.* **20** 825-852

32. Anderson, C. L. (1982) Isolation of the receptor for IgG from a human monocyte cell line (U937) and from human peripheral blood monocytes. *J Exp Med.* **156**, 1794-1806

33. van de Winkel, J. G., and Anderson, C. L. (1991) Biology of human immunoglobulin G Fc receptors. *J Leukoc Biol.* **49**, 511-524

34. Hume, D. A., Halpin, D., Charlton, H., and Gordon, S. (1984) The mononuclear phagocyte system of the mouse defined by immunohistochemical localization of antigen F4/80: Macrophages of endocrine organs. *Proc Natl Acad Sci U S A.* **81**, 4174-4177

35. Ezekowitz, R. A., Sastry, K., Bailly, P., and Warner, A. (1990) Molecular characterization of the human macrophage mannose receptor: demonstration of multiple carbohydrate recognition-like domains and phagocytosis of yeasts in cos-1 cells. *J Exp Med.* **172**, 1785-1794

36. Ehlers, M. R. (2000) CR3: A general purpose adhesion-recognition receptor essential for innate immunity. *Microbes Infect.* **2**, 289-294

37. Arnaout, M. A. (1990) Structure and function of the leukocyte adhesion molecules CD11/CD18. *Blood* **75**, 1037-1050

38. Plow, E. F., and Zhang, L. (1997) A MAC-1 attack: integrin functions directly challenged in knockout mice. *J Clin Invest.* **99**, 1145-1146

39. Cywes, C., Hoppe, H. C., Daffé, M., and Ehlers, M. R. (1997) Nonopsonic binding of *Mycobacterium tuberculosis* to complement receptor type 3 is mediated by capsular polysaccharides and is strain dependent. *Infect Immun.* **65**, 4258-4266

40. Zhou, M. J., and Brown, E. J. (1994) CR3 (mac-1, alpha M beta 2, CD11b/CD18) and Fc gamma RIII cooperate in generation of a neutrophil respiratory burst: requirement for Fc gamma RIII and tyrosine phosphorylation. *J Cell Biol.* **125**, 1407-1416

41. Hestvik, A. L., Hmama, Z., and Av-Gay, Y. (2005) Mycobacterial manipulation of the host cell. *FEMS Microbiol. Rev.* **29**, 1041-1050

42. Russell, D. G. (2011) *Mycobacterium tuberculosis* and the intimate discourse of a chronic infection. *Immunol Rev.* **240**, 252-268

43. Sturgill-Koszycki, S., Schlesinger, P. H., Chakraborty, P., Haddix, P. L., Collins, H. L., Fok, A. K., Allen, R. D., Gluck, S. L., Heuser, J., and Russell, D. G. (1994) Lack of acidification in *Mycobacterium* phagosomes produced by exclusion of the vesicular proton-ATPase. *Science* **263**, 678-681

44. Henry, R., Shaughnessy, L., Loessner, M. J., Alberti-Segui, C., Higgins, D. E., and Swanson, J. A. (2006) Cytolysin-dependent delay of vacuole maturation in macrophages infected with *Listeria monocytogenes*. *Cell Microbiol.* **8**, 107-119

45. Prost, L. R., Daley, M. E., Le Sage, V., Bader, M. W., Le Moual, H., Klevit, R. E., and Miller, S. I. (2007) Activation of the bacterial sensor kinase PhoQ by acidic pH. *Mol. Cell* **26**, 165-174

46. Brüggemann, H., Cazalet, C., and Buchrieser, C. (2006) Adaptation of *Legionella pneumophila* to the host environment: role of protein secretion, effectors and eukaryotic-like proteins. *Curr. Opin. Microbiol.* **9**, 86-94

47. Armstrong, J. A., and Hart, P. D. (1971) Response of cultured macrophages to *Mycobacterium tuberculosis*, with observations on fusion of lysosomes with phagosomes. *J. Exp. Med.* **134**, 713-740

48. Clemens, D. L., and Horwitz, M. A. (1995) Characterization of the *Mycobacterium tuberculosis* phagosome and evidence that phagosomal maturation is inhibited. *J. Exp. Med.* **181**, 257-270

49. Sturgill-Koszycki, S., Schaible, U. E., and Russell, D. G. (1996) *Mycobacterium*-containing phagosomes are accessible to early endosomes and reflect a transitional state in normal phagosome biogenesis. *EMBO J.* **15**, 6960-6968

50. Hoflack, B., and Kornfeld, S. (1985) Lysosomal enzyme binding to mouse P388D1 macrophage membranes lacking the 215-kDa mannose 6-phosphate receptor: evidence for the existence of a second mannose 6-phosphate receptor. *Proc. Natl. Acad. Sci.* **82**, 4428-4432

51. Xu, S., Cooper, A., Sturgill-Koszycki, S., van Heyningen, T., Chatterjee, D., Orme, I., Allen, P., and Russell, D. G. (1994) Intracellular trafficking in *Mycobacterium tuberculosis* and *Mycobacterium avium*-infected macrophages. *J. Immunol.* **153**, 2568-2578

52. Sun, J., Deghmane, A. E., Soualhine, H., Hong, T., Bucci, C., Solodkin, A., and Hmama, Z. (2007) *Mycobacterium bovis* BCG disrupts the interaction of Rab7 with RILP contributing to inhibition of phagosome maturation. *J. Leukoc. Biol.* **82**, 1437-1445

53. Cantalupo, G., Alifano, P., Roberti, V., Bruni, C. B., and Bucci, C. (2001) Rab-interacting lysosomal protein (RILP): the Rab7 effector required for transport to lysosomes. *EMBO J.* **20**, 683-693

54. Moreno, C., Mehlert, A., and Lamb, J. (1988) The inhibitory effects of mycobacterial lipoarabinomannan and polysaccharides upon polyclonal and monoclonal human T cell proliferation. *Clin. Exp. Immunol.* **74**, 206-210

55. Sibley, L. D., Hunter, S. W., Brennan, P. J., and Krahenbuhl, J. L. (1988) Mycobacterial lipoarabinomannan inhibits gamma interferon-mediated activation of macrophages. *Infect. Immun.* **56**, 1232-1236

56. Chan, J., Fan, X. D., Hunter, S. W., Brennan, P. J., and Bloom, B. R. (1991) Lipoarabinomannan, a possible virulence factor involved in persistence of *Mycobacterium tuberculosis* within macrophages. *Infect. Immun.* **59**, 1755-1761

57. Balcewicz-Sablinska, M. K., Keane, J., Kornfeld, H., and Remold, H. G. (1998) Pathogenic *Mycobacterium tuberculosis* evades apoptosis of host macrophages by release of TNF-R2, resulting in inactivation of TNF-alpha. *J. Immunol.* **161**, 2636-2641

58. Chatterjee, D., and Khoo, K. H. (1998) Mycobacterial lipoarabinomannan: an extraordinary lipoheteroglycan with profound physiological effects. *Glycobiology* **8**, 113-120

59. Gilleron, M., Himoudi, N., Adam, O., Constant, P., Venisse, A., Rivière, M., and Puzo, G. (1997) *Mycobacterium smegmatis* phosphoinositols-glyceroarabinomannans: structure and localization of alkali-labile and alkali-stable phosphoinositides. *J. Biol. Chem.* **272**, 117-124

60. Malik, Z. A., Denning, G. M., and Kusner, D. J. (2000) Inhibition of Ca^{2+} signalling by *Mycobacterium tuberculosis* is associated with reduced phagosome-lysosome fusion and increased survival within human macrophages. *J. Exp. Med.* **191**, 287-302

61. Fratti, R. A., Chua, J., Vergne, I., and Deretic, V. (2003) *Mycobacterium tuberculosis* glycosylated phosphatidylinositol causes phagosome maturation arrest. *Proc. Natl. Acad. Sci.* **100**, 5437-5442

62. Fratti, R. A., Backer, J. M., Gruenberg, J., Corvera, S., and Deretic, V. (2001) Role of phosphatidylinositol 3-kinase and Rab5 effectors in phagosomal biogenesis and mycobacterial phagosome maturation arrest. *J. Cell Biol.* **154**, 631-644

63. Derectic, V., Via, L. E., Fratti, R. A., and Deretic, D. (1997) Mycobacterial phagosome maturation, Rab proteins, and intracellular trafficking. *Electrophoresis* **18**, 2542-2547

64. Vergne, I., Chua, J., and Deretic, V. (2003) Tuberculosis toxin blocking phagosome maturation inhibits a novel Ca^{2+}/calmodulin-PI3K hVPS34 cascade. *J. Exp. Med.* **198**, 653-659

65. Christoforidis, S., Miaczynska, M., Ashman, K., Wilm, M., Zhao, L., Yip, S. C., Waterfield, M. D., Backer, J. M., and Zerial, M. (1999) Phosphatidylinositol-3-OH kinases are Rab5 effectors. *Nature Cell Biology* **1**, 249-252

66. Lemmon, M. A. (2003) Phosphoinositide recognition domains. *Traffic* **4**, 201-213

67. McBride, H. M., Rybin, V., Murphy, C., Giner, A., Teasdale, R., and Zerial, M. (1999) Oligomeric complexes link Rab5 effectors with NSF and drive membrane fusion via interactions between EEA1 and syntaxin 13. *Cell* **98**, 377-386

68. Simonsen, A., Gaullier, J. M., D'Arrigo, A., and Stenmark, H. (1999) The Rab5 effector EEA1 interacts directly with syntaxin-6. *J. Biol. Chem.* **274**, 28857-28860

69. Malik, Z. A., Thompson, C. R., Hashimi, S., Porter, B., Iyer, S. S., and Kusner, D. J. (2003) Cutting edge: *Mycobacterium tuberculosis* blocks Ca^{2+} signalling and phagosome maturation in human macrophages via specific inhibition of sphingosine kinase. *J. Immunol.* **170**, 2811-2815

70. Rossolini, G. M., Schippa, S., Riccio, M. L., Berlutti, F., Macaskie, L. E., and Thaller, M. C. (1998) Bacterial nonspecific acid phosphohydrolases: physiology, evolution and use as tools in microbial biotechnology. *Cell Mol. Life Sci.* **54**, 833-850

71. Remaley, A. T., Das, S., Campbell, P. I., Larocca, G. M., Pope, M. T., and Glew, R. H. (1985) Characterization of *Leishmania donovani* acid phosphatases. *J. Biol. Chem.* **260**, 880-886

72. Saleh, M. T., and Belisle, J. T. (2000) Secretion of an acid phosphatase (SapM) by *Mycobacterium tuberculosis* that is similar to eukaryotic acid phosphatases. *J. Bacteriol.* **182**, 6850-6853

73. Bowers, G. N., McComb, R. B., and Upretti, A. (1981) 4-nitrophenyl phosphate characterization of high purity materials for measuring alkaline phosphatase activity in human serum. *Clin. Chem.* **27**, 135-143

74. Murphy, J., and Riley, J. P. (1962) A modified single method for the determination of phosphate in neutral waters. *Anal. Chim. Acta* **27**, 31-36

75. Vergne, I., Chua, J., Lee, H. H., Lucas, M., Belisle, J., and Deretic, V. (2005) Mechanism of phagolysosome biogenesis block by viable *Mycobacterium tuberculosis*. *Proc. Natl. Acad. Sci.* **102**, 4033-4038

76. Bach, H., Papavinasasundaram, K. G., Wong, D., Hmama, Z., and Y., A.-G. (2008) *Mycobacterium tuberculosis* virulence is mediated by PtpA dephosphorylation of human vacuolar protein sorting 33B. *Cell Host Microbe* **3**, 316-322

77. Russell, D. G. (2007) Who puts the tubercle in tuberculosis? *Nature Rev. Microbiol.* **5**, 39-47

78. Singh, P. P., LeMaire, C., Tan, J. C., Zeng, E., and Schorey, J. S. (2011) Exosomes released from *M. tuberculosis* infected cells can suppress IFN-γ mediated activation of naïve macrophages. *PLoS ONE* **6**, e18564

79. Noss, E. H., Pai, R. K., Sellati, T. J., Radolf, J. D., Belisle, J., Golenbock, D. T., Boom, W. H., and Harding, C. V. (2001) Toll-like receptor 2-dependent inhibition of macrophage class II MHC expression and antigen processing by 19-kDa lipoprotein of *Mycobacterium tuberculosis*. *J. Immunol.* **167**, 910-918

80. Young, D. B., and Garbe, T. (1991) Lipoprotein antigens of *M. tuberculosis*. *Res. Microbiol.* **142**, 55-65

81. Pai, R. K., Convery, M., Hamilton, T. A., Boom, W. H., and Harding, C. V. (2003) Inhibition of IFN-ɣ-induced class II transactivator expression by a 19-kDa lipoprotein from *Mycobacterium tuberculosis*: a potential mechanism for immune evasion. *J. Immunol.* **171**, 175-184

82. Pai, R. K., Pennini, M. E., Tobian, A. A., Canaday, D. H., Boom, W. H., and Harding, C. V. (2004) Prolonged toll-like receptor signaling by *Mycobacterium tuberculosis* and its 19-kilodalton lipoprotein inhibits gamma interferon-induced regulation of selected genes in macrophages. *Infect. Immun.* **72**, 6603-6614

83. Brightbill, H. D., Libraty, D. H., Krutzik, S. R., Yang, R. B., Belisle, J. T., Bleharski, J. R., Maitland, M., Norgard, M. V., Plevy, S. E., Smale, S. T., Brennan, P. J., Bloom, B. R., Godowski, P. J., and Modlin, R. L. (1999) Host defense mechanisms triggered by microbial lipoproteins through toll-like receptors. *Science* **285**, 732-736

84. Chu, R. S., Askew, D., Noss, E. H., Tobian, A., Krieg, A. M., and Harding, C. V. (1999) CpG oligodeoxynucleotides down-regulate macrophage class II MHC antigen processing. *J. Immunol.* **163**, 1188

85. Pennini, M. E., Pai, R. K., Schultz, D. C., Boom, W. H., and Harding, C. V. (2006) *Mycobacterium tuberculosis* 19-kDa lipoprotein inhibits IFN-gamma-induced chromatin remodeling of MHC2TA by TLR2 and MAPK signalling. *J. Immunol.* **176**, 4323-4330

86. Landmann, S., Mühlethaler-Mottet, A., Bernasconi, L., Suter, T., Waldburger, J. M., Masternak, K., Arrighi, J. F., Hauser, C., Fontana, A., and Reith, W. (2001) Maturation of dentricitc cells is accompanied by rapid transcriptional silencing of class II transactivator (CIITA) expression. *J. Exp. Med.* **194**, 379-392

87. Cowley, S. C., Babakaiff, R., and Av-Gay, Y. (2002) Expression and localization of the *Mycobacterium tuberculosis* protein tyrosine phosphatase PtpA. *Res. Microbiol.* **153**, 233-241

88. Wong, D., Bach, H., Hmama, Z., and Av-Gay, Y. (2011) *Mycobacterium tuberculosis* protein tyrosine phosphatase A disrupts phagosome acidification by exclusion of host vacuolar H+-ATPase. *Proc. Natl. Acad. Sci.* **108**, 19371-19376

89. Banta, L. M., Robinson, J. S., Klionsky, D. J., and Emr, S. D. (1988) Organelle assembly in yeast: characterization of yeast mutants defective in vacuolar biogenesis and protein sorting. *J. Cell Biol.* **107**, 1369-1383

90. Darsow, T., Reider, S. E., and Emr, S. D. (1997) A multispecificity syntaxin homologue, Vam3p, essential for autophagic and biosynthetic protein transport to the vacuole. *J. Cell Biol.* **138**, 517-529

91. Vida, T., and Gerhardt, B. (1999) A cell-free assay allows reconstitution of Vps33p-dependent transport to the yeast vacuole/lysosome. *J. Cell Biol.* **146**, 85-97

92. Price, A., Wickner, W., and Ungermann, C. (2000b) Proteins needed for vesicle budding from the golgi complex are also required for the docking step of homotypic vacuole fusion. *J. Cell Biol.* **148**, 1223-1229

93. Glick, B. S., and Rothman, J. E. (1987) Possible role for fatty acyl-Coenzyme A in intracellular protein transport. *Nature* **326** 309-312

94. Beckers, C. J., Block, M. R., Glick, B. S., Rothman, J. E., and Balch, W. E. (1989) Vesicular transport between the endoplasmic reticulum and the golgi stack requires the NEM-sensitive fusion protein. *Nature* **339** 397–398

95. Diaz, R., Mayorga, L. S., Weidman, P. J., Rothman, J. E., and Stahl, P. D. (1989) Vesicle fusion following receptor-mediated endocytosis requires a protein active in golgi transport. *Nature* **339**, 398-400

96. Banta, L. M., Vida, T. A., Herman, P. K., and Emr, S. D. (1990) Characterization of yeast Vps33p, a protein required for vacuolar protein sorting and vacuole biogenesis. *Mol. Cell Biol.* **10**, 4638-4649

97. Wurmser, A. E., Sato, T. K., and Emr, S. D. (2000) New component of the vacuolar class C-Vps complex couples nucleotide exchange on the Ypt7 GTPase to SNARE-dependent docking and fusion. *J. Cell Biol.* **151**, 551-562

98. Sato, T. K., Rehling, P., Peterson, M. R., and Emr, S. D. (2000) Class C Vps protein complex regulates vacuolar SNARE pairing and is required for vesicle docking/fusion. *Mol. Cell* **6**, 661-671

99. Seals, D. F., Eitzen, G., Margolis, N., Wickner, W. T., and Price, A. (2000) A Ypt/Rab effector complex containing the Sec1 homolog Vps33p is required for homotypic vacuole fusion. *Proc. Natl. Acad. Sci.* **97**, 9402-9407

100. Brocker, C., Kuhlee, A., Gatsogiannis, C., Balderhaar, H. J. K., Honscher, C., Engelbrecht-Vandré, S., Ungermann, C., and Raunser, S. (2012) Molecular architecture of the multisubunit homotypic fusion and vacuole protein sorting (HOPS) tethering complex. *Proc Natl Acad Sci USA* **109**, 1991-1996

101. Hackam, D. J., Rotstein, O. D., Zhang, W. J., Demaurex, N., Woodside, M., Tsai, O., and Grinstein, S. (1997) Regulation of phagosomal acidification. Differential targeting of Na+/H+ exchangers, Na+/K+-ATPases, and vacuolar-type H+-ATPases. *J. Biol. Chem.* **272**, 29810-29820

102. Sun-Wada, G. H., Tabata, H., Kawamura, N., Aoyama, M., and Wada, Y. (2009) Direct recruitment of H+-ATPase from lysosomes for phagosomal acidification. *J. Cell Sci.* **122**, 2504-2513

103. Mukherjee, S., Ghosh, R. N., and Maxfield, F. R. (1997) Endocytosis. *Physiol Rev.* **77**, 759-803

104. Fadok, V. A., Savill, J. S., Haslet, C., Bratton, D. L., Doherty, D. E., Campbell, P. A., and Henson, P. M. (1992) Different populations of macrophages use either the vitronectin receptor or the phosphatidylserine receptor to recognize and remove apoptotic cells. *Journal of Immunology* **149**, 4029-4035

105. Wyllie, A. H., Kerr, J. F. R., and Currie, A. R. (1980) Cell death: the significance of apoptosis *Int. Reu. CytoI.* **68**, 251-306

106. Duan, L., Gan, H., Arm, J., and Remold, H. G. (2001) Cytosolic phospholipase A2 participates with TNF-Alpha in the induction of apoptosis of human macrophages infected with *Mycobacterium tuberculosis* H37Ra. *J Immunol.* **166**, 7469-7476

107. Nakagawa, I., Amano, A., Mizushima, N., Yamamoto, A., Yamaguchi, H., Kamimoto, T., Nara, A., Funao, J., Nakata, M., Tsuda, K., Hamada, S., and Yoshimori, T. (2004) Autophagy defends cells against invading group A *Streptococcus*. *Science* **306**, 1037-1040

108. Danial, N. N., and Korsmeyer, S. J. (2004) Cell death: critical control points. *Cell* **116**, 205-219

109. Alnemri, E. S., Livingston, D. J., Nicholson, D. W., Salvesen, G., Thornberry, N. A., Wong, W. W., and Yuan, J. (1996) Human ICE/CED-3 protease nomenclature. *Cell* **87**, 171

110. Edinger, A. L., and Thompson, C. B. (2004) Death by design: apoptosis, necrosis and autophagy. *Current Opinion in Cell Biology* **16**, 663-669

111. Boya, P., Reggiori, F., and Codogno, P. (2013) Emerging regulation and functions of autophagy. *Nat Cell Biol.* **15**, 713-720

112. Mizushima, N., Levine, B., Cuervo, A. M., and Klionsky, D. J. (2008) Autophagy fights disease through cellular self-digestion. *Nature* **451**, 1069-1075

113. Mihalache, C. C., and Simon, H. U. (2012) Autophagy regulation in macrophages and neutrophils. *Exp Cell Res.* **318**, 1187-1192

114. Oh, J. E., and Lee, H. K. (2012) Modulation of pathogen recognition by autophagy. *Front Immunol.* **12**, 44

115. Gutierrez, M. G., Master, S. S., Singh, S. B., Taylor, G. A., Colombo, M. I., and Deretic, V. (2004) Autophagy is a defense mechanism inhibiting BCG and *Mycobacterium tuberculosis* survival in infected macrophages. *Cell* **119**, 753-766

116. Proskuryakov, S. Y., Konoplyannikov, A. G., and Gabai, V. L. (2003) Necrosis: a specific form of programmed cell death? *Exp Cell Res.* **283**, 1-16

117. Kasper, D. I., and Zaleznik, D. F. (2001) *Gas gangrene antibiotic-associated colitis and other clostridial infections*, 15th Ed. ed., McGraw-Hill, New York

118. Oddo, M., Renno, T., Attinger, A., Bakker, T., MacDonald, H. R., and Meylan, P. R. (1998) Fas ligand-induced apoptosis of infected human macrophages reduces the viability of intracellular *Mycobacterium tuberculosis*. *J Immunol.* **160**, 5448-5454

119. Winau, F., Weber, S., Sad, S., de Diego, J., Hoops, S. L., Breiden, B., Sandhoff, K., Brinkmann, V., Kaufmann, S. H., and Schaible, U. E. (2006) Apoptotic vesicles crossprime CD8 T cells and protect against tuberculosis. *Immunity* **24**, 105-117

120. Dheda, K., Booth, H., Huggett, J. F., Johnson, M. A., Zumla, A., and Rook, G. A. (2005) Lung remodeling in pulmonary tuberculosis. *J Infect Dis.* **192**, 1201-1209

121. Kaplan, G., Post, F. A., Moreira, A. L., Wainwright, H., Kreiswirth, B. N., Tanverdi, M., Mathema, B., Ramaswamy, S. V., Walther, G., Steyn, L. M., Barry, C. E., and Bekker, L. G. (2003) *Mycobacterium tuberculosis* growth at the cavity surface: a microenvironment with failed immunity. *Infect Immun.* **71**, 7099-7108

122. Lee, J., Repasy, T., Papavinasasundaram, K., Sassetti, C., and Kornfeld, H. (2011) *Mycobacterium tuberculosis* induces an atypical cell death mode to escape from infected macrophages. *PLoS One* **6**, e18367

123. Lee, J., Hartman, M., and Kornfeld, H. (2009) Macrophage apoptosis in tuberculosis. *Yonsei Med J.* **50**, 1-11

124. Aberdein, J. D., Cole, J., Bewley, M. A., Marriott, H. M., and Dockrell, D. H. (2013) Alveolar macrophages in pulmonary host defense – the unrecognized role of apoptosis as a mechanism of intracellular bacterial killing. *Clin Exp Immunol.* **174**, 193-202

125. Placido, R., Mancino, G., Amendola, A., Mariani, F., Vendetti, S., Piacentini, M., Sanduzzi, A., Bocchino, M. L., Zembala, M., and Colizzi, V. (1997) Apoptosis of human monocytes/macrophages in *Mycobacterium tuberculosis* infection. *Journal of Pathology* **181**, 31-38

126. Moore, K. J., and Matlashewski, G. (1994) Intracellular infection by *Leishmania donovani* inhibits macrophage apoptosis *J Immunol* **152**, 2930-2937

127. Keane, J., Balcewicz-Sablinska, M. K., Remold, H. G., Chupp, G. L., Meek, B. B., Fenton, M. J., and Kornfeld, H. (1997) Infection by *Mycobacterium tuberculosis* promotes human alveolar macrophage apoptosis. *Infect Immun.* **65**, 298-304

128. Watson, V. E., Hill, L. L., Owen-Schaub, L. B., Davis, D. W., McConkey, D. J., Jagannath, C., Hunter, R. L., and Actor, J. K. (2000) Apoptosis in *Mycobacterium tuberculosis* infection in mice exhibiting varied immunopathology. *Journal of Pathology* **190**, 211-220

129. Rojas, M., Barrera, L. F., Puzo, G., and Garcia, L. F. (1997) Differential induction of apoptosis by virulent *Mycobacterium tuberculosis* in resistant and susceptible murine macrophages: Role of nitric oxide and mycobacterial products. *J Immunol.* **159**, 1352-1361

130. Velmurugan, K., Chen, B., Miller, J. L., Azogue, S., Gurses, S., Hsu, T., Glickman, M., Jacobs, W. R. J., Porcelli, S. A., and Briken, V. (2007) *Mycobacterium tuberculosis* nuoG is a virulence gene that inhibits apoptosis of infected host cells. *PLoS Pathog.* **3**, e110

131. Hinchey, J., Lee, S., Jeon, B. Y., Basaraba, R. J., Venkataswamy, M. M., Chen, B., Chan, J., Braunstein, M., Orme, I. M., Derrick, S. C., Morris, S. L., Jacobs, W. R. J., and Porcelli, S. A. (2007) Enhanced priming of adaptive immunity by a proapoptotic mutant of *Mycobacterium tuberculosis*. *J Clin Invest.* **117**, 2279-2288

132. Sun, J., Singh, V., Lau, A., Stokes, R. W., Obregón-Henao, A., Orme, I. M., Wong, D., Av-Gay, Y., and Hmama, Z. (2013) *Mycobacterium tuberculosis* nucleoside diphosphate kinase inactivates small GTPases leading to evasion of innate immunity. *PLoS Pathog.* **9**, e1003499

133. Derrick, S. C., and Morris, S. L. (2007) The ESAT6 protein of *Mycobacterium tuberculosis* induces apoptosis of macrophages by activating caspase expression. *Cell Microbiol.* **9**, 1547-1555

134. Santucci, M. B., Amicosante, M., Cicconi, R., Montesano, C., Casarini, M., Giosue, S., Bisetti, A., Colizzi, V., and Fraziano, M. (2000) *Mycobacterium tuberculosis*-induced apoptosis in monocytes/macrophages: Early membrane modifications and intracellular mycobacterial viability. *J Infect Dis.* **181**, 1506-1509

135. Klingler, K., Tchou-Wong, K. M., Brändli, O., Aston, C., Kim, R., Chi, C., and Rom, W. N. (1997) Effects of mycobacteria on regulation of apoptosis in mononuclear phagocytes. *Infect Immun.* **65**, 5272-5278

136. Chen, M., Gan, H., and Remold, H. G. (2006) A mechanism of virulence: virulent *Mycobacterium tuberculosis* strain H37Rv, but not attenuated H37Ra, causes significant mitochondrial inner membrane disruption in macrophages leading to necrosis. *J Immunol.* **176**, 3707-3716

137. Park, J. S., Tamayo, M. H., Gonzalez-Juarrero, M., Orme, I. M., and Ordway, D. J. (2006) Virulent clinical isolates of *Mycobacterium tuberculosis* grow rapidly and induce cellular necrosis but minimal apoptosis in murine macrophages. *J Leukoc Biol.* **79**, 80-86

138. Zhang, J., Jiang, R., Takayama, H., and Tanaka, Y. (2005) Survival of virulent *Mycobacterium tuberculosis* involves preventing apoptosis induced by Bcl-2 up-regulation and release resulting from necrosis in J774 macrophages. *Microbiol Immunol.* **49**, 845-852

139. Porcelli, S. A., and Jacobs, W. R. J. (2008) Tuberculosis: unsealing the apoptotic envelope. *Nat Immunol.* **9**, 1101-1102

140. Butler, R. E., Brodin, P., Jang, J., Jang, M. S., Robertson, B. D., Gicquel, B., and Stewart, G. R. (2012) The balance of apoptotic and necrotic cell death in *Mycobacterium tuberculosis* infected macrophages is not dependent on bacterial virulence. *PLoS One* **7**, e47573

141. Loeuillet, C., Martinon, F., Perez, C., Munoz, M., Thome, M., and Meylan, P. R. (2006) *Mycobacterium tuberculosis* subverts innate immunity to evade specific effectors. *J Immunol.* **177**, 6245-6255

142. Ciaramella, A., Cavone, A., Santucci, M. B., Garg, S. K., Sanarico, N., Bocchino, M., Galati, D., Martino, A., Auricchio, G., D'Orazio, M., Stewart, G. R., Neyrolles, O., Young, D. B., Colizzi, V., and Fraziano, M. (2004) Induction of apoptosis and release of interleukin-1 beta by cell wall-associated 19-kDa lipoprotein during the course of mycobacterial infection. *J Infect Dis.* **190**, 1167-1176

143. Dhiman, R., Raje, M., and Majumdar, S. (2007) Differential expression of NF-kappaB in mycobacteria infected THP-1 affects apoptosis. *Biochim Biophys Acta.* **1770**, 649-658

144. Jalal, S., Arsenault, R., Potter, A. A., Babiuk, L. A., Griebel, P. J., and Napper, S. (2009) Genome to kinome: species-specific peptide arrays for kinome analysis. *Sci Signal.* **2**, pl1

145. Pelech, S., and Zhang, H. (2002) Plasticity of the kinomes in monkey and rat tissues. *Sci STKE* **162**, PE50

146. Ross, P. L., Huang, Y. N., Marchese, J. N., Williamson, B., Parker, K., Hattan, S., Khainovski, N., Pillai, S., Dey, S., Daniels, S., Purkayastha, S., Juhasz, P., Martin, S., Bartlet-Jones, M., He, F., Jacobson, A., and Pappin, D. J. (2004) Multiplexed protein quantitation in *Saccharomyces cerevisiae* using amine reactive isobaric tagging reagents. *Mol. Cell. Proteomics* **3**, 1154-1169

147. Colinge, J., and Bennett, K. L. (2007) Introduction to computational proteomics. *PLoS Comput. Biol.* **3**, 1151-1160

148. Poirier, V., Bach, H., and Av-Gay, Y. (2014) *Mycobacterium tuberculosis* promotes anti-apoptotic activity of the macrophage by PtpA-dependent dephosphorylation of host GSK3α. *J Biol Chem.* **289**, 29376-29385

149. Papavinasasundaram, K. G., Chan, B., Chung, J. H., Colston, M. J., Davis, E. O., and Av-Gay, Y. (2005) Deletion of the *Mycobacterium tuberculosis* pknH gene confers a higher bavillary load during the chronic phase of infection in BALB/c mice. *J.Bacteriol.* **187**, 5751-5760

150. De Maesschalck, R., Jouan-Rimbaud, D., and Massart, D. L. (2000) The Mahalanobis distance. *Chemometrics and Intelligent Laboratory Systems* **50**, 1-18

151. Embi, N., Rylatt, D. B., and Cohen, P. (1980) Glycogen synthase kinase-3 from rabbit skeletal muscle. Separation from cyclic-AMP-dependent protein kinase and phosphorylase kinase. *Eur. J. Biochem.* **107**, 519-527

152. Takahashi-Yanaga, F. (2013) Activator or inhibitor? GSK-3 as a new drug target. *Biochem Pharmacol.* **86**, 191-199

153. Hughes, K., Nikolakaki, E., Plyte, S.E., Totty, N.F., Woodgett, J.R. (1993) Modulation of the glycogen synthase kinase-3 family by tyrosine phosphorylation. *EMBO J.* **12**, 803-808.

154. Bhat, R. V., Shanley, J., Correll, M. P., Fieles, W. E., Keith, R. A., Scott, C. W., and Lee, C. M. (2000) Regulation and localization of tyrosine216 phosphorylation of glycogen synthase kinase-3 beta in cellular and animal models of neuronal degeneration. *Proc. Natl. Acad. Sci.* **97**, 11074-11079

155. Wong, D., Chao, J. D., and Av-Gay, Y. (2013) *Mycobacterium tuberculosis*-secreted phosphatases: from pathogenesis to targets for TB drug development. *Trends Microbiol.* **21**, 100-109

156. Pappin, D. J., Hojrup, P., and Bleasby, A. J. (1993) Rapid identification of proteins by peptide-mass fingerprinting. *Curr Biol.* **3**, 327-332

157. Karim, A. F., Chandra, P., Chopra, A., Siddiqui, Z., Bhaskar, A., Singh, A., and Kumar, D. (2011) Express path analysis identifies a tyrosine kinase Src-centric network regulating divergent host responses to *Mycobacterium tuberculosis* infection. *J. Biol. Chem.* **286**, 40307-40319

158. Cross, D. A., Alessi, D. R., Cohen, P., Andjelkovich, M., and Hemmings, B. A. (1995) Inhibition of glycogen synthase kinase-3 by insulin mediated by protein kinase B. *Nature* **378**, 785-789

159. Hoeflich, K. P., Luo, J., Rubie, E. A., Tsao, M. S., Jin, O., and Woodgett, J. R. (2000) Requirement for glycogen synthase kinase-3 beta in cell survival and NF-kappaB activation. *Nature* **406**, 86-90

160. Wang, Z. B., Liu, Y. Q., and Cui, Y. F. (2005) Pathways to caspase activation. *Cell Biol Int.* **29**, 489-496

161. Bach, H., Sun, J., Hmama, Z., and Av-Gay, Y. (2006) *Mycobacterium avium* subsp. paratuberculosis PtpA is an endogenous tyrosine phosphatase secreted during infection. *Infect. Immun.* **74**, 6540-6546

162. Ripoll, V. M., Irvine, K. M., Ravasi, T., Sweet, M. J., and Hume, D. A. (2007) Gpnmb is induced in macrophages by IFN-gamma and lipopolysaccharide and acts as a feedback regulator of proinflammatory responses. *J Immunol.* **178**, 6557-6566

163. Wu, G., Cao, Y., Fan, B., Zheng, F., Gao, X., Liu, N., Liu, X., and Huang, N. (2011) High-mobility group protein N2 (HMGN2) inhibited the internalization of *Klebsiella pneumoniae* into cultured bladder epithelial cells. *Acta Biochim Biophys Sin (Shanghai)* **43**, 680-687

164. Rivera-Marrero, C. A., Stewart, J., Shafer, W. M., and Roman, J. (2004) The down-regulation of cathepsin G in THP-1 monocytes after infection with *Mycobacterium tuberculosis* is associated with increased intracellular survival of bacilli. *Infect Immun.* **72**, 5712-5721

165. Håkansson, G., Lutay, N., Andersson, M., Hallgren, O., Westergren-Thorsson, G., Svensson, M., and Godaly, G. (2013) Epithelial G protein-coupled receptor kinases regulate the initial inflammatory response during mycobacterial infection. *Immunobiology* **218**, 984-994

166. Lee, B. Y., Jethwaney, D., Schilling, B., Clemens, D. L., Gibson, B. W., and Horwitz, M. A. (2010) The *Mycobacterium bovis* bacille Calmette-Guerin phagosome proteome. *Mol Cell Proteomics.* **9**, 32-53

167. Ghosh, S., and Saxena, R. K. (2004) Early effect of *Mycobacterium tuberculosis* infection on Mac-1 and ICAM-1 expression on mouse peritoneal macrophages. *Exp Mol Med.* **36**, 387-395

168. Ocwieja, K. E., Brady, T. L., Ronen, K., Huegel, A., Roth, S. L., Schaller, T., James, L. C., Towers, G. J., Young, J. A., Chanda, S. K., König, R., Malani, N., Berry, C. C., and Bushman, F. D. (2011) HIV integration targeting: a pathway involving Transportin-3 and the nuclear pore protein RanBP2. *PLoS Pathog.* **7**, e1001313

169. Pan, F., Zhao, Y., Zhu, S., Sun, C., Lei, L., Feng, X., and Han, W. Y. (2012) Different transcriptional profiles of RAW264.7 infected with *Mycobacterium tuberculosis* H37Rv and BCG identified via deep sequencing. *PLoS One* **7**, e51988

170. Imbeault, M., Giguère, K., Ouellet, M., and Tremblay, M. J. (2012) Exon level transcriptomic profiling of HIV-1-infected CD4(+) T cells reveals virus-induced genes and host environment favorable for viral replication. *PLoS Pathog.* **8**, e1002861

171. Guo, F., Xing, Y., Zhou, Z., Dou, Y., Tang, J., Gao, C., and Huan, J. (2012) Guanine-nucleotide exchange factor H1 mediates lipopolysaccharide-induced interleukin 6 and tumor necrosis factor α expression in endothelial cells via activation of nuclear factor κB. *Shock* **37**, 531-538

172. Wareham, A. S., Tree, J. A., Marsh, P. D., Butcher, P. D., Dennis, M., and Sharpe, S. A. (2014) Evidence for a role for interleukin-17, Th17 cells and iron homeostasis in protective immunity against tuberculosis in cynomolgus macaques. *PLoS One* **9**, e88149

173. Umemura, M., and Matsuzaki, G. (2013) Innate and acquired immune responses to mycobacterial infections: involvement of IL-17A/IL-23 axis in protective immunity. *Nihon Hansenbyo Gakkai Zasshi* **82**, 123-132

174. Kozakiewicz, L., Chen, Y., Xu, J., Wang, Y., Dunussi-Joannopoulos, K., Ou, Q., Flynn, J. L., Porcelli, S. A., Jacobs, W. R. J., and Chan, J. (2013) B cells regulate neutrophilia

during *Mycobacterium tuberculosis* infection and BCG vaccination by modulating the interleukin-17 response. *PLoS Pathog.* **9**, e1003472

175. Singh, S. B., Ornatowski, W., Vergne, I., Naylor, J., Delgado, M., Roberts, E., Ponpuak, M., Master, S., Pilli, M., White, E., Komatsu, M., and Deretic, V. (2010) Human IRGM regulates autophagy and cell-autonomous immunity functions through mitochondria. *Nat Cell Biol.* **12**, 1154-1165

176. Ragno, S., Romano, M., Howell, S., Pappin, D. J. C., Jenner, P. J., and Colston, M. J. (2001) Changes in gene expression in macrophages infected with *Mycobacterium tuberculosis*: a combined transcriptomic and proteomic approach. *Immunology* **104** 99-108

177. Krishnan, N., Robertson, B. D., and Thwaites, G. (2013) Pathways of IL-1β secretion by macrophages infected with clinical *Mycobacterium tuberculosis* strains. *Tuberculosis* **93**, 538-547

178. Hu, C. H., Xie, J. P., Li, Y., Yue, J., Xu, Y. Z., and Wang, H. H. (2004) Differential expression of apoptosis-related gene induced by clinical and laboratory *Mycobacterium tuberculosis* strain in macrophages U937 revealed by oligonucleotide microarray. *Yi Chuan Xue Bao* **31**, 231-235

179. Choi, H., Lee, H., Kim, S. R., Gho, Y. S., and Lee, S. K. (2013) Epstein-Barr virus-encoded microRNA BART15-3p promotes cell apoptosis partially by targeting BRUCE. *J Virol.* **87**, 8135-8144

180. Das, R., Koo, M. S., Kim, B. H., Jacob, S. T., Subbian, S., Yao, J., Leng, L., Levy, R., Murchison, C., Burman, W. J., Moore, C. C., Scheld, W. M., David, J. R., Kaplan, G., MacMicking, J. D., and Bucala, R. (2013) Macrophage migration inhibitory factor (MIF) is a critical mediator of the innate immune response to *Mycobacterium tuberculosis*. *Proc Natl Acad Sci U S A.* **110**, E2997-E3006

181. Qiang, X., Yang, W. L., Wu, R., Zhou, M., Jacob, A., Dong, W., Kuncewitch, M., Ji, Y., Yang, H., Wang, H., Fujita, J., Nicastro, J., Coppa, G. F., Tracey, K. J., and Wang, P. (2013) Cold-inducible RNA-binding protein (CIRP) triggers inflammatory responses in hemorrhagic shock and sepsis. *Nat Med.* **19**, 1489-1495

182. Wang, H., Kumar, A., Lamont, R. J., and Scott, D. A. (2014) GSK3β and the control of infectious bacterial diseases. *Trends in Microbiology* **22**, 208-217

183. Herget, M., and Tampé, R. (2007) Intracellular peptide transporters in human - compartmentalization of the "peptidome". *Pflugers Arch.* **453**, 591-600

184. Chen, L., Shi, W., Li, H., Sun, X., Fan, X., Lesage, G., Li, H., Li, Y., Zhang, Y., Zhang, X., Zhang, Y., and Yin, D. (2010) Critical role of toll-like receptor 9 in morphine and *Mycobacterium tuberculosis*-induced apoptosis in mice. *PLoS One* **5**, e9205

185. Lutay, N., Håkansson, G., Alaridah, N., Hallgren, O., Westergren-Thorsson, G., and Godaly, G. (2014) Mycobacteria bypass mucosal NF-kB signalling to induce an epithelial anti-inflammatory IL-22 and IL-10 response. *PLoS One* **9**, e86466

186. Hestvik, A. L., Hmama, Z., and Av-Gay, Y. (2003) Kinome analysis of host response to mycobacterial infection: a novel technique in proteomics. *Infection and Immunity* **71**, 5514-5522

187. Poirier, V., and Av-Gay, Y. (2012) *Mycobacterium tuberculosis* modulators of the macrophage's cellular events. *Microbes Infect.* **14**, 1211-1219

188. Behr, M. A., Wilson, M. A., Gill, W. P., Salamon, H., Schoolnik, G. K., Rane, S., and Small, P. M. (1999) Comparative genomics of BCG vaccines by wholegenome DNA microarray. *Science* **284**, 1520-1523

189. Mahesh, Y., and Schorey, J. S. (2006) The β-glucan receptor dectin-1 functions together with TLR2 to mediate macrophage activation by mycobacteria. *Blood* **108**, 3168-3175

190. Vaux, D. L., and Strasser, A. (1996) The molecular biology of apoptosis. *Proc Natl Acad Sci U S A* **93**, 2239-2244

191. Zychlinsky, A. (1993) Programmed cell death in infectious diseases. *Trends Microbiol.* **1**, 114-117

192. Hsing, C. H., Chen, Y. H., Chen, C. L., Huang, W. C., Lin, M. C., Tseng, P. C., Wang, C. Y., Tsai, C. C., Choi, P. C., and Lin, C. F. (2012) Anesthetic propofol causes glycogen synthase kinase-3β-regulated lysosomal/mitochondrial apoptosis in macrophages. *Anesthesiology* **116**, 868-881

193. Beurel, E., and Jope, R. S. (2006) The paradoxical pro- and anti-apoptotic actions of GSK3 in the intrinsic and extrinsic apoptosis signalling pathways. *Prog Neurobiol.* **79**, 173-189

194. Fratazzi, C., Arbeit, D. R., Carini, C., and Remold, H. G. (1997) Programmed cell death of *Mycobacterium avium* serovar 4-infected human macrophages prevents the mycobacteria from spreading and induces mycobacterial growth inhibition by freshly added, uninfected macrophages. *J. Immunol.* **158**, 4320-4327

195. Riendeau, C. J., and Kornfeld, H. (2003) THP-1 cell apoptosis in response to mycobacterial infection. *Infect. Immun.* **71**, 254-259

196. Nau, G. J., Richmond, J.F.L., Schlesinger, A., Jennings, E.G., Lander, E.S., and Young, R.A. (2002) Human macrophage activation programs induced by bacterial pathogens. *Proc Natl Acad Sci* **99**, 1503–1508

197. McGarvey, J. A., Wagner, D., and Bermudez, L.E. . (2004) Differential gene expression in mononuclear phagocytes infected with pathogenic and non-pathogenic mycobacteria. *Clin Exp Immunol* **136**, 490–500

198. Ehrt, S., Schnappinger, D., Bekiranov, S., Drenkow, J., Shi, S., Gingeras, T.R., Gaasterland, T., Schoolnik, G., and Nathan, C. (2001) Reprogramming of the macrophage transcriptome in response to interferon-gamma and *Mycobacterium tuberculosis*: signalling roles of nitric oxide synthase-2 and phagocyte oxidase. *J Exp Med* **194**, 1123-1140

199. Wang, J. P., Rought, S.E., Corbeil, J., and Guiney, D.G. . (2003) Gene expression profiling detects patterns of human macrophage responses following *M. tuberculosis* infection. . *FEMS Immunol Med Microbiol* **39**, 163–712

200. Schnappingera, D., Schoolnikb, G.K., and Ehrt, S. (2006) Expression profiling of host pathogen interactions: how *Mycobacterium tuberculosis* and the macrophage adapt to one another. *MIcrobes and Infection* **8**, 1132–1140

201. Wu, K., Dong, D., Fang, H., Levillain, F., Jin, W., Mei, J., Gicquel, B., Du, Y., Wang, K., Gao, Q., Neyrolles, O., and Zhang, J. (2012) An interferon-related signature in the transcriptional core response of human macrophages to *Mycobacterium tuberculosis* infection. *PLoS One* **7**, e38367

202. Subbian, S., Bandyopadhyay, N., Tsenova, L., Brien, O.P., Khetani, V., Kushner, N.L., Peixoto, B., Soteropoulos, P., Bader, J.S., Karakousis, P.C., Fallows, D., and Kaplan, G. (2013) Early innate immunity determines outcome of Mycobacterium tuberculosis pulmonary infection in rabbits. *Cell Commun Signal.* **11**, 60

203. Berry, M. P., Graham, C.M., McNab, F.W., Xu, Z., Bloch, S.A., Oni, T., *et al.* (2010) An interferon-inducible neutrophil-driven blood transcriptional signature in human tuberculosis. *Nature* **466** 973–977

204. Mistry, R., Cliff, J.M., Clayton, C.L., Beyers, N., Mohamed, Y.S., Wilson, P.A. *et al.* (2007) Gene-expression patterns in whole blood identify subjects at risk for recurrent tuberculosis. *J Infect Dis* **195**, 357–365

205. Lesho, E., Forestierob, F.J., Hiratab, M.H., Hiratab, R.D., Ceconb, L., Meloc, F.F., Paikd, S.H., Muratad, Y., Fergusond, E.W., Wange, Z., Ooid, G.T. (2011) Transcriptional responses of host peripheral blood cells to tuberculosis infection. *Tuberculosis* **91**, 390–399

206. Maertzdorf, J., Repsilber, D., Parida, S.K., Stanley, K., Roberts, T., Black, G. *et al.* (2011) Human gene expression profiles of susceptibility and resistance in tuberculosis. *Genes Immun* **12**, 15–22

207. Thuong, N. T., Dunstan, S.J., Chau, T.T., Thorsson, V., Simmons, C.P., Quyen, N.T. *et al.* (2008) Identification of tuberculosis susceptibility genes with human macrophage gene expression profiles. *PLoS Pathog* **4**, e1000229

208. Chaussabel, D., Semnani, R. T., McDowell, M. A., Sacks, D., Sher, A., and Nutman, T. B. (2003) Unique gene expression profiles of human macrophages and dendritic cells to phylogenetically distinct parasites. *Blood* **102**, 672-681

209. Bartke, T., Pohl, C., Pyrowolakis, G., and Jentsch, S. (2004) Dual role of BRUCE as an antiapoptotic IAP and a chimeric E2/E3 ubiquitin ligase. *Mol Cell.* **14**, 801-811

210. Tarn, W. Y., and Steitz, J. A. (1997) Pre-mRNA splicing: the discovery of a new spliceosome doubles the challenge. *Trends Biochem Sci.* **22**, 132-137

211. Riemekasten, G., Langnickel, D., Enghard, P., Undeutsch, R., Humrich, J., Ebling, F. M., Hocher, B., Humaljoki, T., Neumayer, H., Burmester, G. R., Hahn, B. H., Radbruch, A., and Hiepe, F. (2004) Intravenous injection of a D1 protein of the Smith proteins postpones murine lupus and induces type 1 regulatory T cells. *J Immunol.* **173**, 5835-5842

212. Höchst, B., Schildberg, F. A., Sauerborn, P., Gäbel, Y. A., Gevensleben, H., Goltz, D., Heukamp, L. C., Türler, A., Ballmaier, M., Gieseke, F., Müller, I., Kalff, J., Kurts, C., Knolle, P. A., and Diehl, L. (2013) Activated human hepatic stellate cells induce myeloid derived suppressor cells from peripheral blood monocytes in a CD44-dependent fashion. *J Hepatol.* **59**, 528-535

213. Manigold, T., and Racanelli, V. (2007) T-cell regulation by CD4 regulatory T cells during hepatitis B and C virus infections: facts and controversies. *Lancet Infect Dis.* **7**, 804-813

214. Gerosa, F., Nisii, C., Righetti, S., Micciolo, R., Marchesini, M., Cazzadori, A., and Trinchieri, G. (1999) CD4(+) T cell clones producing both interferon-gamma and interleukin-10 predominate in bronchoalveolar lavages of active pulmonary tuberculosis patients. *Clin Immunol.* **92**, 224-234

215. Trinchieri, G. (2001) Regulatory role of T cells producing both interferon gamma and interleukin 10 in persistent infection. *J Exp Med.* **194**, F53-57

216. Côté, J. F., and Vuori, K. (2002) Identification of an evolutionarily conserved superfamily of DOCK180-related proteins with guanine nucleotide exchange activity. *J Cell Sci.* **115**, 4901-4913

217. Yelo, E., Bernardo, M. V., Gimeno, L., Alcaraz-García, M. J., Majado, M. J., and Parrado, A. (2008) Dock10, a novel CZH protein selectively induced by interleukin-4 in human B lymphocytes. *Mol Immunol.* **45**, 3411-3418

218. Dlugovitzky, D., Bay, M. L., Rateni, L., Urízar, L., Rondelli, C. F., Largacha, C., Farroni, M. A., Molteni, O., and Bottasso, O. A. (1999) In vitro synthesis of interferon-gamma, interleukin-4, transforming growth factor-beta and interleukin-1 beta by peripheral blood mononuclear cells from tuberculosis patients: relationship with the severity of pulmonary involvement. *Scand J Immunol.* **49**, 210-217

219. López Ramírez, G. M., Rom, W. N., Ciotoli, C., Talbot, A., Martiniuk, F., Cronstein, B., and Reibman, J. (1994) *Mycobacterium tuberculosis* alters expression of adhesion molecules on monocytic cells. *Infect Immun.* **62**, 2515-2520

220. Wilkinson, R. J., Patel, P., Llewelyn, M., Hirsch, C. S., Pasvol, G., Snounou, G., Davidson, R. N., and Toossi, Z. (1999) Influence of polymorphism in the genes for the interleukin (IL)-1 receptor antagonist and IL-1beta on tuberculosis. *J Exp Med* **189**, 1863–1874

221. Murray, H. W., Nathan, C. F., and Cohn, Z. A. (1980) Macrophage oxygen-dependent antimicrobial activity. IV. Role of endogenous scavengers of oxygen intermediates. *J Exp Med.* **152**, 1610-1624

222. Murray, H. W., and Cohn, Z. A. (1980) Macrophage oxygen-dependent antimicrobial activity. III. Enhanced oxidative metabolism as an expression of macrophage activation. *J Exp Med.* **152**, 1596-1609

223. Yuo, A., Kitagawa, S., Motoyoshi, K., Azuma, E., Saito, M., and Takaku, F. (1992) Rapid priming of human monocytes by human hematopoietic growth factors: granulocyte-macrophage colony-stimulating factor (CSF), macrophage-CSF, and interleukin-3 selectively enhance superoxide release triggered by receptor-mediated agonists. *Blood* **79**, 1553-1557

224. Oddo, M., Calandra, T., Bucala, R., and Meylan, P. R. (2005) Macrophage migration inhibitory factor reduces the growth of virulent *Mycobacterium tuberculosis* in human macrophages. *Infect Immun.* **73**, 3783-3786

225. Kagnoff, M. F., and Eckmann, L. . (2001) Analysis of host responses to microbial infection using gene expression profiling. *Curr. Opin. Microbiol.* **4**, 246-250

226. Gygi, S. P., Rochon, Y., Franza, B.R., and Aebersold, R. . (1999) Correlation between protein and mRNA abundance in yeast. *Molecular and Cellular Biology* **19**, 1720–1730.

227. Belle, A., Tanay, A., Bitincka, L., Shamir, R., and O'Shea, E.K. (2006) Quantification of protein half-lives in the budding yeast proteome. *Proc. Natl. Acad. Sci.* **103**, 13004–13009

228. Xue, J. H., Nonoguchi, K., Fukumoto, M., Sato, T., Nishiyama, H., Higashitsuji, H., Itoh, K., and Fujita, J. (1999) Effects of ischemia and H2O2 on the cold stress protein CIRP expression in rat neuronal cells. *Free Radic Biol Med.* **27**, 1238-1244

229. Sheikh, M. S., Carrier, F., Papathanasiou, M. A., Hollander, M. C., Zhan, Q., Yu, K., and Fornace, A. J. J. (1997) Identification of several human homologs of hamster DNA damage-inducible transcripts. Cloning and characterization of a novel UV-inducible cDNA that codes for a putative RNA-binding protein. *J Biol Chem.* **272**, 26720-26726

230. Wellmann, S., Bührer, C., Moderegger, E., Zelmer, A., Kirschner, R., Koehne, P., Fujita, J., and Seeger, K. (2004) Oxygen-regulated expression of the RNA-binding proteins RBM3 and CIRP by a HIF-1-independent mechanism. *J Cell Sci.* **117**, 1785-1794

231. Makarova, O. V., Makarov, E. M., Liu, S., Vornlocher, H. P., and Lührmann, R. (2002) Protein 61K, encoded by a gene (PRPF31) linked to autosomal dominant retinitis pigmentosa, is required for U4/U6*U5 tri-snRNP formation and pre-mRNA splicing. *EMBO J.* **21**, 1148-1157

232. Yokogawa, T., Shimada, N., Takeuchi, N., Benkowski, L., Suzuki, T., Omori, A., Ueda, T., Nishikawa, K., Spremulli, L. L., and Watanabe, K. (2000) Characterization and tRNA recognition of mammalian mitochondrial seryl-tRNA synthetase. *J Biol Chem.* **275**, 19913-19920

233. Belostotsky, R., Ben-Shalom, E., Rinat, C., Becker-Cohen, R., Feinstein, S., Zeligson, S., Segel, R., Elpeleg, O., Nassar, S., and Frishberg, Y. (2011) Mutations in the mitochondrial seryl-tRNA synthetase cause hyperuricemia, pulmonary hypertension, renal failure in infancy and alkalosis, HUPRA syndrome. *Am J Hum Genet.* **88**, 193-200

234. Rayasam, G. V., Tulasi, V. K., Sodhi, R., Davis, J. A., and Ray, A. (2009) Glycogen synthase kinase 3: more than a namesake. *Br J Pharmacol* **156**, 885-898

235. MacAulay, K., Doble, B. W., Patel, S., Hansotia, T., Sinclair, E. M., Drucker, D. J., Nagy, A., and Woodgett, J. R. (2007) Glycogen synthase kinase 3 alpha-specific regulation of murine hepatic glycogen metabolism. *Cell Metab.* **6**, 329-337

236. Piazza, F., Manni, S., Tubi, L. Q., Montini, B., Pavan, L., Colpo, A., Gnoato, M., Cabrelle, A., Adami, F., Zambello, R., Trentin, L., Gurrieri, C., and Semenzato, G. (2010) Glycogen synthase kinase-3 regulates multiple myeloma cell growth and bortezomib-induced cell death. *BMC Cancer* **10**

237. Wilson, W., and Baldwin, A. S. (2008) Maintenance of constitutive IkappaB kinase activity by glycogen synthase kinase-3alpha/beta in pancreatic cancer. *Cancer Res.* **68**, 8156-8163